General Disclaimer

One or more of the Following Statements may affect this Document

- This document has been reproduced from the best copy furnished by the organizational source. It is being released in the interest of making available as much information as possible.

- This document may contain data, which exceeds the sheet parameters. It was furnished in this condition by the organizational source and is the best copy available.

- This document may contain tone-on-tone or color graphs, charts and/or pictures, which have been reproduced in black and white.

- This document is paginated as submitted by the original source.

- Portions of this document are not fully legible due to the historical nature of some of the material. However, it is the best reproduction available from the original submission.

Produced by the NASA Center for Aerospace Information (CASI)

(NASA-CR-170729) LOW CONCENTRATION RATION SOLAR ARRAY FOR LOW EARTH ORBIT MULTI-100 kW APPLICATION Mid-term Report (Rockwell International Corp.) 146 p HC A07/MF A01 CSCL 10A G3/44

N83-20360

Unclas 03048

SSD82-0172

LOW CONCENTRATION RATIO SOLAR ARRAY FOR LOW EARTH ORBIT MULTI-100 kW APPLICATION

MID-TERM REPORT

NOVEMBER 1982

PREPARED FOR:

NATIONAL AERONAUTICS AND SPACE ADMINISTRATION
GEORGE C. MARSHALL SPACE FLIGHT CENTER,
AL 35812

CONTRACT NAS8-34214

MAR 1983
RECEIVED
NASA STI FACILITY
ACCESS DEPT.

Rockwell International
Space Operations/Integration &
Satellite Systems Division

SSD82-0172

LOW CONCENTRATION RATIO SOLAR ARRAY FOR LOW EARTH ORBIT MULTI-100 kW APPLICATION

MID-TERM REPORT

NOVEMBER 1982

PREPARED FOR:

NATIONAL AERONAUTICS AND SPACE ADMINISTRATION
GEORGE C. MARSHALL SPACE FLIGHT CENTER,
AL 35812

CONTRACT NAS8-34214

Rockwell International
Space Operations/Integration &
Satellite Systems Division

TECHNICAL REPORT INDEX/ABSTRACT

ACCESSION NUMBER							DOCUMENT SECURITY CLASSIFICATION	
							UNCLASSIFIED	

TITLE OF DOCUMENT	LIBRARY USE ONLY
Low Concentration Ratio Solar Array For Low Earth Orbit Multi-100 kW Application, Mid-Term Report	
AUTHOR(S) Nalbandian, S. J., et. al.	

CODE	ORIGINATING AGENCY AND OTHER SOURCES	DOCUMENT NUMBER
	Rockwell International Corporation Space Operations/Integration & Satellite Systems Division	SSD 82-0172

PUBLICATION DATE	CONTRACT NUMBER
November 1982	NAS8-34214

DESCRIPTIVE TERMS

Concentrators, Solar Arrays, Concentrator Arrays, Concentrating Silicon Solar Cells, concentrating gallium arsenide cells, Low earth orbit multi-100 kW solar array design.

ABSTRACT

This report describes an ongoing preliminary design effort directed toward a low-concentration-ratio photovoltaic array system based on 1984 technology and capable of delivering multi-hundred kilowatts (300 kW to 1000 kW range) in low earth orbit. The array system consists of two or more array modules each capable of delivering between 80 kW to 172 kW using silicon solar cells or gallium arsenide solar cells respectively.

The array module deployed area is 1320 square meters and consists of 4356 pryamidal concentrator elements. The module, when stowed in the Space Shuttle's payload bay, has a stowage volume of a cube with 3.24 meters on a side. The concentrator elements are sized for a geometric concentration ratio (GCR) of six with an aperture area of 0.5 meters x 0.5 meters.

The report discusses the structural analysis and design trades leading to the baseline design. It also describes the configuration, as well as optical, thermal and electrical performance analyses that support the design and overall performance estimates for the array.

ORIGINAL PAGE IS
OF POOR QUALITY

FOREWORD

This mid-term report describes the effort performed for the preliminary design of low-cost concentrator multi-hundred kilowatt solar arrays. The primary emphasis in this report is placed on activities performed between June 18, 1981 and August 1982, as required by Contract NAS8-34214 Statement of Work. The report was prepared by the Space Operations/Integration and Satellite Systems Division of Rockwell International Corporation for the NASA George C. Marshall Space Flight Center (MSFC), Huntsville, Alabama. The NASA technical Contractor Officer Representative for the activity is Mr. W. L. Crabtree. The contents of this document are not necessarily endorsed by the NASA-MSFC.

Mr. S. J. Nalbandian is project supervisor. Principal contributors to the project were: J. B. Adkins, M. Biss, and D. Reed, Jr. in design and mechanisms, J. L. Edwards in structures; Dr. E. P. French in optical and electro-thermal analysis; M. W. Mills in electrical design, and Z. Backovsky in thermal analysis and demonstration testing; and A. M. Pope in development planning. Mr. H. S. Greenberg provided initial support in definition of design and structual configuration for the array module.

CONTENTS

Section		Page
1.0	INTRODUCTION	1-1
	1.1 RESULTS OF PRIOR STUDIES	1-1
	1.2 PROGRAM OBJECTIVES	1-1
	1.3 PROGRAM APPROACH	1-2
	1.4 SUMMARY OF RESULTS TO DATE	1-3
2.0	CONCENTRATOR ARRAY DESIGN CRITERIA	2-1
	2.1 LAUNCH	2-1
	2.2 DEPLOYMENT	2-1
	2.3 ORBITAL OPERATION	2-1
	2.4 REQUIREMENTS	2-2
	2.5 DESIGN PARAMETERS	2-2
3.0	BASELINE DESIGN DESCRIPTION	3-1
	3.1 MODULE CONFIGURATION	3-1
	3.2 CONTAINER STRUCTURE	3-7
	3.3 MODULE INTEGRATION HARDWARE	3-13
	3.4 CONCENTRATOR ELEMENTS	3-16
4.0	ARRAY TRADE STUDIES AND PERFORMANCE ANALYSIS	4-1
	4.1 TRADE STUDIES	4-1
	4.2 STRUCTURAL ANALYSIS	4-4
	4.3 THERMAL ANALYSIS	4-19
	4.4 OPTICAL PERFORMANCE	4-27
	4.5 ELECTRICAL ANALYSIS	4-37
	4.6 ARRAY MODULE PERFORMANCE	4-46
5.0	COMPONENT DEMONSTRATION TESTS (TASK II)	5-1
	5.1 STRUCTURAL AND DYNAMIC MODELS	5-1
	5.2 REFLECTOR MATERIAL AND FABRICATION TESTS	5-4
	5.3 SOLAR PANEL FABRICATION AND TESTING	5-6
	5.4 FULL SCALE CONCENTRATOR TESTS	5-9
6.0	DEVELOPMENT PLANNING AND FUTURE EFFORT	6-1
	6.1 TECHNOLOGY ASSESSMENT	6-1

PRECEDING PAGE BLANK NOT FILMED

Section		Page
	6.2 SUPPORTING RESEARCH TECHNOLOGY (SRT) PLAN . . .	6-2
	6.3 GROUND TEST MODEL FABRICATION PLAN	6-3
	6.4 DESIGN UPDATE	6-3
7.0	REFERENCES	7-1
	APPENDIX	
	A. DRAWINGS	A-1

ILLUSTRATIONS

Figure		Page
1.4-1	Program Logic	1-4
1.4-2	Project Schedule	1-5
1.4-3	Concentrator Array Module Nomenclature	1-6
1.4-4	Container Structures/Mechanisms/Subsystems	1-7
3.0-1	Drawing Tree, Preliminary Design	3-2
3.0-2	Drawing Tree, Test Hardware	3-3
3.1-1	Solar Array/Shuttle Interface	3-4
3.1-2	Array Module Stowage In Shuttle	3-5
3.1-3	Concentrator Array Module Design Configuration	3-7
3.2-1	Container Structures/Mechanisms/Subsystems	3-9
3.4-1	Reflector Panels	3-18
3.4-2	Concentrator Element (Stretched Film or Rigid Panel	3-20
3.4-3	Solar Panel Design	3-22
4.2-1	User Spacecraft and Mathematical Model	4-5
4.2-2	Stationkeeping Acceleration	4-5
4.2-3	Mast Structural Capability (Single Laced)	4-8
4.2-4	Mast Structural Capability (Hybrid)	4-8
4.2-5	Container/Housing	4-10
4.2-6	Container/End-Cap	4-11
4.2-7	Power Output as a Function of Cable Tension	4-12
4.2-8	Module Deployment Response	4-13
4.2-9	Latching Mechanism Loads	4-14
4.2-10	Cradled Concept	4-18
4.3-1	Coupled Thermal-Electric Model Results (Silicon Baseline)	4-21
4.3-2	Coupled Thermal-Electric Model Results (GaAs Baseline)	4-22
4.3-3	Scale Effect on Radiator/Substrate	4-23
4.3-4	Transient Temperatures for Frame-Film Reflectors	4-25
4.3-5	Differential Expansion Results	4-25
4.4-1	Coordinate System for Pyramidal Concentrators	4-28
4.4-2	Geometry of Limiting Ray (Conventional Design)	4-28
4.4-3	Typical Ray Trace Histories	4-31
4.4-4	Optical Performance--Fully Reflecting Corners (Geometric CR=6.0; Reflectivity 90%)	4-33
4.4-5	Optical Performance--Nonreflecting Corners (Geometric CR=6.0; Reflectivity 90%)	4-34
4.4-6	Optical Performance-Nonreflecting Corner Tips (Geometric CR=6.0; Reflectivity 90%)	4-35
4.4-7	Ray-Tracing Results-Average Flux Incident on Solar Panel	4-36
4.5-1	Measured Low CR Optimized Solar Cell Output Characteristics	4-38
4.5-2	Solar Cell Characteristics and Performance Models (BOL)	4-39
4.5-3	Coupled Thermal Electrical Math Model	4-40
4.5-4	Electrical String Design (Silicon)	4-45
4.6-1	Life Cycle Energy Comparisons	4-50
5.1-1	Articulated Model Deploying from Stowed Position	5-2
5.1-2	Four Element Model Undergoing Extension	5-3
5.4-1	Full Scale Concentrator Tests	5-11

TABLES

Table		Page
1.4-1	Power Levels for Module Configurations	1-8
1.4-2	Concentrator Component Operating Temperature Ranges.	1-9
2.5-1	System Requirements for Structural Design	2-3
3.4-1	Stack Breakdown.	3-21
3.4-2	Solar Panel Characteristics.	3-21
4.0-1	Concept Verification Major Design Issues	4-2
4.1-1	Summary of Trade Studies.	4-3
4.2-1	Comparison of Module Extension Limits	4-7
4.2-2	Dimensional Stability and Deflections (Single Module)	4-16
4.2-3	Stationkeeping Deflections	4-17
4.2-4	Mass Summary.	4-17
4.2-5	STS Compatibility-Quasi-Steady State Flight Loads (Acceleration in g's)	4-18
4.3-1	Container Thermal Distortion	4-26
4.4-1	Optical Performance of CR=6 Concentrators	4-32
4.5-1	Harness Design Characteristics.	4.43
4.6-1	Weight and Cost Estimates for Baseline Modules	4-47
4.6-2	Performance Estimates for Baseline Modules.	4-48
5.3-1	Test Requirements for Solar Panels	5-7
5.4-1	Differences between the Baseline Design and Test Hardware	5-10
6.1-1	Technology Assessment-Identification of Technology Deficiencies	6-1
6.3-1	Model Fabrication Plan	6-4

PRECEDING PAGE BLANK NOT FILMED

1.0 INTRODUCTION

Space Transportation System (Shuttle) operational usage in the 1980's will allow routine access to earth-orbiting space systems (e.g., space base scientific and public service platform missions). These low earth orbit (~500 km) space systems are expected to require power system capabilities of multi-100-kW power levels to perform a variety of missions. The ability to provide the required power levels is limited by the cost of solar arrays within use of existing technology.

1.1 RESULTS OF PRIOR STUDIES

NASA Marshall Space Flight Center has recently funded studies[1][2][3]* which show that a concentrator solar array concept can reduce the recurring array and operational costs by a factor of three or more over that attainable with current planar arrays.

For the recurring solar array costs goals to be met and the desired performance characteristics to be maintained, technology advancements are needed in three major areas for solar array configurations. These are:

1. Lower cost, large area, lightweight deployable structures that lead to a compact stowage volume compatible for launch to orbit by the Shuttle vehicle.
2. Lower cost, larger-area, higher-efficiency solar cells suitable for low-concentration ratio (CR) applications.
3. Lightweight concentrator configurations designed to provide the desired concentration ratio and compatible with the solar array deployment scheme selected and the severe temperature cycling incurred in low earth orbit.

1.2 PROGRAM OBJECTIVES

A large-area array, with a geometric CR of about six suns, has been selected as a relatively low risk development to demonstrate technology

*Superscript numbers in paranthesis indicate references.

readiness by the end of 1984. This program has as its prime objective the preliminary design of a solar array system capable of providing in excess of 300 kW power, deliverable to the user system in orbit by a single Shuttle launch. Up to four solar array modules (each having a power output greater than 75 kW) would comprise the array. The preliminary design effort, including critical technology demonstrations, is planned to be completed in June 1983. The concentrator array design provides for utilization of either silicon (Si) or gallium arsenide (GaAs) solar cells for conversion of solar energy to electrical power.

1.3 PROGRAM APPROACH

The approach builds upon results of Rockwell's previous study to provide a preliminary design consistent with the goals of the project, namely technology readiness in the mid-1980's, compatibility with a Shuttle launch, and low recurring cost (life cycle cost). The work is being carried out under four technical tasks.

Task 1 is a preliminary design effort using the pyramidal concentrator element concept defined in Reference (1) as a point of departure. A selected array configuration has been derived through an orderly series of trade studies. These, together with the mission and orbital considerations typical of operation in low earth orbit, have been used to establish a baseline solar array configuration. Each major subsystem (primary structure, integration hardware, reflector/concentrator structure, and solar cell stack/radiator) has been studied separately in order to optimize the array system and to assess technology deficiencies. Near the end of the contract effort the results of design analysis, technology reassessment, and subelement demonstration tests (Task 2) will be used to update the preliminary design of the array system.

Task 2 deals with the demonstration testing of certain subelements and components. It is designed to provide early insight into component performance and to show confidence that the design concept will work. This task is a major activity of the contract (over one-third of the overall effort). The subelements tested will include solar cells (both GaAs and Si) mounted on a passive substrate/radiator and a full size reflector/concentrator element. Solar cells, radiator and concentrators will be integrated for functional testing. Models demonstrating the stowed and deployment method are also included.

Task 3 addresses development planning for multi-hundred kilowatt arrays. Areas of technology for which there is now insufficient engineering knowledge to support a sound preliminary design will be identified. A supporting research technology (SRT) plan containing schedules and cost estimates will be developed. Technologies which will require experimental demonstration in order to establish near-term feasibility will be identified. Test requirements, tooling, equipment, and facilities will be established with estimates for costs and schedules for demonstration testing. In addition, a plan will be prepared covering the design and fabrication of a ground test demonstration model for the array as a whole.

Task 4 considers the integration requirements of the array. Mission and orbital constraints typical in low earth orbit will be used in an analysis of system interfaces pertaining to the Shuttle orbiter (STS) and those pertaining to large user space vehicle systems. A generic approach will be used for the latter since specific missions have not been identified in this procurement. Task 4 will result in definition of specific interface compatibility of the array system for potential low earth orbit mission applications.

1.4 SUMMARY OF RESULTS TO DATE

At the mid-point in the program, substantial results have been achieved in each task area. Figure 1.4-1 illustrates overall program logic. A baseline design of the array has been defined and drawings have been prepared showing the stowed configuration, structural details of the modules and the design of individual concentrators. The design has been supported by a number of trade studies and by detailed structural, thermal, optical and electrical analyses. Models have been constructed to illustrate module deployment and concentrator element extension. Fabrication tests have been carried out for both film and rigid panel reflector types. Procurement of both silicon and gallium arsenide solar panels has been accomplished and construction is underway. Technology assessment continues and array integration requirements are being defined as required to support the design effort.

Figure 1.4-2 depicts current schedule status. The following paragraphs summarize briefly the accomplishments to date. They will be covered in greater detail in later sections of the report.

ORIGINAL PAGE IS
OF POOR QUALITY

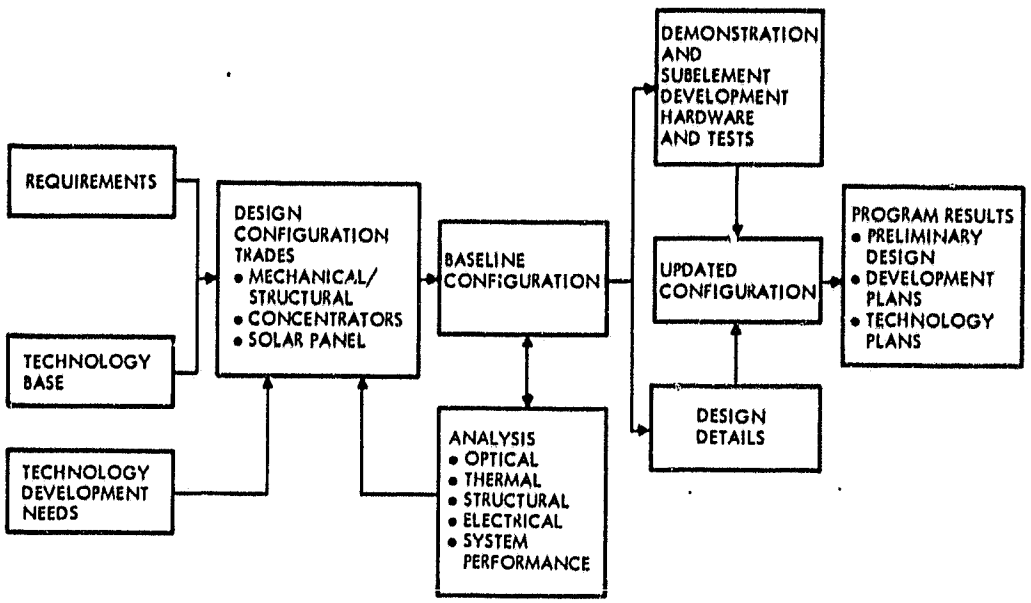

Figure 1.4-1. Program Logic

1.4.1 BASELINE DESIGN

The primary facet of the program is to study the feasibility of replacing expensive solar cells with a much less costly concentrator system without prohibitive performance (weight and deployed area penalty). The design approach is novel in the space application because of the extreme number of duplicate parts in the structures, mechanisms, and power generation hardware. The single array module, with its component nomenclature is shown in Figure 1.4-3. The array system would consist of at least two array modules. The basic power generating component in the system is a concentrator element. The element consists of a four-sided, inverted, truncated pyramid reflector with an aperture of 0.5 m per side and a geometric concentration ratio (GCR) of six. At the bottom of the concentrator element is the solar panel. The solar panel consists of solar cells mounted on a radiator panel. The concentrator elements fold along the corners and down the center of the two side reflector panels, forming the reflective surface with two full end panels, and two sets of half-panels. The concentrator/assembled in multiples of two containers. Each container (see Figure 1.4-4) is 0.54 m high by 3.24 m square. The array module consists of six containers with a stowage volume of 3.24 m cubed. There are 11 concentrator stacks and 1 deployable mast per side of each double set of

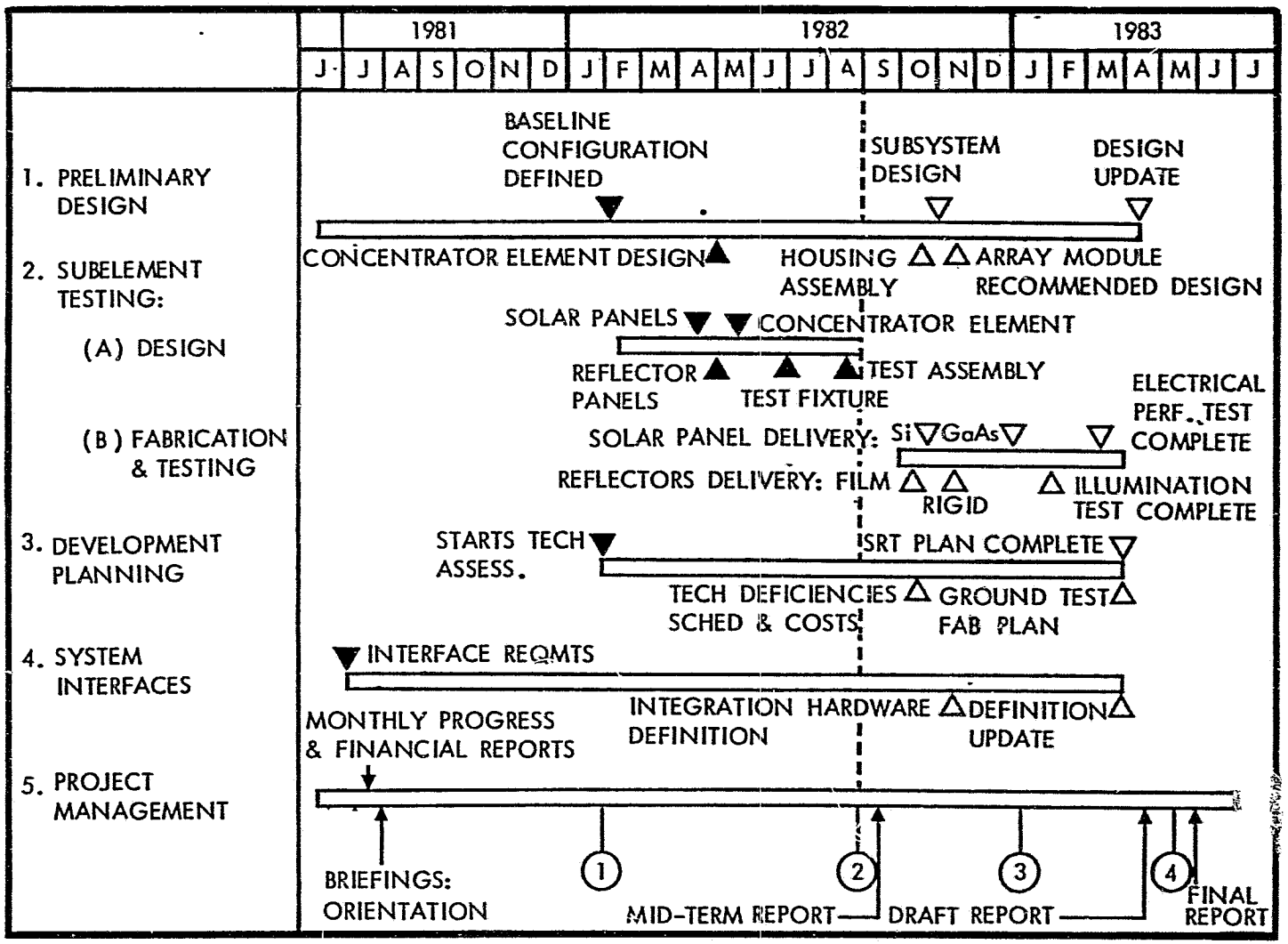

Figure 1.4-2. Project Schedule

ORIGINAL PAGE IS
OF POOR QUALITY

ORIGINAL PAGE IS
OF POOR QUALITY

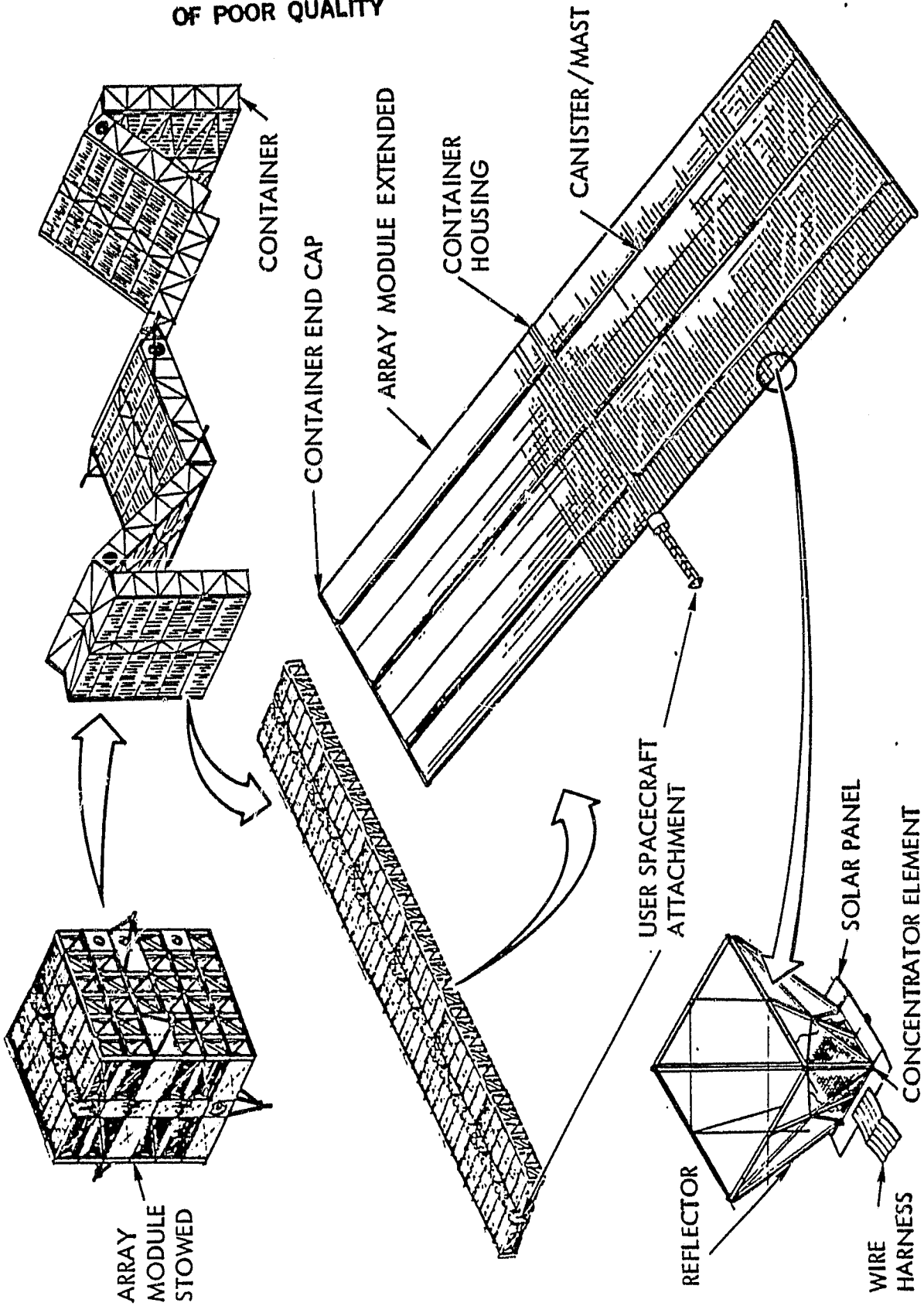

Figure 1.4-3. Concentrator Array Module Nomenclature

ORIGINAL PAGE IS
OF POOR QUALITY

Figure 1.4-4. Container Structures/Mechanisms/Subsystems

containers. The single module contains 33 concentrator stacks and 3 masts per side (double extension) with not more than 12 concentrator stacks between each mast. In a fully-extended condition, about 2½ of the 66 concentrator elements per stack would remain erected in the container housing. The concentrator elements are supported by cables connected between the end cap and the housing. The cables are maintained under tension through a constant force spring (CFS) mechanism.

The modular design allows for flexibility in sizing the array system for various power levels. The baseline array module consists of six containers; however, the module could be modified to consist of sets of two or four containers. In addition two containers can be connected end to end to form a dual container that is 6.28 m long. A dual module would then consist of six dual containers. Table 1.4-1 provides power levels available by various module configurations.

Table 1.4-1. Power Levels for Module Configurations

Containers per Module	Single Extension (kW)		Double Extension (kW)	
	GaAs Cells	Si Cells	GaAs Cells	Si Cells
6 (Baseline Module)	86	40	172	80
2	28.6	13.3	57.3	26.6
4	57.3	26.7	114.6	53.3
12 (Dual Module)	172	80	344	160

1.4.2 TRADE STUDIES AND DESIGN ANALYSIS

The principal design trades involved the choices of module geometry and concentrator size. The primary objective in both cases was to reach a design which would yield the highest power output per Shuttle load. The resulting module is cubical, occupying one quarter of the payload bay. The articulating sections housing the folded concentrator elements deploy in one direction like a carpenter's rule. Once deployed, the concentrators are extended in both directions by extendible masts acting back-to-back. Concentrator elements size (0.25 m^2 aperture) was selected because it required low radiator mass, it produced a favorable module aspect ratio for large systems while at the same time yielding acceptable structural characteristics.

ORIGINAL PAGE IS
OF POOR QUALITY

Structural analysis has been used to assess vibration frequencies which must avoid resonance with potential driving sources but remain high enough to provide reasonable settling times. Structural elements such as masts/containers and end caps have been analyzed to determine if they have sufficient strength to prevent failure under loads, both in the stowed configuration and deployed in orbit. The mast/container design for the baseline module configuration has been prepared by Astro Research Corporation (Astro) under subcontract effort. Structural element stiffness was also assessed to determine if it was sufficient to limit deformation to acceptable levels. Finally, both modules and individual concentrator elements were evaluated as to their capability of surviving steady-state or transient thermal stresses.

Detailed optical analysis has been made of the pyramidal concentrator configuration using ray-tracing methods. Optical efficiency and illumination non-uniformity has been assessed as a function of pointing error over the range 0° to 15°. The results have shown that the concentrator design is forgiving of moderate pointing error (performance losses of 3% or less for angles up to 3°). Much of the reflector heating comes from rays reflected from the upper corners. These rays contribute little to useful illumination of the solar panel. Heat load on the reflectors may therefore be decreased substantially by making the corners non-reflective.

A variety of special thermal analyses have been performed to assess the adequacy of the baseline design. These studies served to establish temperature distributions, to evaluate thermal stresses and thermal distortion effects and to uncover any serious design problems. Component temperature ranges during normal operation are summarized in Table 1.4-2.

Table 1.4-2. Concentrator Component Operating Temperature Ranges

Component	Temperature Range (°C)	
	Gallium Arsenide	Silicon
Reflector panels	48 - 134	50 - 136
Solar Cells	96 - 130	115 - 144
Radiator	57 - 91	64 - 97
Harness	29 - 46	34 - 50

Coupled thermal-electrical mathematical models of both Si and GaAs concentrators have been analyzed to determine the effect of non-uniform illumination on electrical output. The results show that by using larger cells and parallel electrical design, mismatch losses associated with illumination non-uniformity can be minimized. The analysis, which takes into account cell electrical performance, the distribution of direct and reflected sunlight obtained from ray tracing, heat conduction through the substrate-radiator and hindered thermal radiation from reflectors and radiator, due to the presence of adjacent concentrators, gives improved estimates of array power output. The higher efficiency and lower temperature sensitivity of gallium arsenide cells at operating temperature gives them a big advantage over silicon cells. Peak output (BOL) for a GaAs concentrator was 40.2 watts as compared with 18.9 watts for silicon.

2.0 CONCENTRATOR ARRAY DESIGN CRITERIA

The design requirements for the array encompass three mission phases: launch, deployment, and orbital operations. No specific missions have been identified. Rather, the design is a generic one for high-power space systems Shuttle-launched into low earth orbit.

2.1 LAUNCH

In its stowed configuration the solar concentrator array module must be of a size that fits within the Shuttle bay dynamic envelope, allows air lock ingress/egress, installation of orbital maneuvering system (OMS) kits and payload ground handling mechanism clearances as well as staying within the Shuttle cargo bay longitudinal center of gravity envelope.[4] Module attachments to the Shuttle orbiter should be compatible with the location and load capability of the orbiter attachments and/or cradle installation. The attachments should provide access for removal of the array module by means of the remote maneuvering system (RMS) in orbit.

2.2 DEPLOYMENT

This phase includes (1) the detachment and removal of the solar array modules from the orbiter's cargo bay and attachment to the user satellite, (2) articulation and deployment of the folded array module containers, and (3) extension of the deployable masts and individual concentrator elements.

2.3 ORBITAL OPERATION

The array modules are designed to keep life-cycle energy costs low for low-earth-orbit satellites. Performance factors such as array module power per unit weight and power per unit deployed area are considered important to the extent of their influence on cost effectiveness in orbit. Modularity is a major consideration in developing an acceptable design concept that can be used for a wide range of power needs of future satellites.

2.4 REQUIREMENTS

The specific guidelines used in this effort are listed below:

- Concentration ratio (CR) range of 2 to 6
- Four-sided reflector concentrator module approach (truncate pyramid)
- Low life cycle cost targeted for $30/watt recurring (1978 dollars)
- Use 1984 technology readiness date
- Design for low earth orbit (LEO) application (~500 km assumed)
- Design should be consistent with both silicon and GaAs cells
- Stowage method should be fold-up
- Design should provide maximum kW per Shuttle launch consistent with other guidelines
- Watts/kg goal not specified but to be governed by transportation cost penalties and reasonable extension of state of the art
- Practical configurations compatible with orbiter cargo compartment and on-orbit maintenance operations
- Rating of 300 kW to 1000 kW (Modular design approach)

2.5 DESIGN PARAMETERS

Other system application requirements assumed in lieu of a specific mission application are listed in Table 2.5-1. The array module configuration selected to meet these goals are discussed in Section 3.

Table 2.5-1. System Requirements for Structural Design

- Launch phase—STS compatibility
  - Orbiter cargo bay dynamic envelope
  - Quasi-steady state flight loads—acceleration in g's

	N_x*	N_y*	N_z*
• Boost environment	+2 -5	±3	±5
• Landing	+1.8 -2.0	±1.5	+4.2 -1.0

- Orbital operation
  - Attitude control
    - Stationkeeping acceleration range from 0.001 g to 0.01 g
    - Control system frequency separation (>0.02 Hz)
  - Thermal loading (not to exceed ±1° in pointing error)
  - Array orientation (not to exceed ±0.5° in pointing error)
  - Atmospheric drag (4.3×10^{-4} N/m^2)
  - Solar pressure (4.5×10^{-6} N/m^2 in GEO)
  - Gravity gradient (7.3×10^{-5} N/m^2)

*Shuttle orbiter coordinates

3.0 BASELINE DESIGN DESCRIPTION

The solar array preliminary design is embodied in a set of drawings which, together with associated callouts and specifications, provides a physical description of the system as a whole and its associated subsystems. Figures 3.0-1 and 3.0-2 are drawing trees showing the relationship between individual subassembly drawings making up the total preliminary design and test hardware. Those drawings now completed are accented with a set of the top assemblies shown in the Appendix A.

The baseline design has been broken down into three major subsystems: the container structure, module integration hardware and the power-generating or concentrator element. Figure 1.4-3 illustrates the nomenclature adopted for the solar array. The fundamental building block is the container which, when assembled into a single module and deployed, forms a large rectangle area 19.4 m x 68 m. Modules attach to the user spacecraft along longitudinal centerline of the container housing. The module structure consists of a set of six container housings attached end-to-end containing the folded concentrator stacks, deployable masts and their canisters, and end caps which are extended by the masts. The power-generating components of the array are the concentrator elements containing reflector panels which concentrate light onto the solar panels and a flat wire harness to combine and collect the power output of individual elements of the module.

3.1 MODULE CONFIGURATION

The solar array is designed to be transported in the form of modules within the 4.6-m-diameter, 14.4-m-long dynamic envelope of the shuttle payload bay. The cubical, single-module or rectangular prism dual-module designs illustrated in Figure 3.1-1 provide the compact stowage of up to four single or two dual modules per Shuttle flight (see Figure 3.1-2). Compactly folded concentrator elements contained within the modules are protected from damage due to vibration and acoustic loads during launch by means of separation buttons on vulnerable surfaces. Structural integrity of the containers is maintained by means of either latching devices which hold the individual containers together in the stowed configuration or by a cradle system which maintains the module structure under compression during launch condition. Acceleration

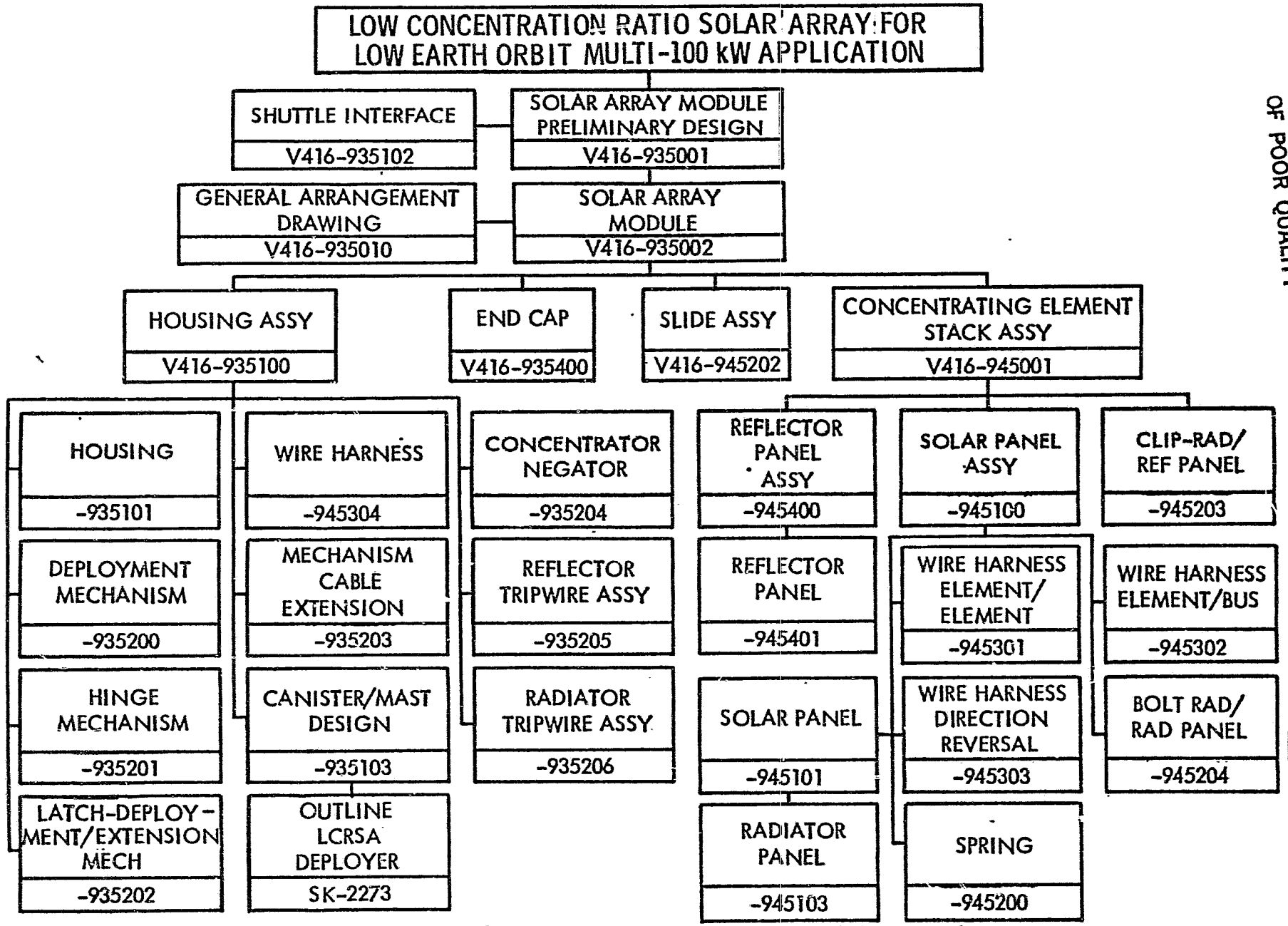

Figure 3.0-1. Drawing Tree, Preliminary Design

ORIGINAL PAGE IS OF POOR QUALITY

Space Operations/Integration & Satellite Systems Division
Rockwell International

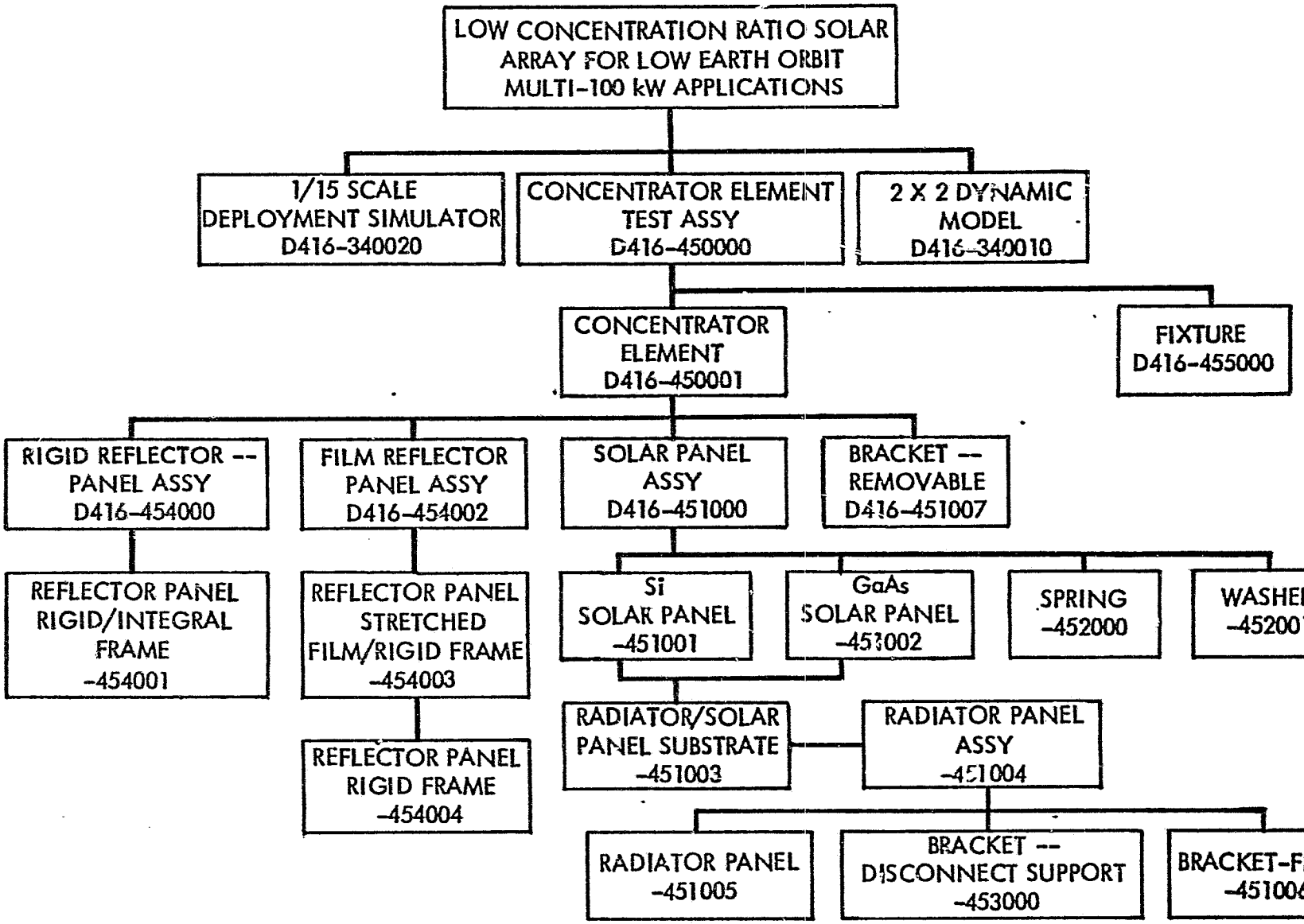

Figure 3.0-2. Drawing Tree, Test Hardware

ORIGINAL PAGE IS OF POOR QUALITY

ORIGINAL PAGE IS
OF POOR QUALITY

DRIVERS

- POWER OUTPUT REQUIRED
- SHUTTLE INTERFACE
- WEIGHT
- COST
- SHUTTLE C.G. ABORT ENVELOPE
- LAUNCH LOADS
  - STATIC/DYNAMIC
  - ACOUSTIC

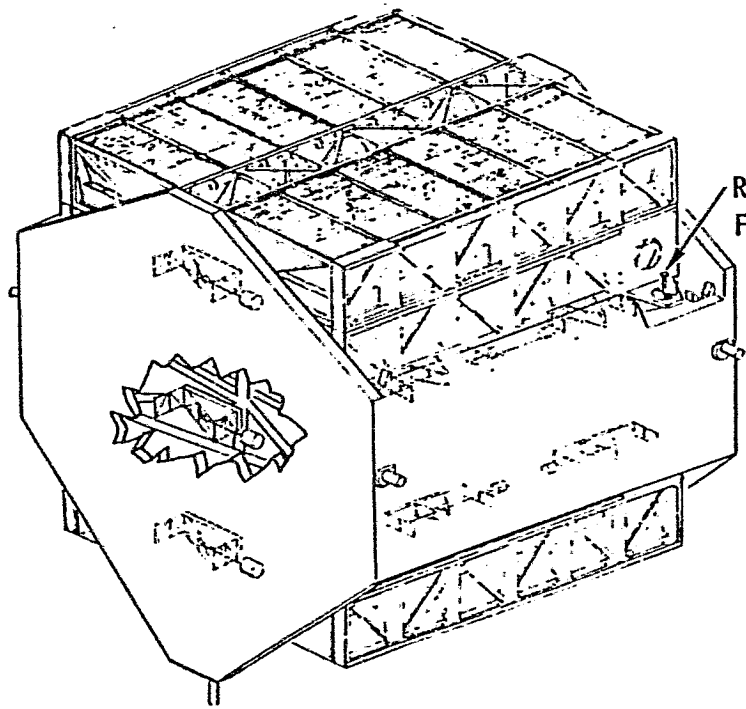

CRADLED CONCEPT

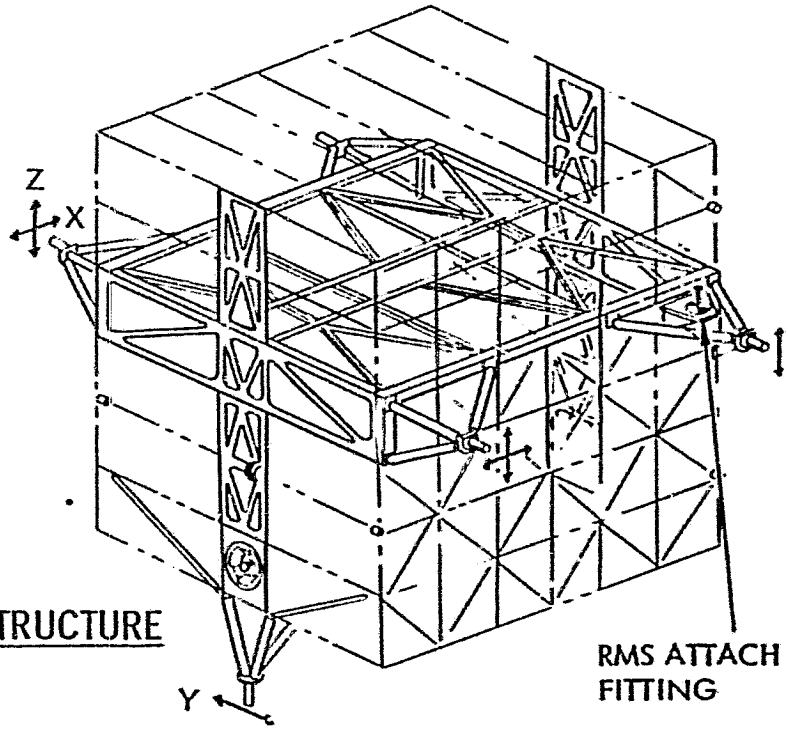

INTEGRAL STRUCTURE

Figure 3.1-1. Solar Array/Shuttle Interface

Space Operations/Integration &
Satellite Systems Division
Rockwell International

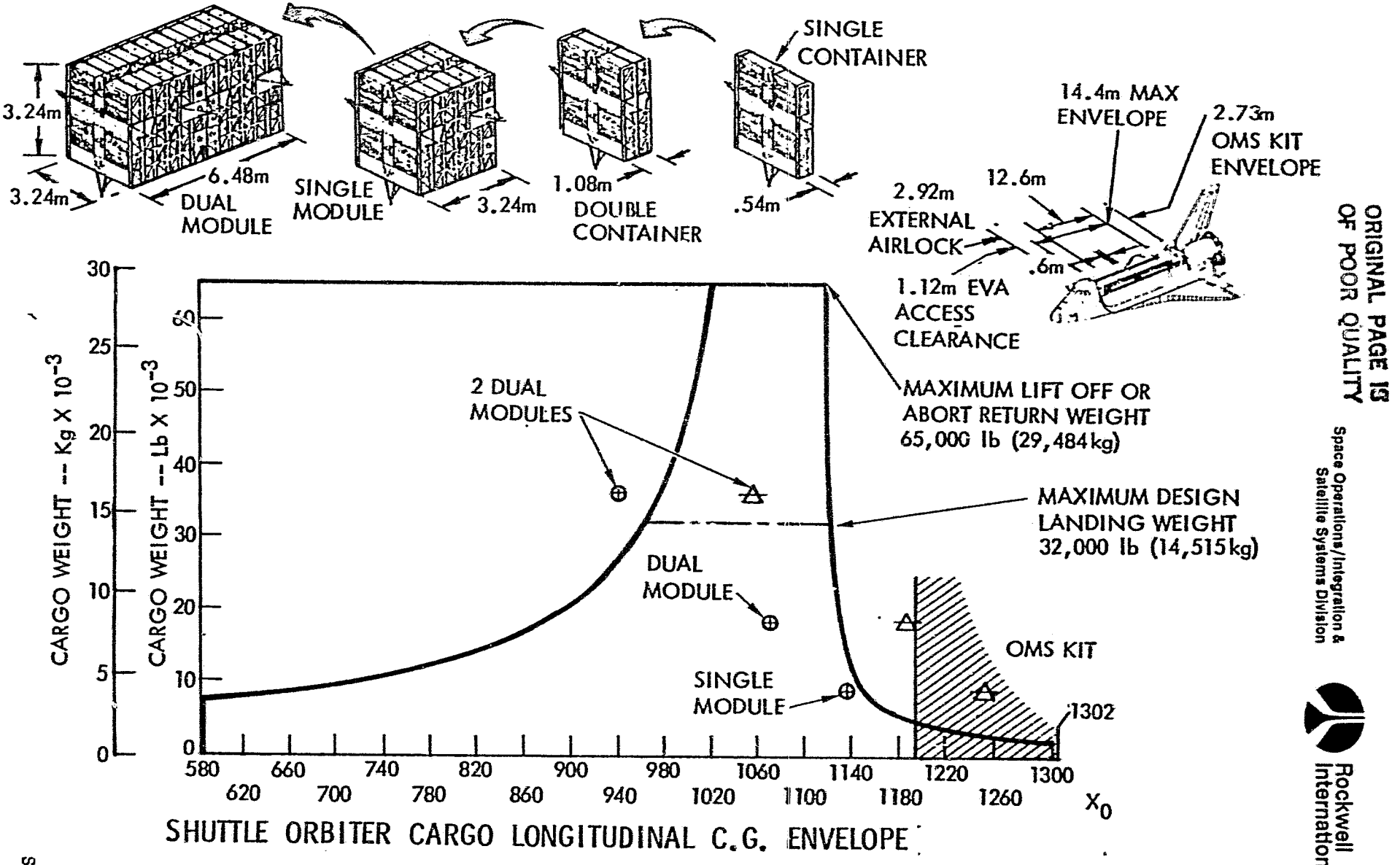

Figure 3.1-2. Array Module Stowage in SHuttle

ORIGINAL PAGE IS OF POOR QUALITY

Space Operations/Integration & Satellite Systems Division
Rockwell International

loads are carried out through attach points and transmitted to the Shuttle structure through a cradle or support structure.

The single module packages in the form of a cube 3.24 m long per side will be removed from the bay and deployed using the remote maneuvering system (RMS) arm grappling the fixture attached to the module. The six folded sections of the housing will deploy in accordian fashion, driven by rotary incremental actuators. Five such actuators, each redundant in itself, and each producing 6.8 N-m of torque will execute the 180° rotation at each joint to produce the 19.4-m-long deployed container section (see Figure 3.1-3). The total time required for this maneuver is 29 minutes. Each actuator provides 17.0 N-m holding torque while the linear incremental actuators drive the latching mechanism closed, taking 10 seconds. Extension of the array is then accomplished by the two sets of three canister-deployed continuous longeron double/single-laced (hybrid) masts which extend the end cap, carrying out the concentrator extension mechanism (CSM) cables and the first concentrator element in each stack. Each mast extends a total of 32.4 m from the end of its canister.

ORIGINAL PAGE IS
OF POOR QUALITY

Figure 3.1-3. Concentrator Array Module Design Configuration

SSD82-0172

3.2 CONTAINER STRUCTURE

Figure 3.2-1 illustrates the baseline design of a single container. Listed below is the description of each subelement or subsystem housing in the container. The module consists of six containers with two masts/canisters (Figure 3.2-1) in three of the containers. The other three containers have concentrator elements stowed in lieu of the masts/canisters shown in Figure 3.2-1. Thus a sub-module can be formed using pairs of containers consisting of one with masts/canisters and another without.

3.2.1 HOUSING

The housing is the focal point of the structural system with all subsystems being attached to the housing. The prime drivers in the sizing of the housings were the concentrator element size, Shuttle compatibility, and static and dynamic loads. Also due to the large number of parts involved a common, simple, mass-producible concept was required. The design that was settled was a design symmetrical about the longitudinal centerline. Each housing is 0.54 m high x 3.24 m wide x 3.24 m long. There are two types of housings, one with five concentrator stack bays and a mast bay per side, and one with six concentrator stack bays per side.

The housing is a truss-type structure made from two machined parts, four types of extrusion, one type of bent sheet metal and flat sheet metal shear webs, and gussets. All parts are of 2024-T6 aluminum with graphite epoxy pultrusion as an alternative. Down the center of the housing is a truss-type box 0.54 m high x 0.50 m wide with the longerons being T-extrusions running the full length of the housing on both outer corners, top and bottom. All parts begin or end at these longerons. The latch mechanisms, hinge mechanism, deployment motor, wire harnesses, CEM's, CSTM's, solar panel tripwire mechanism, reflector panel tripwire mechanism and the other mechanical subsystems are mounted inside this box section. On the outboard sides of this central box are the concentrator stack bays. Each bay is 0.54 m long (having six equal bays per side). On the housings with mast bays, a concentrator stack bay is modified by closing out the top and bottom of the structure with shear panels, and adding structures to which the extension motors and structural tie-downs are mounted. The bays are divided by a truss structure having the launch support tubes at the top to carry the launch loads of the concentrator element stacks. On the end cap/housing interface there is an L-extrusion with shear pins at the base and

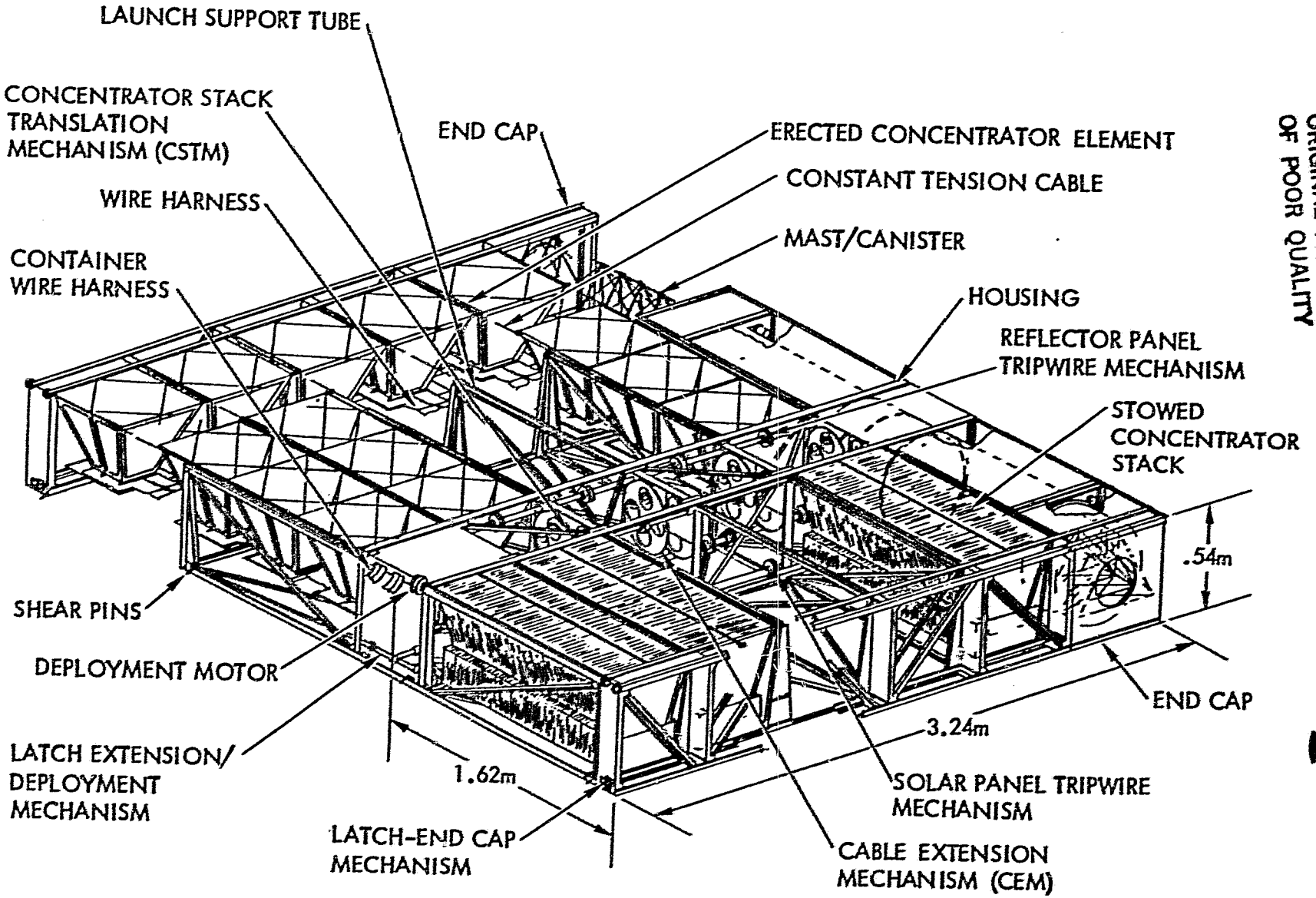

Figure 3.2-1. Container Structures/Mechanisms/Subsystems

ORIGINAL PAGE IS
OF POOR QUALITY

vertical bent sheet metal stiffeners to support the launch support tubes. The launch support tubes also attach to the end cap to dump longitudinal launch loads into the end cap. Inside the launch support tubes exists a thin bonded silicon rubber sheet with a slightly smaller inside diameter than the slide mechanism outside diameter. This allows the extension of the concentrator elements to be semi-controlled. The cable extension mechanism (CEM) cable runs down the center of the launch support tubes and attaches to the end cap.

3.2.2 END CAP

The end cap is extended by the masts and is used to extend the concentrator elements from the housing, extend the constant tension cables from their mechanisms, and to carry the loads during stationkeeping from the concentrator elements to the masts. The end caps are held in place during launch by a combination of shear pins, latches, and if one is required, the cradle system. The structure was designed to use very few parts to produce the structure. In the structural design, all the end caps can be built from one type of machined part, two types of extrusion, and one type of bent sheet metal along with flat sheet metal gussets and shear panels. The baseline design calls for 2024-T6 aluminum with an alternate of graphite/epoxy pultrusions for lighter weight.

3.2.3 CANISTER/MAST DESIGN

The concept calls for a deployable structure to extend the end caps from the housing, drawing the CEM cables and the first concentrator in each stack out of the housing. The mast also carries the on-orbit stationkeeping loads from the end caps and concentrator elements to the housing. The mast chosen is a hybrid-type single/double-laced continuous longeron, canister-deployed mast using S-glass/epoxy for the longerons, battens and diagonals. The canister envelope is to be 1.62 m long with maximum outside diameter of 0.50 m. The mast itself will be 0.44 m diameter and 32.4 m long, fully extended. The longerons are a square cross section 6.6 mm × 6.6 mm, the battens are a rectangle cross section of (W/T = 2.75) 3.74 mm × 10.11 mm, and the diagonals are a round cross section 3.3 mm diameter, all are of pultruded S-glass epoxy. The baseline design mast is capable of sustaining up to a 0.008 g level before longeron buckling occurs. The masts are spaced to carry approximately 12 concentrator element stacks each. The drive motors are each controlled through

a central servo control unit to allow for uniform extension. Each motor drives a bull gear with a pinion, requires 260 watts of power, and takes 27 minutes to fully extend one side of the array. The prime drivers in sizing the mast were the maximum outside diameter of the canister, the g loading during on-orbit stationkeeping, and the maximum stowed length of the canister.

3.2.4 CONCENTRATOR STACK TRANSLATION MECHANISM (CSTM)

The CSTM assembly consists of a pair of CFS's mounted to a small pulley. Each assembly is mounted to the backside of a CEM and attached by a 0.51 mm stainless steel cable to the last slide assembly in each set of concentrator element stacks. At the end of the mast extension, during thermal growth, or on-orbit stationkeeping, the CSTM maintains the extended stacks under 7.2 N of pretension, allowing the last two and one-half concentrators to remain erected in the housing and translate within the launch support tubes. The maximum extension of the CSTM cable is 1.0 m. The pulley is manufactured from a thermoplastic, and the CFS's are stainless steel wound on the pulley. There are 78 identical CSTM's required in the single module concept.

3.2.5 LATCH-END CAP EXTENSION MECHANISM

At the interface between the end cap and the housing on the end of the housing with the container/container latching mechanism is a device called the latch-end cap extension mechanism. The assembly allows activation of the latching mechanism in the end cap while the end cap is adjacent to the housing but does not interfere with the end cap extension. The mechanism is attached by a control rod to the latch deployment/extension mechanism bell crank. When the bell crank is actuated, the control rod activates a slider linkage mechanism across the housing/end cap interface closing and locking the latch using a spring retained over-center hinge. The latch-end cap extension mechanism is made from 2024-T6 aluminum and requires ten assemblies for either single- or double-module concepts.

3.2.6 CABLE EXTENSION MECHANISM (CEM)

The mechanism consists of a pulley assembly 0.31 m diameter that plays out braided stainless steel cable 0.51 mm diameter, 35 m long at constant tension using two constant force springs. At full extension, the cable is under 20 N

tension providing planar stability for the concentrator elements. There is one CEM between each concentrator element stack per direction and one per direction on each end of the stacks. The mechanism is a simple design calling for only seven kinds of parts each. The pulley and spring housings are thermoplastic, the constant force springs are stainless steel, and the structure is aluminum sheet metal. There are seventy-eight CEM assemblies in the single module concept.

3.2.7 SLIDE ASSEMBLY

The slide assembly functions as the tie point for the concentrator stack/stack interface, the concentrator stack/launch support tube interface, the concentrator stack/CEM cable interface, and the concentrator element stack spacer. The slide mechanism is a two-part molded thermoplastic part that is assembled on the CEM cable with adjacent concentrator element stacks. When the assembly process is finished, it allows continuous sheet, as opposed to individual rows. There are approximately 4500 slide assemblies for the single module concept.

3.2.8 REFLECTOR PANEL TRIPWIRE MECHANISM

The reflector panel tripwire mechanism works in conjunction with, and in much the same manner as the solar panel tripwire mechanism. The cables run from the end cap to the housing on the top of the concentrator elements. There are two 0.51 mm stainless steel cables per concentrator element stack. The cables run from the top center of the end cap in an alternate zigzag fashion from one reflector half panel eyelet to the next concentrator element reflector half panel on the opposite side of the bay. This pattern continues all the way back to the housing. Upon leaving the last concentrator element, the cables enter the center of the housing box structure longeron cap in each concentrator stack bay, through the wire tension sensor, and to the torque tube pulley system. The pulley/torque tube system is made from graphite/epoxy tube and attached by bearing/flange to the housing. The tube runs the length of the housing. The torque tube/pulley assembly is driven by a hollow shaft motor mounted to the housing. The pulleys are made from a thermoplastic and mounted to the torque tube. When the cable is drawn in, the panel hinges are over-centered, similar to the solar panels, and the panels stow. There are two total assemblies in each housing, twelve per single module, all using redundant parts.

3.2.9 SOLAR PANEL TRIPWIRE MECHANISM

Incorporated into the design of the system is the ability to stow the module after it has been extended, either for orbit transfer or at end of life for return to earth for refurbishment. The solar panels have torsionally loaded springs at their hinge line, and need an external force applied to trip the over-center hinge/spring mechanism to assure proper stowage. When the concentrator elements are in the stowed configuration, the solar panels are perpendicular to the housing base with the panel hinge line being at the bottom. In the erected configuration, the solar panels are parallel with the base but translated up. The radiator panel tripwire mechanism consists of one set of 0.51 mm stainless steel cables per concentrator stack bay and a torque tube/pulley system inside the housing. The cables start at the lower outboard corners of each stack bay and run from solar panel hinge to solar panel hinge on the same side of the stack bay. After running through all 66 concentrator elements, the cable runs through the lower housing box longeron, the cable tension sensor, and to the torque tube/pulley system. The pulley system is allowed to play out cable as the concentrator elements are deployed, allowing no restriction of the elements. During stowage, the mechanism is engaged taking up cable, over-centering the hinges, on the solar panel allowing the stowage sequence to take place. The design and materials are the same as the reflector panel tripwire mechanism.

3.3 MODULE INTEGRATION HARDWARE

The housings are assembled as containers (fully assembled with all subsystems) and joined to the other containers to form a module, they are alternately hinged top and bottom so that they fold like a carpenter's rule. The design calls for staggering the mast/element and all element housings so that there are never more than 12 concentrator element stacks between each mast. When fully assembled with end caps, the stowed single module configuration is a cube 3.24 m on a side, and when deployed, it is 0.54 m high x 3.24 m wide x 19.4 m long. For the dual module concept, they are assembled in much the same manner with only five hinge lines (6.48 m apart instead of 3.24 m), the five additional points being fixed on the ground by replacing the deployment motors with a machined fitting, and the latching mechanisms by bolts. Due to the minimum gauge extrusion chosen, the structure is already close to minimum practical manufacturing capability for this type of design, so there is no structural weight penalty for the dual module concept. The dual module envelope is 6.48 m long x 3.24 m wide x 3.24 m high stowed and deploys to an envelope of 0.54 m high x 3.24 m wide x 38.9 m long.

3.3.1 HINGE MECHANISM

The containers are hinged together along common centerlines. In both the single- and double-module concepts, there are five hinge lines. On the hinge lines, along the top of the container/container interfaces, there are six hinge points: two hinge points on each end cap, two in the central area of the housing, one at the end of one longeron, and the other hinge being the deployment motor at the end of the other longeron. On the hinge lines along the bottom of the container/container interface, there are eight hinge points: six the same as the top and two additional on the outboard edge of each housing adjacent to the end caps. The hinge structure is designed such that the parts are interchangeable. The central housing structure also requires machined parts. The parts are left- and right-handed, but can be used as a pair at all container/container interfaces. With the addition of one machined part to replace the deployment motor and the insertion of bolts to replace the latch mechanism, the single module concept can be converted to a dual module. The hinge mechanism is made from off-the-shelf ball bearings and machined 2024-T6 aluminum plate.

3.3.2 DEPLOYMENT MECHANISM

Each container interfaces with the next via a set of ball bearing hinges and a deployment motor. The motor chosen is a rotary incremental actuator. The baseline actuator is a small angle permanent magnet stepper attached to a harmonic drive speed reducer. The motor has a build-in redundant motor to maintain a minimum envelope. The harmonic drive ratio is 100:1 with an output capability of 0.432 kg-sec^2 m (10 slug-ft^2), a holding torque of 17 N-m (150 in.-lb) powered, 5.7 N-m (50 in.-lb) unpowered, and a power requirement of 8 watts (24 V dc). The total weight of each motor is 0.91 kg (2 lb). Due to the compact size of the actuators, the motors can be used on either the single- or dual-module concepts without paying an additional weight or power penalty. There are a total of five motors required whether it is the single- or dual-module concept.

3.3.3 LATCH-DEPLOYMENT/EXTENSION MECHANISM

The housing to housing and end cap to end cap latch mechanisms share a common design, allowing for mass production of the latches. By installing different clevis inserts in the latch mechanism, they all become interchangeable. There are four latch mechanisms per container, two located in the housing box structure at the end of the longerons, opposite the deployment motor and hinge mechanism, and two in each end cap. The latches are driven by control rods from a bell crank assembly, which in turn is driven by a linear incremental actuator. The actuator is a small angle permanent magnet stepper with an output force of 44.5 N (10 lb) and a holding force of 13.3 N (3.0 lb). The latches on the end caps are actuated by control rods from the bell crank to the latch-end cap extension mechanism, which in turn actuates the latch mechanism locking the containers together. The latch mechanism is an over-center hinge design so all loads are transferred through the latch housing to the structure and not back to the bell crank or motor.

The latch housing is made from 2024-T6 aluminum and the linkage is made from stainless steel. There are a total of 20 latch mechanisms for the single module concept.

3.3.4 SHEAR PINS

The module structure makes extensive use of shear pins. By using a common design, the shear pins become a mass producible item. During the launch configuration, the container/container interfaces are retained in the transverse axis using shear pins. The end caps are also held in their respective transverse axis using them. As the module is deployed, the containers hinge about their deployment axis and latch with the adjacent container. During on-orbit maneuvering the shear pin design translates the shear and torsional loads across the container/container interface, and the latch and deployment mechanism takes the tension loads. The shear pins are made from stainless steel, with the single module concept requiring approximately 175 shear pin assemblies.

3.3.5 WIRE HARNESS (CONTAINER/CONTAINER)

The wire harness in the housing runs from one end of the housing box structure to the other. The wire harness acts as the bus for the individual concentrator stacks, and has disconnects on either end for the housing/housing interface. The wire harness is made from a Kapton insulator with a copper bus. The bus will be two conductors wide, 0.125m wide each, and 0.30mm thick. There are up to ten of these layers deep (where housing ends in a user attach fitting). The total number of these harnesses required for the single module concept is six.

3.4 CONCENTRATOR ELEMENTS

The fundamental premise behind the design of a concentrating array is the substitution of optical surfaces (the concentrator) for much of the area normally occupied by solar cells. In order for this approach to be effective, the concentrator must be light in weight, much cheaper than the cells it replaces, and must have reasonably high optical efficiency. These requirements impose severe limitations on concentrator design. A variety of approaches have been considered. Some have been rejected in favor of two candidate options which have been retained. A final selection will be made after further study and experimental work.

For the present concept of a truncated pentahedral concentrator element with an aperture of 0.5 m × 0.5 m × 0.37 m high, and with a solar cell area at the base of the reflector panels of 0.2 m × 0.2 m has been chosen for the baseline. The concentrator elements fold along the corners of the reflector panels and down the center of the side reflector panels. The solar panels attach to the bottom of the reflector panels and hinge along the same concentrator element centerline. They also hinge along the base of the full reflector panels. The concentrator element design is compatible with either the GaAs or the Si solar panels. With the present design, the assembled, stowed, single concentrator element total thickness is 20 mm.

3.4.1 REFLECTOR PANELS

Figure 3.4-1 illustrates the major approaches considered. They break down into two categories, rigid panels and stretched films. Under the rigid panel category, the honeycomb panels are the strongest and most rigid; and they can be constructed with simple tooling well within familiar fabrication technology. They tend to be heavy, however, and there is concern that the optical quality will be compromised by dimpling of facesheets. A molded chopped fiber impregnated thermal plastic is the present baseline concept to produce a set of single lightweight, thin panels that are taped together at the hinge lines using 0.05 mm aluminized Kapton tape. An alternate concept of molding the panels as one single unit with the hinge molded in with only one taped hinge line is also being studied. The rigid panel baseline design is presently undergoing fabrication prior to optical performance tests.

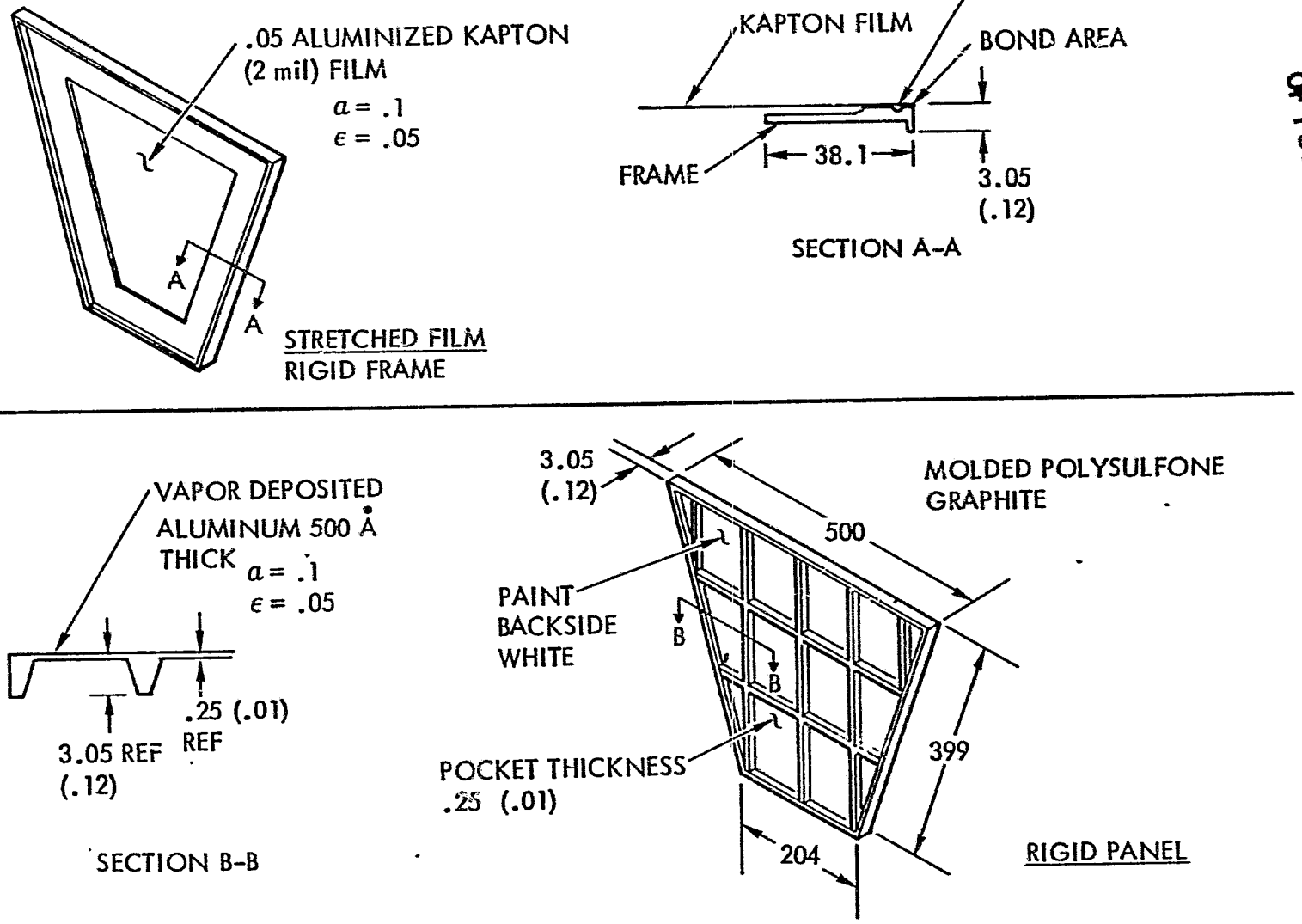

NOTE: ALL DIMS IN MILLIMETERS (INCHES IN PARENTHESES) EXCEPT AS NOTED

Figure 3.4-1. Reflector Panels

ORIGINAL PAGE IS
OF POOR QUALITY

The lightest concept considered for reflector panel construction is a stretched film supported by catenary wires. This concept has been eliminated from further consideration because of difficulties in achieving a credible design for the mechanisms which erect and tension the support wires. The favored approach is the use of rigid-frame support for stretched aluminized Kapton film panels. This concept and the solid, rigid panel concept referred to above can be used interchangeably in the construction of the four-panel pyramidal concentrator configuration.

The frame on the stretched film concept is made in much the same manner as the rigid panel. The baseline concept calls for a chopped fiber impregnated thermal plastic frame molded as a single panel or as an alternate, a fully-molded concentrator element assembly with integrally-molded hinges and one taped hinge. The panels are then secondary-bonded to 0.05 mm double-aluminized Kapton film. The film has a specular surface on the reflector side and a diffuse surface on the frame side.

Figure 3.4-2 illustrates the use of either the stretched film or the rigid panel version to make up a complete concentrator element consisting of two whole panels and two sets of hinged half-panels. The corners of the whole panels are suspended from the CEM cables by means of a slide wire mechanism, leaving the hinged panels and the hinged radiator free to fold compactly for stowage. Table 3.4-1 lists the thicknesses of the concentrator parts in stowed conditions.

3.4.2 SOLAR PANEL AND HARNESS

It is a design requirement that the solar array be compatible with both silicon (Si) and gallium arsenide (GaAs) solar cells. Because of detailed differences in available cell sizes and in cell characteristics, solar panel designs for the two-cell types will be different in some respects. Every effort has been made to minimize these differences without seriously compromising the capabilities of either. Table 3.4-2 lists the characteristics of the two panels. Differences in the areal density between the two-cell types is compensated for by reducing the thickness of the radiator/substrate for the GaAs panel.

ORIGINAL PAGE IS
OF POOR QUALITY

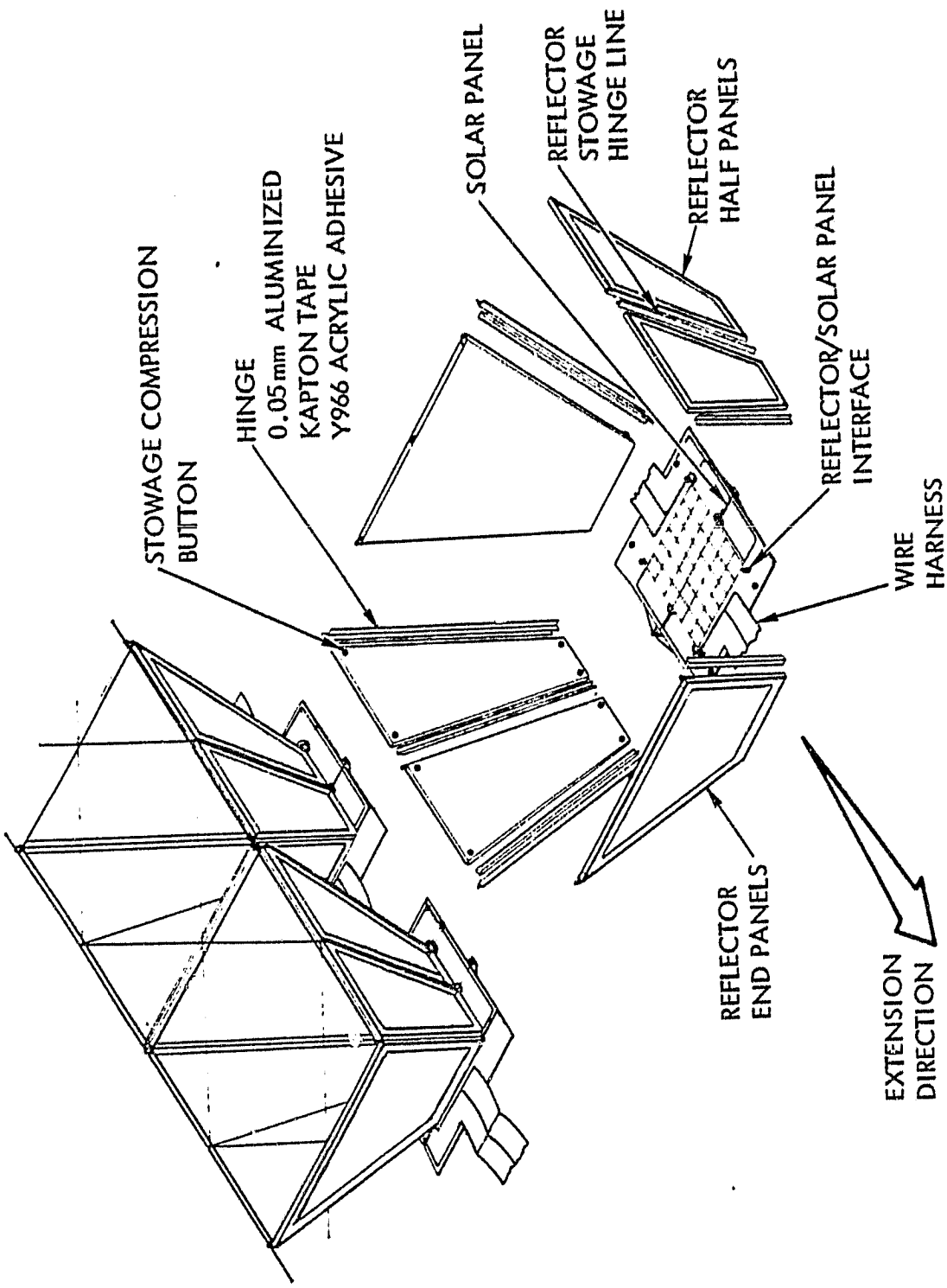

Figure 3.4-2. Concentrator Element (Stretched Film or Rigid Frame)

Table 3.4-1. Stack Breakdown

Part	Thickness	Quantity	Total
Reflector end panels	3.25	2	6.5
Reflector half panels	3.25	2	6.5
Solar half panels*	1.0	2	2.0
Miscellaneous	0.83	6	5.0
Total			20 mm
Note: All dimensions are in mm			
*Si valve shown, GaAs panels are 0.6mm to provide comparable concentrator element weight.			

Table 3.4-2. Solar Panel Characteristics

Solar Cell Characteristics	Si	GaAs
Conversion efficiency,	14	18
Solar absorptance	0.70	0.75
Low CR optimized	Yes	Yes
BSR	Yes	N/A
BSF	No	N/A
Thickness (mm)	0.25	0.30
Surface dimensions (mm)	50x50	20x20
Cover type/thickness (mm)	Fused silica/0.2	Fused silica/0.2
Substrate/Radiator Characteristics		
Thickness (mm)	0.6	0.5
A_R/A_p	2.0	2.0
Solar absorptance	0.22	0.22
Emissivity	0.85	0.85

Figure 3.4-3 illustrates the mechanical design of the radiator/substrate which is common to both cell types. The radiator is the area extending beyond the solar panel and has twice the area of the substrate. It folds using over-center hinges so that the cell covered surfaces do not touch in the stowed condition (15mm gap). The half-panels are identical parts having turned up flanges on the sides and thermoplastic shoulder bolts holding the panels together. Around both shoulder bolts are torsion springs that cause the panels to open. Stamped into the radiator panel is a small flange that fits over the lug on the base of reflector panel. A spring clip then fits over the assembly to lock the flange over the lug. On the other end of the solar panel/reflector panel hinge line, a small right angle bracket fits on the panel over the reflector panel lug and is riveted to the solar panel. The lug is retained in the bracket by a cotter pin.

CELL TYPE	PANEL SIZE			CELL SIZE
	A	B	C	
Si	353	353	.6	50 x 50
GaAs	353	353	.5	20 x 20

RADIATOR DESIGN DRIVERS

- THERMAL CONDUCTIVITY
- INTERCHANGEABLE PANELS
- HINGED INTERFACE
- COMPACT PACKAGING
- CELL PROTECTION
- SIMPLE HARNESS INTERFACE
- CONSISTENT MASS FOR Si OR GaAs

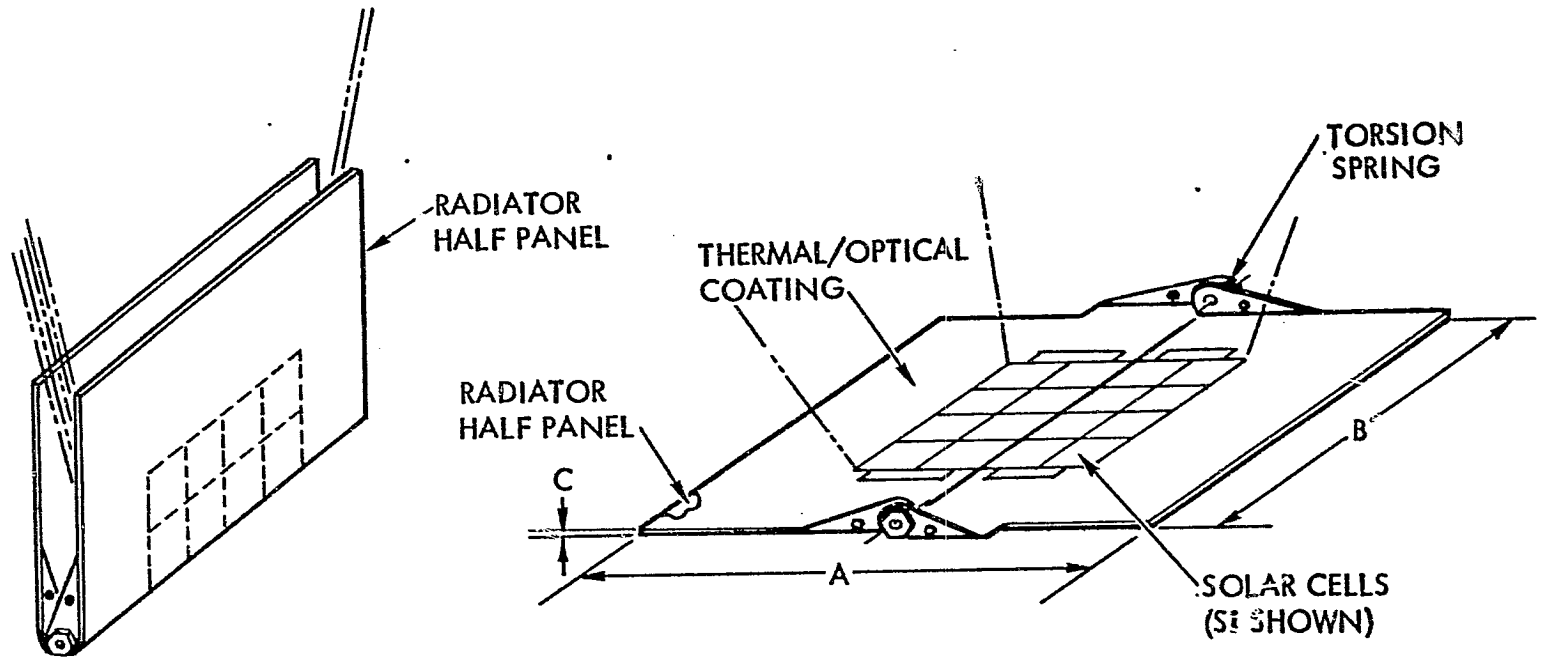

ALL DIMENSIONS ARE IN MILLIMETERS, WIRE HARNESS OMITTED FOR CLARITY

Figure 3.4-3. Solar Panel Design

ORIGINAL PAGE IS OF POOR QUALITY

The silicon design radiator panels are made from 6061-T6 aluminum 0.64 mm (0.5 mm for GaAs) thick. A white thermal control coating is then applied. A layer of insulation is then bonded to the panel. The insulator is 0.025 mm Kapton film bonded with a low viscosity high temperature epoxy. The solar cells are then installed and the wire harness attached to the cells and fully bonded to the radiator panels.

3.4.2.1 Electrical Design for Silicon Cells

The electrical design of the silicon solar panel is comprised of two basic tasks, the design of the concentrator element and the design of the solar array module and the electrical strings of which it is comprised. This distinction is made because of the vastly different and largely independent set of design requirements which affect the two levels of the array design.

The solar panel design is driven by the available cell sizes, the inherent physical properties of the devices, and the environment in which the device must operate.

For silicon solar cells there are two basic limitations on device size. The first limit is the Czochralski crystal growth technique which presently limits boule diameter to approximately 102 mm (4 in.). As a result, cell size is restricted to approximately a 59 mm x 59 mm maximum. This large cell fabrication technology for planar array application is being pursued under the auspices of the NASA Power Extension Package (PEP) program by Applied Solar Energy Corporation (ASEC). ASEC is the silicon solar panel subcontractor for this project. This limitation was resolved as follows:

The baseline concentrator design requires the solar panel to be approximately 200 mm x 200 mm when deployed. Each half-panel is then 100 mm x 200 mm. As each half-panel within the element is isolated from its mate, the array of solar cells must fit within this area. Obviously, a 59 mm x 59 mm cell would not be appropriate for this panel size due to a resultantly poor packing factor. If the boules were grown in a nominal 70 mm (3 in.) diameter, the cells could be made 50 mm x 50 mm. This device would fit the available envelope and still embody the large-area/low-cost production concept. ASEC has made a preliminary assessment of the large device and has suggested the use of smaller area devices such as 25 mm x 50 mm. This suggestion is only preliminary and the cell size selection will be investigated further.

The second limitation is the effective series resistance of a device which is to be used for concentrator application. Preliminary assessments of the applicability of large-area devices to concentrators do not appear favorable. The high-current density and long transmission distances in the n-contact grids of a concentrating solar cell appear to result in prohibitively high series resistance losses. This is usually overcome by changing the grid pattern and using more than one n-bar contact. The revised grid pattern is not a problem. However, the use of more than one n-bar contact results in a packing factor penalty which would negate the benefit of the multiple n-bars.

The use of multiple wraparound n-bar contacts would eliminate the series resistance and packing factor losses in a large-area device. This solution, however, is not without limitations. These devices have not economically been made in production quantities. The solar cell electrical interconnects in a wraparound panel design become a constraining factor. The wraparound contacts dictate the use of in-plane stress relief within the interconnect. The in-plane stress relief interconnect design is impeded by having to be immersed in a material which could reduce the effective stress-relieving ability of the interconnect design. The thermal conduction requirements in a concentrating solar array are such that the rear cell surface must be totally immersed in the void-free adhesive which holds the cells to the radiators. Due to the requirement to keep the cell-substrate bond line thin, the interconnect is trapped in a narrow region. The in-plane interconnect material is prevented from deforming out of plane to any degree, and material fatigue is enhanced. The interconnect design for a ten-year LEO mission must survive a difficult environment (typically, 55,000 temperature cycles from -100°C to +125°C). Many planar solar arrays have been designed for similar missions, including the high expansion aluminum substrate characteristics. The stringent requirements seem to favor an out-of-plane stress relief interconnect design.

The selected baseline design is a conventional front/back contact cell, a silver mesh interconnect with an out-of-plane stress relief loop bonded to an insulated aluminum radiator with a silicone elastometer adhesive. These aspects of the design embody no new technologies. The low-CR optimized cell and interconnect have to be more fully developed and qualified for space application.

The technology needed to use a welding process for solar array manufacturing is new. A welding process was selected for interconnecting the cells within the array and for attaching the wire harness to the array. This selection was based upon two criteria, the relatively high operating temperature of the solar panel and the long, low earth on-orbit life for the array. These two factors, when applied to the relatively well known fatigue life characteristics of soldered interconnections, raise serious questions about the ability of a soldered system to survive the mission environment. The welding interconnection process is not well understood, and represents a technology development item. The proponents of this process claim it can meet both the high operating temperature and long cycle life over wide temperature extremes required for this solar array application. The potential capabilities of this process have yet to be realized in a solar array manufacturing environment.

Once the cell size has been selected and an interconnection and fabrication scheme have been selected, the electrical characteristics of the concentrator element assembly have been fixed. The technique used to determine these characteristics is covered in Section 4.5. The electrical characteristics of a half-panel within an operating concentrator element are:

- Maximum power (MP) 9.04 watts
- Voltage at MP 1.40 volts
- Current at MP 6.50 amperes

These half-panels must be series interconnected in order to develop a reasonable voltage for transmission of the large amounts of electrical power which this array produces. The selection of a transmission voltage should be based upon a user spacecraft system study and not on the solar array characteristics alone. In this case, where no user spacecraft was defined, engineering judgment dictated a bus voltage to be in the range of 150 to 300 V. In the absence of any more specific design criteria, a further judgment was made. All concentrator elements within a deployed row are interconnected in series (i.e., one deployed row of 66 concentrators equals one electrical string).

The design of an electrical string is driven by two considerations: (1) minimize the length of the conduction path, and (2) minimize the generated magnetic fields caused by "current loops" in the electrical network.

For the baseline silicon design with 66 concentrator elements (132 half-panels), the output characteristics for an operating electrical string are:

- Maximum power (MP) = 1200 watts
- Voltage at MP = 185 volts
- Current at MP = 6.50 amperes

(Note: These numbers do not include harness and diode losses, which will be discussed later.) There are also 66 electrical strings per solar array module (33 rows deployed per side).

Every half-panel is protected from reverse bias damage by the use of peripheral current bypass (shunt) diodes. These are bonded to the top surface of the radiator outside the confines of the reflectors. The need for bypass diodes is established by the relatively high bus voltage dictated by any high-power solar array and the electrical power subsystem in general. The effects of shadowing, associated with deployable solar arrays when coupled with these relatively high voltages, could pose a serious threat to the solar array. An analysis has been performed to determine the approximate reverse bias potentials which could occur in the baseline design. In the absence of a specific mission scenario, several assumptions as to operation of the solar array within an electrical power subsystem and a given orbital environment must be made. Typical of these is whether the array is series or shunt regulated, and what the operational temperature of the partially deployed array would be. The results of this analysis show reverse bias potentials on the order of -20 V can be expected across a non-illuminated half-panel. (Four-series cells translate into -5 V per cell.) This potential is not considered particularly dangerous with respect to known space-type solar cells. There are uncertainties in the preliminary analysis which, when coupled with relatively unknown reverse bias characteristics of the baseline large-area, low-CR optimized silicon solar cells, could reverse this assessment. It is intended that some preliminary data be collected as to the reverse bias characteristics during the concentrator testing. An assessment of this situation determined that bypass diode protection is a viable approach to eliminating a possible problem with the baseline design. This is supported by the ease with which this design feature can be incorporated into the baseline design.

If later cost and performance analyses result in a reversal of this assessment, the removal of the bypass diodes will not cause any major impact on the design. The cost impact of this design feature on the total array cost is relatively small in any case.

The individual electrical strings are isolated from the main power bus by isolation diodes. These diodes perform two functions:

- They prevent an electrical string whose open-circuit voltage is less than the bus voltage from becoming a net electrical power consumer.
- They can prevent certain short-circuit failure modes of the wire harness from being a catastrophic failures.

A series/parallel redundant configuration was chosen for the baseline design. This configuration is required to meet the "no single-point failures ..." criterion which has been adopted in this array design. Again, any specific failure mode analysis to demonstrate the performance of the isolation diodes requires certain assumptions as to solar array operation within the user spacecraft electrical power subsystem to be made. It can be shown that under certain circumstances anything less than series/parallel redundant diodes will not allow the solar array to pass the "no single-point failure" criterion. This assessment is not unique to this solar array design; it has validity in a large number of, if not all, applications. The physical location of the diodes with respect to the overall layout has not yet been determined. A failure mode/diode location analysis is planned, and a location will be selected.

As is the case with most protective devices, certain design penalties are incurred. The penalties which are imposed on the design are small when compared to the benefits of the diode configuration. There is a distribution system efficiency penalty with the efficiency of the diode package at approximately 0.99 for a 185 V bus. Another penalty to the design is cost. The total cost of the diodes (both isolation and bypass) is small when compared to the total solar array module cost. Diode unit costs are relatively low when compared to solar cell unit costs, and these are relatively few diodes.

If the results of the failure mode analysis results in the diodes being collocated, we can explore the possibility of assembling all four diodes in a single package. This package reduces the number of piece-parts which must be assembled by the array manufacturer, and reduces by a factor of four the number of piece-parts subjected to burn-in and test by the diode manufacturer. This burn-in and test is a major cost and schedule driver in space-qualified diodes. The repackaging would allow the opportunity for the diode manufacturing engineer and the array manufacturer to collaborate on a package design which is better optimized thermally, etc., for solar arrays than the axial lead designs which are so often used. Diode packaging techniques which allow very speedy integration to a flat cable harness and result in low overall assembly costs can be explored. The cost of testing the diodes after installation in the array, in such a large array, may equal or exceed the cost of purchasing and installing the parts. There are several techniques for speeding this testing which have been implemented on flight programs; they are unique and serve to reduce testing costs.

3.4.2.2 Electrical Design for Gallium Arsenide (GaAs) Cells

The general design drivers for the GaAs half-panels are identical to those for the silicon half-panels. It is the detailed implementation which differs. The cell size, bypass diode placement, panel output characteristics, solar cell interconnect selection, etc., are all likely to be different from the silicon half-panel design. The contractual requirement for a design which is consistent with both silicon and GaAs solar cells has, however, been achieved. The consistency lies in the concentrator element physical characteristics and in compatibility of either design with a single structural/mechanical design. The electrical design is comprised of two basis tasks—that of concentrator element design, and design of the solar array module.

The GaAs solar panel design, like the silicon design, is driven by available cell sizes. For GaAs solar cells there are presently only two cell sizes from which to choose: 20 mm × 20 mm, and 20 mm × 40 mm. This may change as GaAs cell manufacturing technology is developed. The inherent brittleness of the GaAs cell substrate will present a considerable challenge, and may prove to be a limiting factor, in the maximum area per device which is economically

feasible. It is not clear, at this time, that large-area devices are the best approach to lowest cost per watt with this substrate/device type. Ultimately, the selection of a cell size will be driven by the cost factor, and the concentrator configuration will be designed to utilize the lowest-cost device.

The selection between the two available cell sizes was driven by the dimensions of the concentrator element which require the cells to be located within a 100 mm × 200 mm envelope on the half-panel. This requires an integral number of cells to fit within the 100 mm envelope dimension. This simple consideration, plus restraints on cell/interconnect orientation due to the concentrator configuration, tends to favor the 20 mm x 20 mm over the 20 mm × 40 mm cell size. The only development contract currently under way to produce GaAs devices (USAF low cost GaAs solar cell development) has adopted this 20 mm × 20 mm cell size as a program goal. The results of this development will not be available until mid-1984. The development of a larger area device would likely proceed, but could not be cost-competitive until development was complete. Our contractual requirement is for end of 1984 technology readiness. This is consistent with existing development contracts for a 20 mm × 20 mm cell. No such contracts exist for a larger cell, and including this cell in a baseline design would require technology development at a rate beyond existing planning.

There are fifty 20 mm × 20 mm solar cells on each half-panel. The illumination distribution (see Section 4.4) suggested a high degree of electrical paralleling within the half-panel to minimize output mismatch losses. The selected configuration is to electrically connect five cells in parallel ($N_p = 5$) and to connect ten of these cell assemblies in series ($N_S = 10$). This design should perform as though it were comprised of ten extremely large area (2000 mm^2) GaAs devices in series.

To protect the devices from the space radiation environment, a fused silica coverslide is applied to the cell top surface. The selection of fused silica was based upon several considerations; among these are availability, cost, and resistance to radiation degradation. The adhesive used to bond these covers could be either DC93-500 or (if proven to be less expensive) fluorinated ethylene-propylene (FEP). The FEP option would also eliminate the relatively expensive ultra violet filter which must be applied to the fused silica to protect the DC93-500. It may also be possible to use

a matte front surface coverglass to eliminate the magnesium fluoride (MgF_2) anti-reflection coating. An additional array fabrication step is included to further protect the cells from particulate radiation. The area surrounding the ohmic contact will be coated, after array assembly, to increase the effective shielding density over this surface.

The array on each half-panel must be protected from reverse-bias effects. The technique adopted in the baseline GaAs design is the same as that used in the silicon design—peripheral bypass diodes. The reverse-bias characteristics of the GaAs devices and the response of the baseline design in the operational scenario determine the placement of the diode shunts within the electrical string. In the absence of comprehensive, statistically based test data on mass-produced GaAs solar cells, the selection of this tap point is somewhat arbitrary. This is complicated by lack of in-depth operational scenario for the solar array. To help alleviate the former problem, Rockwell will perform some reverse-bias testing on GaAs devices in conjunction with hardware testing (see Section 5.3). These test data will establish a performance benchmark which will be used in updating the baseline design. The operational characteristics will become better defined as further work is performed in support of this contract. The assumptions made to date, with regard to cell and operational performance, have driven the design to an electrical tap with a shunt diode at every two series cells. This is a conservative approach which may be modified as information becomes available. Isolation diode protection is identical to the silicon string design, i.e., series/parallel redundant.

The interconnection of these half-panels into an electrical string is handled in the same way as in the silicon design. The difference lies in the number of concentrator elements needed to develop bus voltage. The higher per cell output voltage and the greater number of series cells per half-panel dictate fewer series concentrators per electrical string. Each deployed row will contain four strings. In this configuration, the output characteristics of an electrical string would then be:

- Output power = 662 watts
- Current = 2.39 amperes
- Voltage = 277 volts

The assembly of the cells into an array will utilize a welding process. This assembly technique is subject to all the restrictions and reservations described in the discussion of the silicon design.

The interconnect design will be the out-of-plane stress relief type. This was selected because of the front/back contact configuration which will most likely be used on the early production GaAs cells. The cell will be bonded to the substrate/radiator using a silicone elastomer adhesive. A relatively low-cost system could be a mixture of RTV-566 and RTV-567. Bond-line thickness control is critical to regulate mass properties, to ensure adequate curing of the adhesive, and to maintain good thermal conduction between the cell and the radiator.

Wire harness design is similar to the silicon array. The current density is determined per the technique discussed in Section 4.5.3. Because there are four strings per deployed row of concentrators, there are additional conductors necessary to deliver power from the electrical strings which terminate away from the root of the extended row. This is unlike the silicon design which has only one string per deployed row.

The coverglass material selected for the GaAs devices is fused silica. The adhesive is DC93-500. The FEP/frosted, fused silica covering system may not be applicable to GaAs devices due to the extreme temperature and pressure cycle needed to reflow the adhesive. This process may, especially if a curved-platen technique were to be needed, cause excessive breakage of the brittle GaAs cell. The developmental emphasis should remain upon low-cost production of cells and substrates, not on a potentially lower-cost covering process. The GaAs upper ohmic contact will—like the silicon design—be coated to protect against low energy protons and other particulate radiation.

3.4.2.3 Harness Design

The interconnection of the individual concentrator element assemblies into an electrical string is accomplished through the use of flat, flexible printed-circuit wire harnesses. This type of wire harness offers several distinct advantages over a conventional round wire-bundle harness. Production of this type of harness is highly automated, resulting in relatively low unit cost. The harness is flat and thin, offering unparalleled packaging options

when space is at a premium, as in the fully stowed configuration. The thinness results in an extremely flexible harness which is necessary for the complete unfolding of the harness during deployment of the concentrators from the densely stowed condition with a minimum of stress. Wire routing can be as complex as necessary without the production problems associated with round wire conductors because the wiring layout is fixed by artwork. This same artwork, when coupled with a photo resist/etching process, accounts for the ease and consistency with which even complicated routings are reproduced.

Multi-layer printed circuitry is common, but at the expense of thinness and flexibility. Two laminated harness layers are used within the deployed rows. This is used in an area such that no storage (thinness) or bending (flexibility) penalties are incurred. The main power bus, which runs centrally through the housing, builds up to twelve separate layers as additional container housing are picked up before entering the user attach fittings on the last housing. This harness is ten separate layers thick where it passes over the last rotating hinge line. The layers are not laminated together so as to maintain as flexible a harness as possible.

The harness is sized so as to maintain an optimum current density in all sections under nominal conditions. This optimization is described in Section 4.5.3. The optimum current density is maintained by varying the cross-sectional area of the conductor to accommodate the current in the circuit branch. For printed circuitry, this is achieved by varying the width of the conductors which are uniform in thickness, or by using multiple parallel layers of conductors, or both.

The selected materials are copper conductors, laminated between layers of Kapton by a modified acrylic adhesive. The copper used within the electrical strings is 0.14 mm thick, with 0.025 mm adhesive and insulator layers. The copper used within the housing is 0.28 mm thick with similar adhesives and insulators. Localized plating of the copper may be needed to enhance weldability.

4.0 ARRAY TRADE STUDIES AND PERFORMANCE ANALYSIS

Section 3 describes in detail the features of the GaAs and silicon versions of the baseline design. This section gives an account of the trade studies and parametric analytical studies from which the design was derived.

The overall credibility of the final array design which results from this program will rest upon design judgement, analytical predictions and test results. Table 4.0-1 lists the important design issues which have been identified and categorizes them in terms of method of verification. Some issues, such as those relating to mechanisms, mechanical supports and connectors, are not readily solved by analysis alone, yet embody familiar principles and techniques. For these issues design judgement is appropriate. There are a number of issues, particularly those relating to structural, optical, thermal and electrical performance, where good quantitative prediction methods exist. Here, parametric analysis is most effective in establishing component design features. Finally there are other issues, some critical to the design, which are sufficiently novel that they require experimental demonstration of their feasibility.

4.1 TRADE STUDIES

The baseline design rests upon the results of a large number of trade studies based upon structural, electrical, optical and thermal analyses. These trade studies are summarized in Table 4.1-1. The structural trades deal with geometrical constraints as well as with the stresses and deformations associated with thermal gradients and static and dynamic loads. Electrical trades were carried out at the cell, panel and module level in order to optimize output with respect to cost and weight. Much of the optical analysis performed so far has been directed toward predicting sensitivity to pointing errors. However, it also served to select optimum thermo-optical reflector characteristics. Thermal analysis, too, has been used primarily to assess output performance of the baseline design but also served to optimize radiator size and thickness and to select reflector back-surface coatings.

In the following sections details of the individual trades and analyses are presented in more detail.

Table 4.0-1. Concept Verification Major Design Issues

ITEM NO.	DESIGN ISSUES	DESIGN JUDGMENT	ANALYSIS	TESTING
1	CONCENTRATOR PACKAGES WITHIN PRESCRIBED ENVELOPE		X	X
2	SOLAR CELL, RADIATOR SUITABILITY FOR LAUNCH		X	
3	CONTAINERS AND TIE SYSTEM SUITABILITY FOR LAUNCH	X	X	
4	RELEASE OF SUPPORT FITTINGS (IF NECESSARY)	X		
5	REMOVAL FROM SHUTTLE/POSITION FOR DEPLOYMENT	X		
6	DEPLOYMENT OF CONTAINERS AND LOCKING OF JOINTS	X		
7	RELEASE OF END CAPS FROM MODULAR TIES	X		
8	MAST EXTENSION	EXISTING DESIGN		
9	EXTENSION OF CONCENTRATORS AND SOLAR PANELS	X		X
10	EXTENSION OF CABLES AND POWER TRANSMISSION LINES	X		X
11	FINAL LOCKING OF ARRAY	X		
12	DEVELOPMENT/MAINTENANCE OF REQUIRED CABLE TENSION	X	X	
13	REFLECTOR SPECULAR QUALITY TO REQUIREMENT			X
14	REFLECTOR FLATNESS QUALITY TO REQUIREMENT		X	X
15	REFLECTOR ARRAY DIMENSIONAL QUALITY	X		X
16	REFLECTOR POINTING ACCURACY TO REQUIREMENT		X	
17	SOLAR ARRAY MODULE CONFIGURATION GENERAL STABILITY		X	
18	SOLAR ARRAY MODULE CONFIGURATION USER SPACECRAFT LOAD SUITABILITY		X	
19	SOLAR CELL/RADIATOR PERFORMANCE		X	X
20	TOTAL CONCEPT WEIGHT VERIFICATION		X	X

ORIGINAL PAGE IS OF POOR QUALITY

Table 4.1-1. Summary of Trade Studies

TRADE ISSUE	BASELINE DESIGN CHOICE	RATIONALE
STRUCTURAL		
MODULE STOWED DIMENSIONS	CUBE, 3.24m PER SIDE	ORIENTATION-GEOMETRICALLY INSENSITIVE, ONE-QUARTER BAY LENGTH
STACKING PARAMETER, N	N = 6	EFFICIENT, LOW MASS RADIATOR; ADEQUATE MAST DIAMETER
SINGLE-AXIS VS DUAL-AXIS DEPLOYMENT	SINGLE AXIS	EFFICIENT USE OF CANISTER STOWAGE, LESS COMPLEX, SIMPLER USER VEHICLE INTERFACE
SHEAR-PANEL VS DRAG TRUSS HOUSING DESIGN	DRAG TRUSS	LIGHTER WEIGHT, LOW COST
MAST DESIGN	CANISTER DEPLOYED HYBRID (SINGLE- AND DOUBLE-LACED) CONTINUOUS LONGERON	STRENGTH TO STOWAGE FOR CANISTER ENVELOPE
ELECTRICAL		
SILICON CELL SIZE	50 mm X 50 mm X 0.25 mm	LARGEST AVAILABLE SIZE FITTING PANEL AREA WITH GOOD PACKING DENSITY
GALLIUM ARSENIDE CELL SIZE	20 mm X 20 mm X 0.30 mm	SAME AS ABOVE
INTERCONNECT DESIGN	SILVER MESH WELDED, OUT-OF-PLANE STRESS RELIEF LOOP	LARGE NUMBER OF THERMAL CYCLES
STRING DESIGN	PARALLEL CELLS IN EACH HALF-PANEL GaAs -- FOUR ELECTRICAL STRINGS PER ROW; Si -- ONE ELECTRICAL STRING PER ROW	MINIMIZES ILLUMINATION MISMATCH LOSSES MODERATE MODULE VOLTAGE
HARNESS DESIGN	FLAT FLEXIBLE CABLE, COUNTER CURRENT HARNESS	EXCELLENT PACKAGING, NECESSARY FLEXIBILITY, MINIMIZES EMI
OPTICAL		
TREATMENT OF REFLECTOR COVERS	FULL SPECULAR REFLECTIVITY	HIGHEST ELECTRICAL OUTPUT; ACCEPTABLE REFLECTOR TEMPERATURES
THERMAL		
RADIATOR SIZE & THICKNESS	RADIATOR AREA TWICE SOLAR PANEL; 0.5/0.6 mm (GaAs/Si) Al SHEET	MINIMIZES RADIATOR SPECIFIC WEIGHT -- MAINTAINS ACCEPTABLE Si CELL TEMP
REFLECTOR BACK SURFACE TREATMENT	HIGH DIFFUSE REFLECTIVITY	IMPROVED RADIATOR HEAT REJECTION (TOP SIDE)

ORIGINAL PAGE IS
OF POOR QUALITY

4.2 STRUCTURAL ANALYSIS

The major portion of the analysis was concerned with on-orbit structural requirements. The overall system must have general stability, at least an order of magnitude frequency separation with possible excitation frequencies, and sustain dynamic loads induced by spacecraft maneuvers. A NASTRAN mathematical model was developed to evaluate the overall stability and the parameters that would affect the stability. The results indicated that cable tensions would have to increase the 137 N per cable to create mast buckling. The same model was utilized to determine the overall fundamental frequency for both single and dual modules. The first mode of a single module is 0.027 Hz which is 71 times the LEO gravity gradient disturbance frequency.

The first mode frequency of a dual module is 0.01 Hz which is 26 times the LEO gravity gradient disturbance frequency. The model was utilized to determine transient responses created by a stationkeeping acceleration.

Stationkeeping maneuvers are initiated by firing thrusters to increase a systems orbital velocity. The increased velocity (ΔV) creates an apogee 180° from the point of thrusting.

Firing the thruster a second time while at the apogee produces a circular orbit of increased altitude. The increased altitude (ΔH) is a function of initial altitude, thrust magnitude, thrust duration, and system mass.

Structurally, the stationkeeping acceleration (V/time) is the solar arrays most critical design parameter, and throughout the preliminary design and analysis a 0.01 g acceleration criteria was utilized.

After developing a baseline configuration, a hypothetical system configuration was mathematically modeled to determine system response to stationkeeping maneuvers (see Figure 4.2-1).

Feasible "Large Space Structure" boosters could vary from 110 N (25 lb) to 450 N (100 lb), thus an upper limit system thrusting (P_{thr}) would be four 450 N boosters or 1800 N total.

Figure 4.2-2 represents maximum acceleration levels on various system configurations (masses) as a function of thrust magnitudes. Mast extension capability, ultimately the system performance, is determined by maximum

ORIGINAL PAGE IS
OF POOR QUALITY

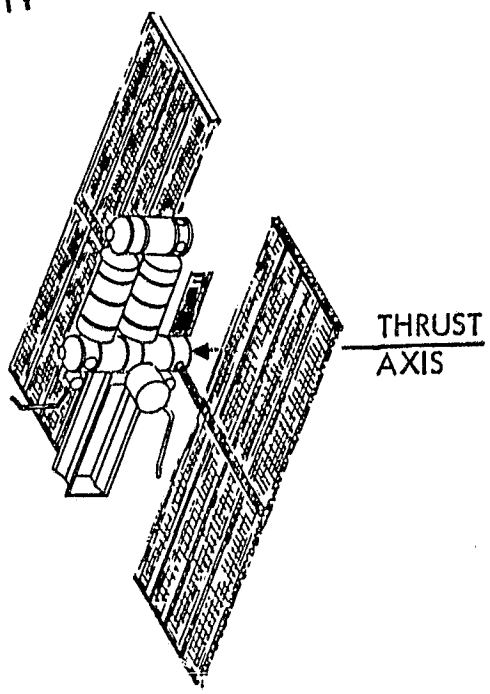

Figure 4.2-1. User Spacecraft and Mathematical Model

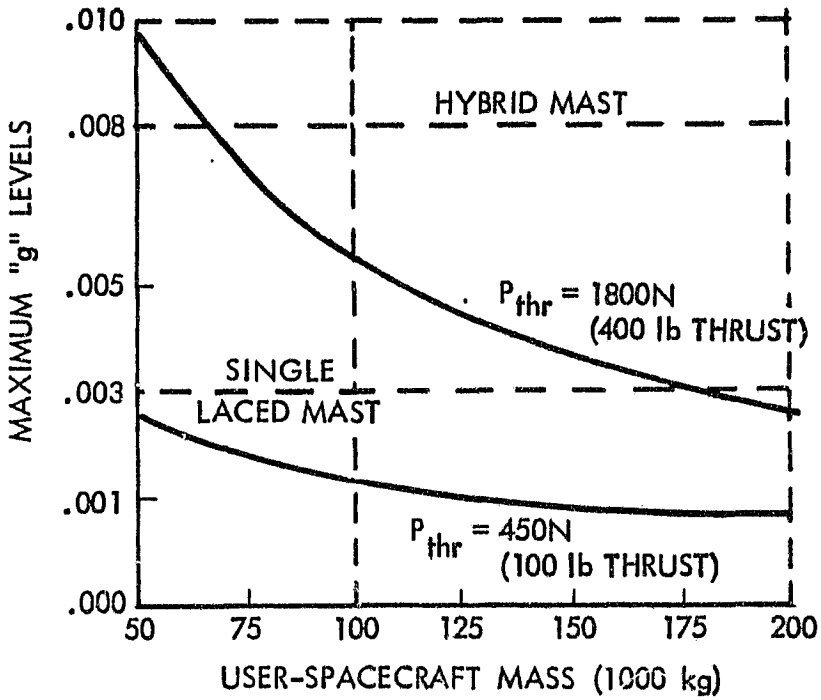

Figure 4.2-2. Stationkeeping Accelerations

applied bending moment. The bending moment is a function of the stationkeeping acceleration applied to the user spacecraft and the systems maximum response. The results on Figure 4.2-2 are the maximum systems responses at the container housing.

The choice of the structural baseline design was made after several trades in each subsystem area. The housing structure started as a set of integrally machined panels; then, the structural design changed to shear panels and extrusions; but, because of the low structural loading and high weight, the truss structure was considered. A trade was run between a tension cable/compression member-type and a standard drag truss. The drag truss structure was chosen over the others because of the simple manufacturing, relatively few different types of parts, inexpensive tooling and light weight. The mast/canister trades also enveloped several trades.

The overall dimensions of the deployed and extended module represent the simultaneous satisfaction of several extension length criteria:

- *Mast Stowage Limit*—The maximum extended length of continuous longeron canister deployed single/double-laced mast 0.44 m in diameter which can be stowed in the 1.62 m canisters.
- *Concentrator Stowage Limit*—The maximum extended length (0.5 m per concentrator) which can be spanned by the number of folded concentrators (20 mm per concentrator) stowable in the container housings.
- *Mast Stress Limit*—The mast length capable of carrying the 0.008 g station-keeping load with 1.5 safety factor.

Table 4.2-1 illustrates these limit lengths and the corresponding number of extended concentrators which could be accommodated.

The concept of making the module restowable also called for the container modifications. The solar panel and reflector panel tripwire mechanisms have been presented but are not necessary to the concept if it is determined that the module will not require retraction in orbit (i.e., orbit transfer or return to earth at end-of-life).

Table 4.2-1. Comparison of Module Extension Limits

Limit Criteria	Extension Length	Equivalent No. of Concentrators
Mast stowage	35	70
Concentrator stowage	40	80
Mass stress	32.4	66

4.2.1 SIZING STRUCTURAL MEMBERS

The structure components were designed to withstand dual modules connected end-to-end and a targeted stationkeeping acceleration range of 0.001 to 0.01 g. A 1.5 ultimate load factor was utilized in sizing all structural members.

4.2.1.1 Canister Deployed Continuous Longeron Astro Mast

Mast structural capability depends upon internal design (single or double laced) mast diameter and the applied structural loads. The primary load factor is stationkeeping acceleration. In addition, the cables supporting the concentrator elements exert a tension between container and end cap which compressed the mast. The reacting mass includes the concentrator elements, the containers, and caps, and the masts themselves.

Figure 4.2-3 shows various Astro mast deployment capabilities as a function of mast radii and stationkeeping accelerations. The figure also shows the required canister lengths associated with the radius and deployed lengths. The maximum canister envelope is approximately 0.49 m which limits the maximum mast radius to 0.44 m.

The structural capability of a 0.44 m diameter mast extended 32.6 (root length) is 0.003 g acceleration. Increasing the stationkeeping acceleration above 0.003 g requires a stronger single/double laced mast combination.

Figure 4.2-4 represents the structural capabilities of a single/double laced mast (hybrid mast) as a function radius, accelerations and batten stiffness (EI_b/EI_e).

Double lacing requires more stowage area, thus to maintain a 1.62 canister height envelope requires retangular battens to increase packing efficiency. Utilizing a 0.44 m hybrid mast with batten width to thickness ratio (W/t) of 2.5 allows 0.008 g stationkeeping maneuver.

ORIGINAL PAGE IS
OF POOR QUALITY

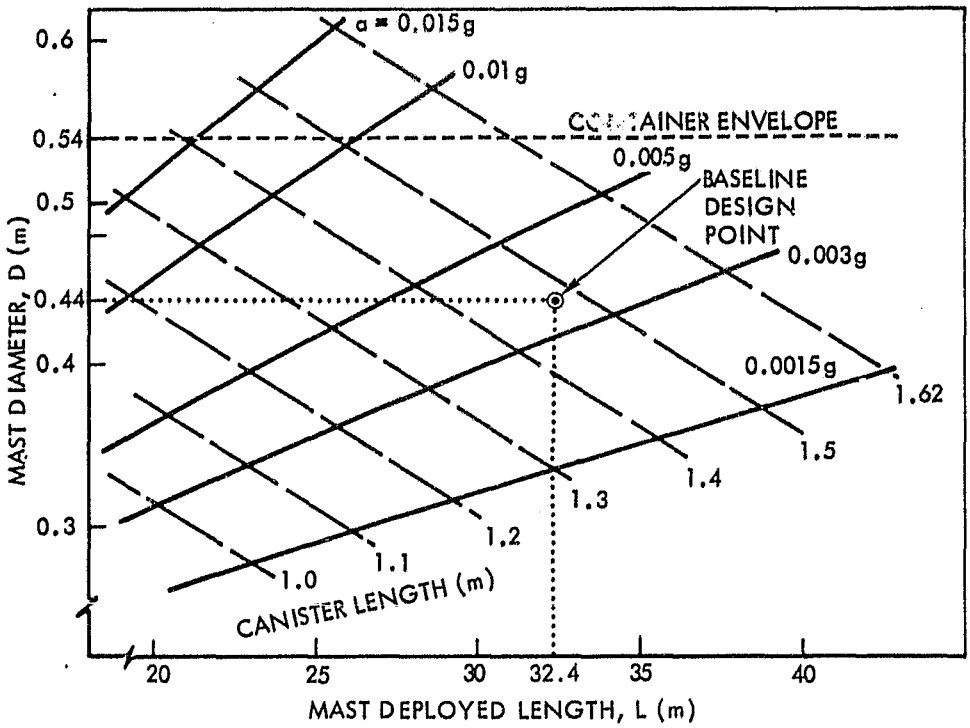

Figure 4.2-3. Mast Structural Capability (Single Laced)

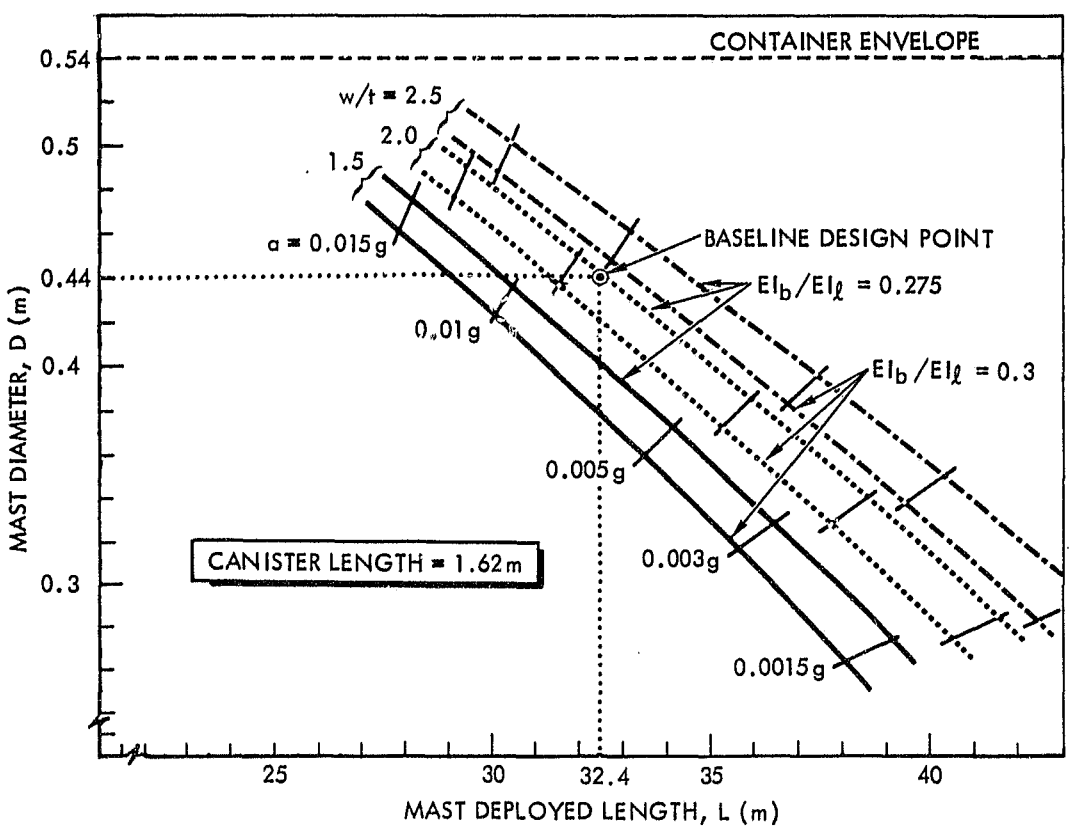

Figure 4.2-4. Mast Structural Capability (Hybrid)

4.2.1.2 Container/Housing and End-Caps

Structural strength in the direction normal to the mast axes is provided by the interconnected container housings (at the canister end) and by interconnected end caps to which the extending ends of the mast are attached. Early designs used shear panels of solid aluminum sheet for both housing and end caps. However, minimum gauge requirements imposed by reasonable-cost manufacturing procedures resulted in high weights for these components. Considerably lighter structures were achieved by the use of diagonally braced strusses as shown in Figure 4.2-5.

Figures 4.2-5 and 4.2-6 provide weight breakdowns, structural capabilities and applied loads for housing and end-cap respectively.

4.2.1.3 Concentrator Support Cables and Tensioners

The individual concentrator elements, each approximately 0.70 kg are supported on cables suspended between the end-caps and the negator mechanisms located in the container/housing. A second tensioning mechanism is applied to the concentrator elements themselves to prevent translations during an in-phase stationkeeping maneuver. The concentrator tensioners will also ensure reflector hinge flatness. The present design value of 20 N per cable and 7 N per concentrator row is more than sufficient to maintain planar integrity during normal operation. During a stationkeeping maneuver, however, there is a translation and rotation of the concentrator elements.

The concentrator oscillations initiated by the maneuver will "settle" as a function of cable tension (frequency) and system damping. Figure 4.2-7 represents the settling time and approximate power output as a function of cable tension. The 1.5% damping value utilized in this analysis is based on vibrational tests conducted by Astro Research. Multi-jointed structures similar in nature to continuous longer mast has damping values ranging from 1.1 to 2.0%.

4.2.1.4 Deployment Actuators

The deploying array will be supported at mid-span, allowing translation and rotations in both directions which eliminates inertial loads being transferred to the RMS [Figure 4.2-8(a)]. The deployment actuators were sized utilizing Schaeffer Magnetics specifications. A Type 2 actuator produces

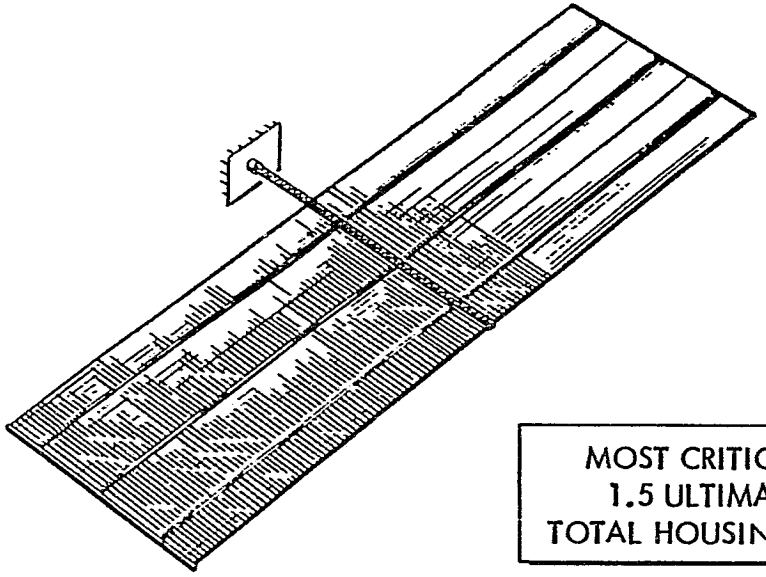

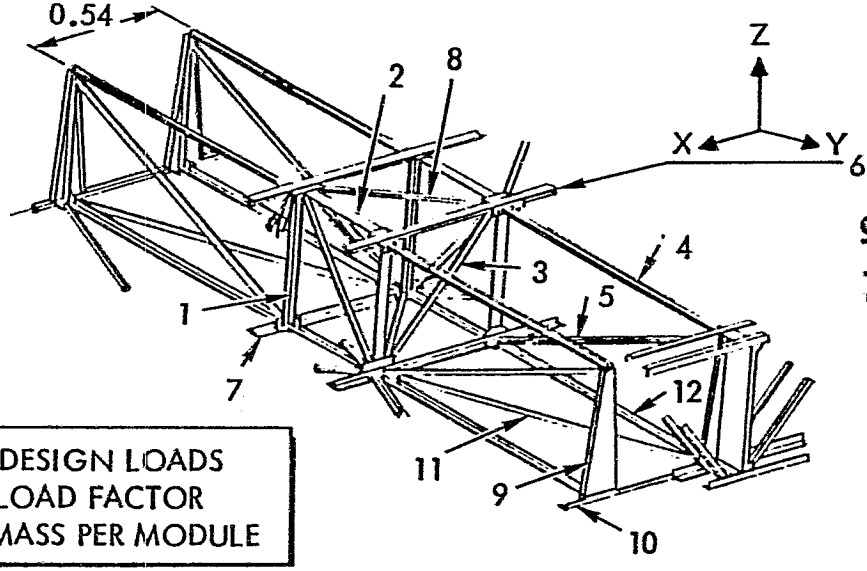

MOST CRITICAL DESIGN LOADS
1.5 ULTIMATE LOAD FACTOR
TOTAL HOUSING MASS PER MODULE

MEMBER	AREA (mm^2)	CAPABILITY	MOST CRITICAL LOAD CONDITION	APPLIED LOAD (ULT.)	TOTAL MASS PER MODULE (kg)
1	75	10,500 N	LAUNCH ($N_Z = \pm 5$)	10,200 N (AXIAL)	9.4
2	40	5,500 N	LAUNCH ($N_Y = \pm 3$)	1,700 N (AXIAL)	4.6
3	75	10,500 N	STA KP (.01 g) (TORSIONAL)	6,400 N (AXIAL)	10.4
4*	220	950 N/mm^2	LAUNCH ($N_Z = \pm 5$) (BENDING)	700 N/mm^2	107.0
5	40	1,500 N	STATIONKEEPING	NEGLIGIBLE	12.3
6	100	22,400 N	STATIONKEEPING (.01 g)	22,400 N (AXIAL)	21.5
7	40	5,000 N	LAUNCH STABILITY	—	3.4
8	75	10,500 N	STA KPG (.01 g) (TORSIONAL)	6,400 N (AXIAL)	11.4
9	40	9,400 N	LAUNCH STABILITY	—	5.0
10	40	9,400 N	LAUNCH STABILITY	—	4.3
11	40	1,500 N	LAUNCH STABILITY	—	9.8
12	75	2,040 N	LAUNCH STABILITY	—	22.9
				TOTAL	222.0

*STAINLESS STEEL LAUNCH SUPPORT TUBE

Figure 4.2-5. Container/Housing

ORIGINAL PAGE IS
OF POOR QUALITY

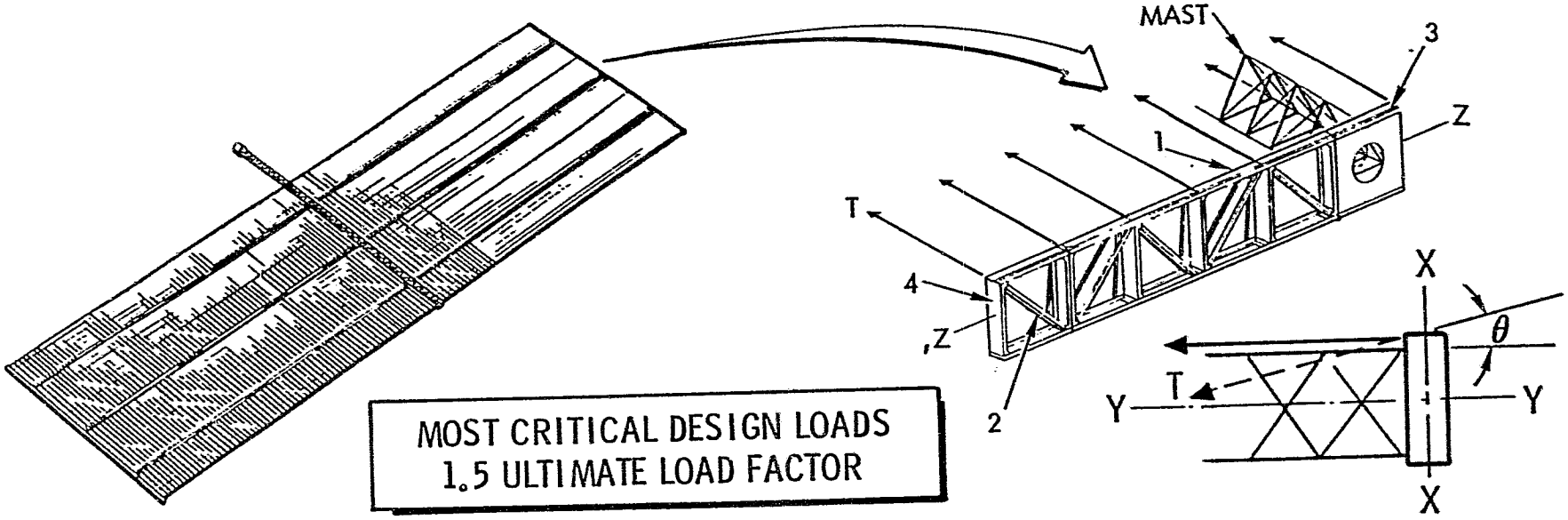

MOST CRITICAL DESIGN LOADS
1.5 ULTIMATE LOAD FACTOR

MEMBER	AREA	CAPABILITY	MOST CRITICAL LOAD CONDITION T = 27N	APPLIED LOAD (ULT)	NUMBER REQUIRED PER SIDE	TOTAL MASS (kg)
1	40 mm^2	4700N	BENDING X-X	4500N	4	8.6
2	40 mm^2	4600N	TORSION Z-Z	2000N	72	6.1
	THICKNESS					
3	.75 mm	250 N/mm^2	SHEAR (HINGES)		38	5.3
4	.75 mm	250 N/mm^2	SHEAR (TORSION)		42	5.9
TOTAL (PER SIDE)						25.9

Figure 4.2-6. Container/End-Cap

ORIGINAL PAGE IS
OF POOR QUALITY

- .008g STATIONKEEPING ACCELERATION (HYBRID MAST)
- 1.5% DAMPING

20N SUPPORT CABLE (WITHIN PRESENT TECHNOLOGY)

7N CONCENTRATOR TENSIONER
98% POWER OUTPUT .9 MIN
99+% POWER OUTPUT 4.2 MIN

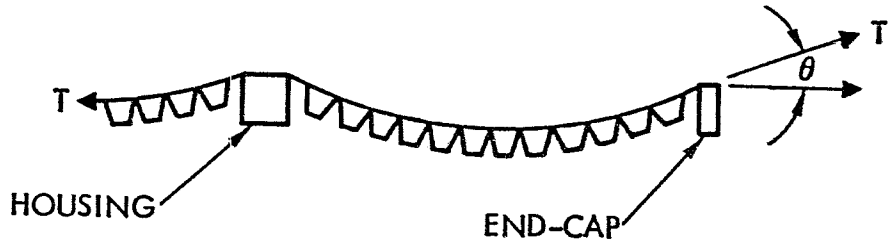

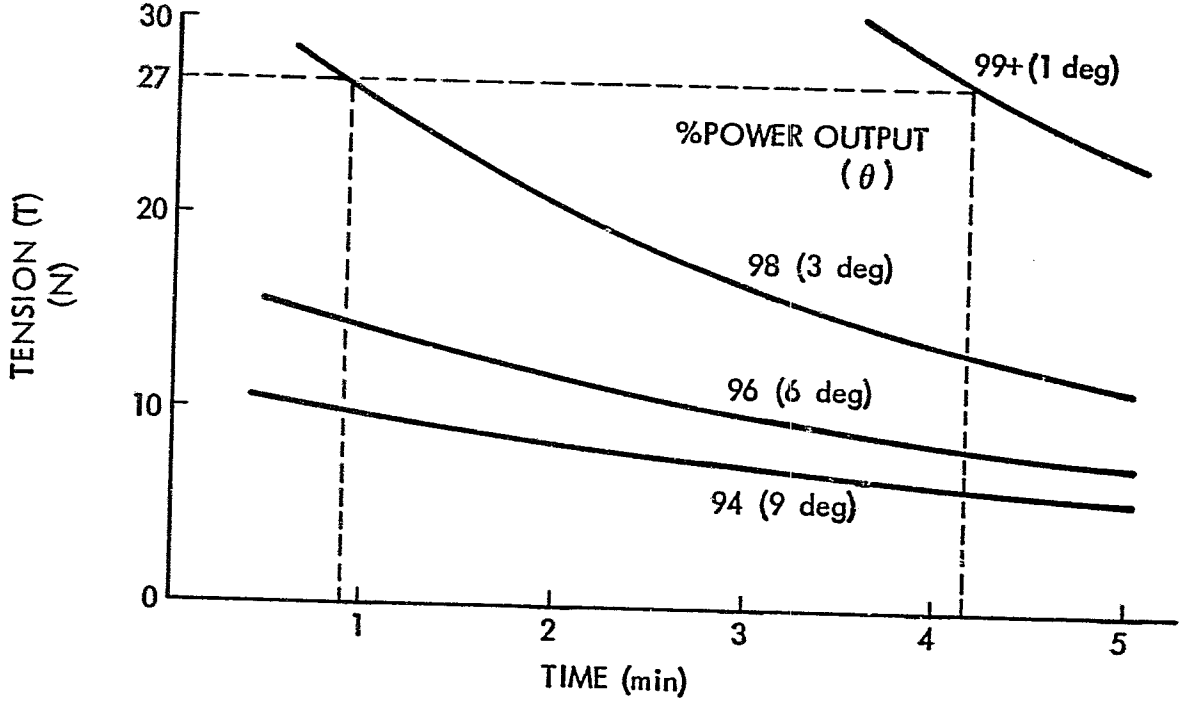

Figure 4.2-7. Power Output as a Function of Cable Tension

ORIGINAL PAGE IS
OF POOR QUALITY

ORIGINAL PAGE IS
OF POOR QUALITY

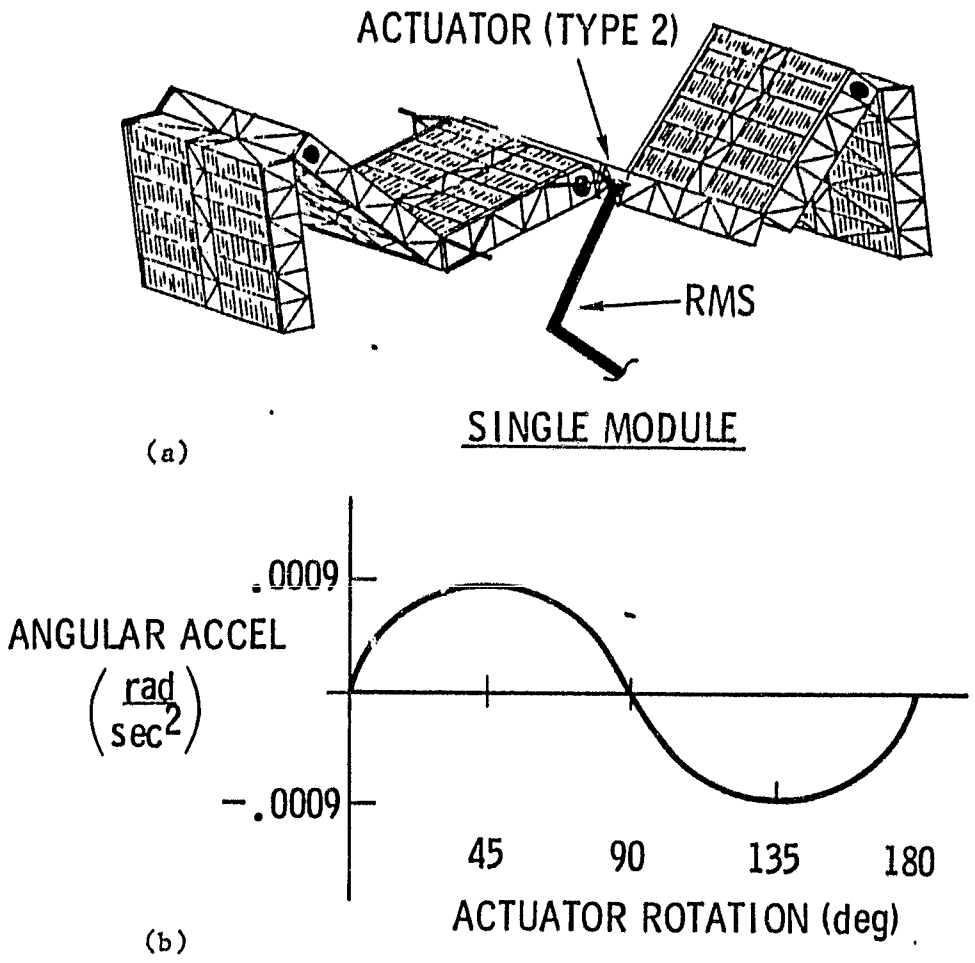

Figure 4.2-8. Module Deployment Response

7.0 Nm output torque and when activated will create 0.0009 rad/sec^2 radial acceleration of the two 3 section container in opposite directions. Full rotation (180°) of the No. 1 actuator (Type 2) at a 7.0 Nm constant torque requires approximately 29 minutes [Figure 4.2-8(b)]. Installing a Type 3 actuator which produces 45 Nm torque will rotate through 180° in approximately 5 minutes. Full rotation of the second and third sets of actuators would require less time since the 7.0 Nm torques would produce greater radial accelerations.

ORIGINAL PAGE IS
OF POOR QUALITY

4.2.1.5 Container/Housing Latching Mechanism

Active latching is required at deployment hinge joints to ensure longeron stiffness and tensile strength continuity. During orbit make-up maneuvers, the maximum longeron bending moments are produced at the spacecraft array interfacing. The mast critical latch load is the first joint closest to the user spacecraft (excluding the user attach point). Applying a 0.01 g orbit make-up to a dual module array creates a 16,000 Nm (Figure 4.2-9) bending moment at the first deployment joint. Two active latches attach to the container longerons opposite the joint hinges and capable of 16,000 N plus 300 N (4,400 lb) preload, will ensure longeron structural integrity and acceptable stiffness.

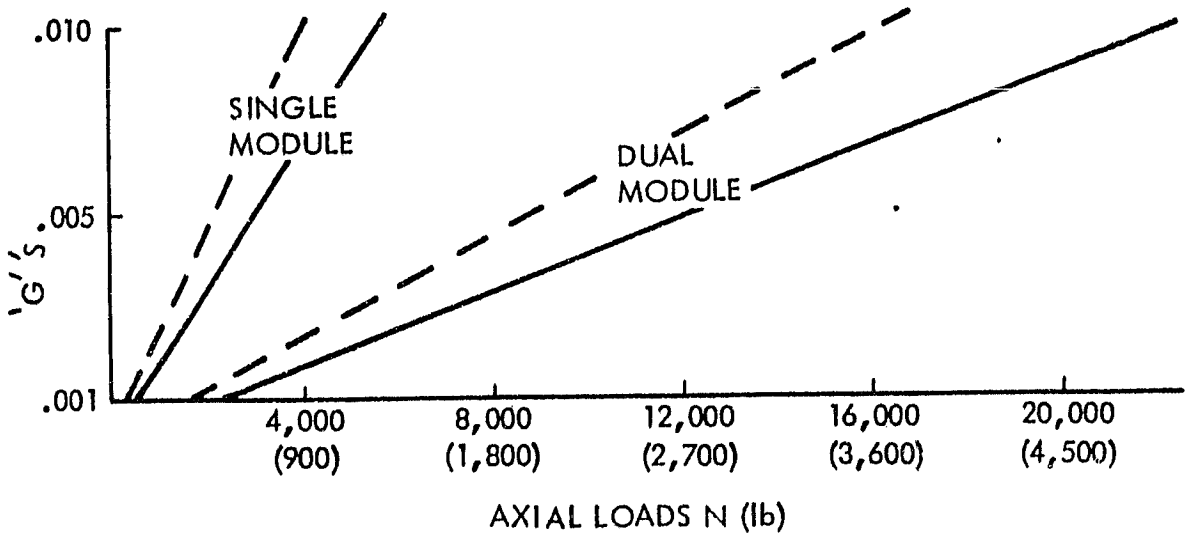

Figure 4.2-9. Latching Mechanism Loads

4.2.2 OVERALL STRUCTURAL CHARACTERISTICS

4.2.2.1 Module Deflections

Solar heating of the sun-facing side of masts, housing and end-caps can result in thermal distortion of the module when concentrators are extended. Absorption of solar energy by the top surfaces and shadowing of the lower ones results in a thermal gradient estimated to be 25°C. The resulting differential expansion produces bending of the structure and a corresponding rotation of the concentrator optical axes. However, as shown in Table 4.2-2 the pointing errors introduced by this effect are not large and will not result in serious thermal distortions. Solar heating does not create concentrator support cable distortions but atmospheric drag (4.5×10^{-4} N/m^2) will produce 0.01 degree pointing errors, as shown in the figure.

4.2.2.2 Stationkeeping Distortions

Table 4.2-3 represents the most critical deflections created by stationkeeping maneuvers. The preliminary design stationkeeping range is from 0.001 g to 0.01 g, thus the table shows the deflection at both limits. The overall housing deflections are affected by the number of modules connected together, but the other structural components are independent of the number of modules.

4.2.2.3 Mass Summary

A mass breakdown of the structural components and subsystems is presented in Table 4.2-4 The table lists the components, the mass of each component, the number required per 3.24 m cubic module, and the total mass per module. Two masses are presented (4377 kg and 3987 kg) and are the results of utilizing film-frame concentrators or rigid panel concentrators, respectively.

Table 4.2-2. Dimensional Stability and Deflections (Single Module)

STRUCTURAL ELEMENT	NORMAL OPERATIONS (OUT-OF-PLANE CURVATURE) (DEGREE)	.01g STATIONKEEPING MANUEVER (OUT-OF-PLANE TRANSLATION) (m)
MAST	0.001 (THERMAL)	3.0
CONTAINER/HOUSING	0.57 (THERMAL)	0.3
CONTAINER/END-CAP	0.57 (THERMAL)	NEGLIGIBLE
CONCENTRATOR SUPPORT CABLE	0.01 (ATM. DRAG)	0.7
SUB TOTAL	0.81	–
MANUFACTURING TOLERANCES	±0.25	–
ARRAY POINTING	±0.5	–
TOTAL SUN POINTING ERROR	1.4	
REMARKS	3.0 DEGREES USED IN PERFORMANCE ESTIMATES	STATIONKEEPING TRANSLATIONS (DISPLACEMENTS) ARE STRUCTURALLY ACCEPTABLE

ORIGINAL PAGE IS OF POOR QUALITY

ORIGINAL PAGE IS
OF POOR QUALITY

Table 4.2-3. Stationkeeping Deflections

ITEM	DEFLECTIONS (m)			
	SINGLE MODULE		DUAL MODULE	
ACCELERATION LEVEL	0.001 g	0.01 g	0.001 g	0.01 g
MAST	0.30	3.00	0.30	3.0
HOUSING	0.03	0.30	0.50	5.3
SUPPORT CABLES	0.07	0.70	0.07	0.7

Table 4.2-4. Mass Summary

COMPONENT OR SUBSYSTEM	MASS (kg)	NO. REQ'D	TOTAL MASS (kg)
MAST (INCLUDING CANISTER)	100	6	600
CONTAINER/HOUSING (INCLUDING LATCHES)	227	1	227
CONTAINER/END-CAP (INCLUDING LATCHES)	36	2	72
CABLE EXTENSION MECH. (INCL. CABLES)	2	78	156
CONCENTRATOR TENSIONERS	1.5	78	117
DEPLOYMENT ACTUATOR	1.0	5	5
ELECTRICAL HARNESS			500
REFLECTOR PANELS			
FILM-FRAME	0.287	4356	1250
RIGID PANEL (0.25 mm THICK)	0.197		860
REFLECTOR HARNESS			122
SOLAR PANEL AND RADIATOR	0.305	4356	1328
TOTALS		FILM FRAME	4377
		RIGID PANEL	3987

ORIGINAL PAGE IS
OF POOR QUALITY

4.2.3 LAUNCH LOAD ENVIRONMENT

The baseline configuration is designed primarily for on-orbit operational loads. The stowed geometry is compatible to the Shuttle bay, but no on-orbit weight penalty is involved. Table 4.2-5 lists the limit load accelerations during an STS launch. The internal support members of the stowed configuration are designed to withstand launch environment and transfer all loads to the exterior of the module to be picked up by the external support mechanism, Figure *4.2-10.*

Table 4.2-5. STS Compatibility—Quasi-Steady State Flight Loads (Acceleration in g's)

	N_x	N_y	N_z
Boost Environment	+2 -5	±3	±5
Landing	+1.8 -2.0	±1.5	+4.2 -1.0

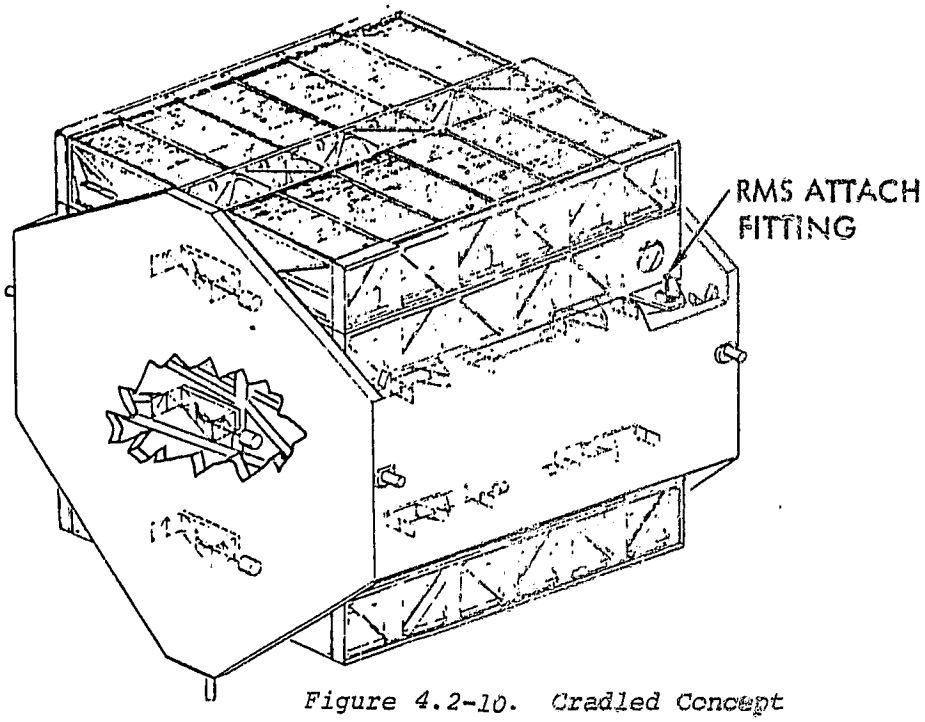

Figure 4.2-10. Cradled Concept

4.3 THERMAL ANALYSIS

Thermal analysis of the array as a whole and of its components supports the design process in several ways. Component temperature predictions are needed throughout in order to guide the selection of appropriate materials and surface treatments. Temperature distributions and temperature transients are required to assess thermal stress levels and thermal distortion effects. Finally, the electrical output of the solar panel is strongly temperature-dependent. Early in the program simplified thermal analyses were carried out in support of the design effort. These studies served to establish temperature distributions and to evaluate thermal stresses and thermal distortion effects as well as to optimize radiator size and thickness. In general the results did not uncover any serious design problems.

More accurate evaluation of concentrator temperatures has now been completed. It takes into account the coupled thermal and electrical behavior of the solar cell panel. This includes the (non-uniform) absorption of solar energy, heat loss by radiation and conduction and the conversion of light to electrical power. This was accomplished by the simultaneous solution of thermal and electrical networks using a Rockwell-developed thermal analyzer code. The thermal behavior of the concentrator was solved by the built-in logic of the analyzer code while the electrical behavior of the solar cell network was solved by a special Newton-Raphson procedure.

Separate mathematical models were generated for the gallium and silicon baseline concentrators. Each incorporated individual models of cell electrical performance, the distribution of direct and reflected sunlight, heat conduction through the substrate-radiator and a thermal radiation model which considered the hindered view from reflectors and radiator due to the presence of adjacent concentrators.

4.3.1 REFLECTOR PANEL TEMPERATURES

The temperature distribution over the reflector panels is determined by the distribution of incident and reflected sunlight (evaluated by the ray-tracing methods described in the next section) and by the presence of adjacent concentrators which hinder reradiation.

Typical concentrator temperature distributions are illustrated in Figures 4.3-1 and 4.3-2 which show the effects of fully reflecting corners and low (0.15) rear-surface emissivity on reflector panel temperature distribution. Multiple reflections from rays originating in the corners tends to heat the lower portion of the reflector panels. Low emissivity on both front (~0.05) and back surfaces of the panels results in fairly high temperatures. Although these temperatures are not expected to cause problems, they can be reduced by one of several methods. The outer (non-reflecting) surfaces of the reflector panels can be coated with high-emissivity material to improve heat rejection. However, a portion of that rejected heat must go to the radiators, thus impairing their performance in keeping the solar cells cool. Another approach is to make the reflector corners non-specular (diffuse), thus reducing the amount of multiple reflection which contributes to the overheating. This method, however, results in large overall light losses with consequent reduction in electrical output. A third alternative is to make only the upper corners of the reflectors diffuse. That region contributes most to the heating and very little to the illumination of the cells.

4.3.2 RADIATOR/SUBSTRATE MASS OPTIMIZATION

Heat is carried away from the solar cells by conduction in an aluminum sheet which serves as both substrate and radiator. Its effectiveness in distributing heat depends on its size and thickness. These factors, in turn, determine the mass of the sheet per unit of aperture area[5]. For a particular aperture size and relative radiator area, sheet mass can be reduced by decreasing its thickness. However, this results in an increase in cell temperature with consequent loss in electrical conversion efficiency. By reducing the scale of the concentrator, on the other hand, the same performance can be achieved with a thinner sheet, reducing the mass per unit aperture by almost 50%. Figure 4.3-3 illustrates this point. This scale effect on radiator performance is one of the reasons for choosing the N=6 baseline configuration.

4.3.3 THERMAL CYCLING OF FILM REFLECTORS

Two options are under consideration for reflector panel design, namely rigid and stretched film. In the stretched film design, aluminized Kapton is bonded to a rigid frame made of molded chopped fiber. In operation the

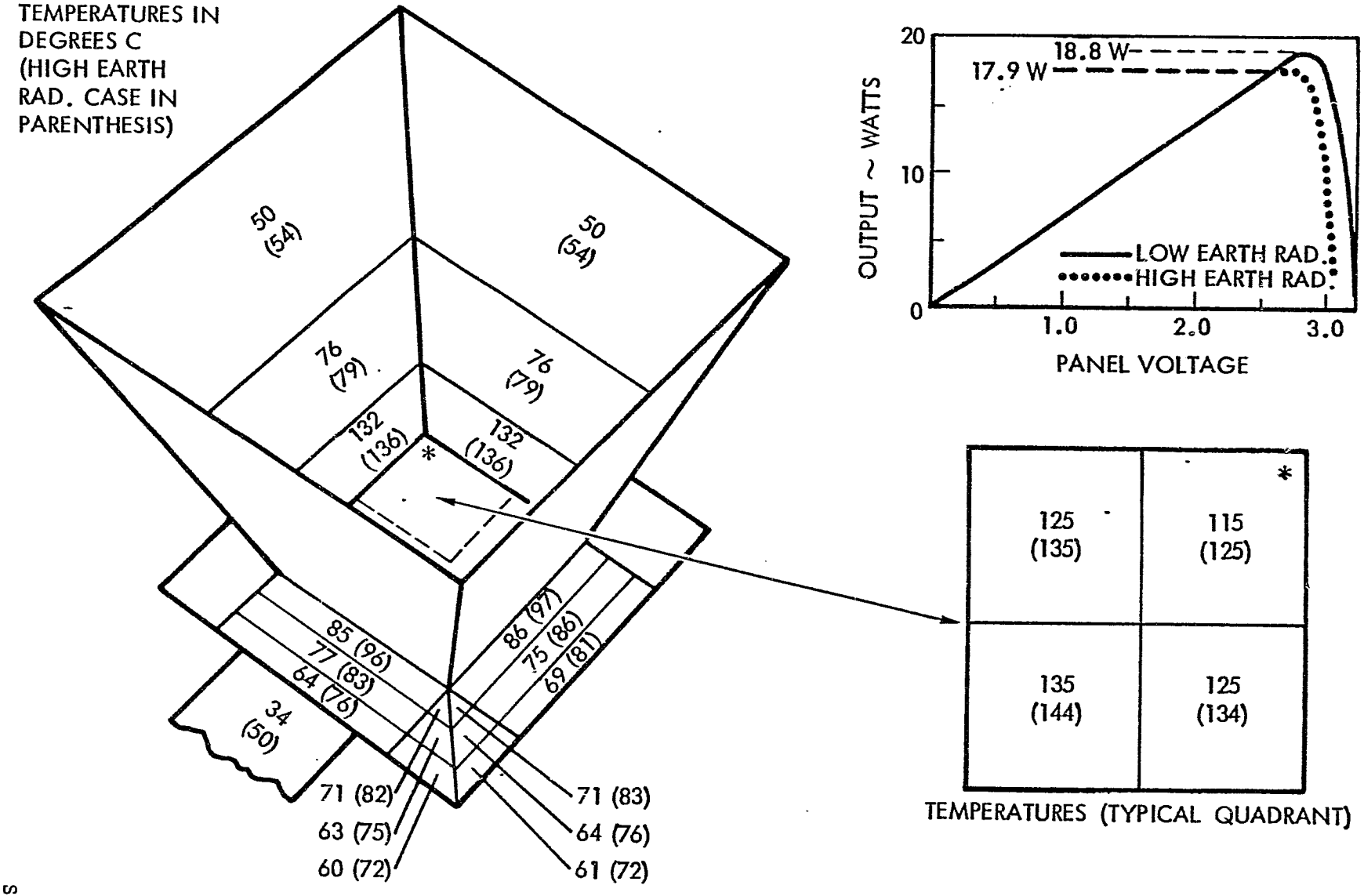

Figure 4.3-1. Coupled Thermal-Electric Model Results (Silicon Baseline)

ORIGINAL PAGE IS OF POOR QUALITY

Space Operations/Integration & Satellite Systems Division

Rockwell International

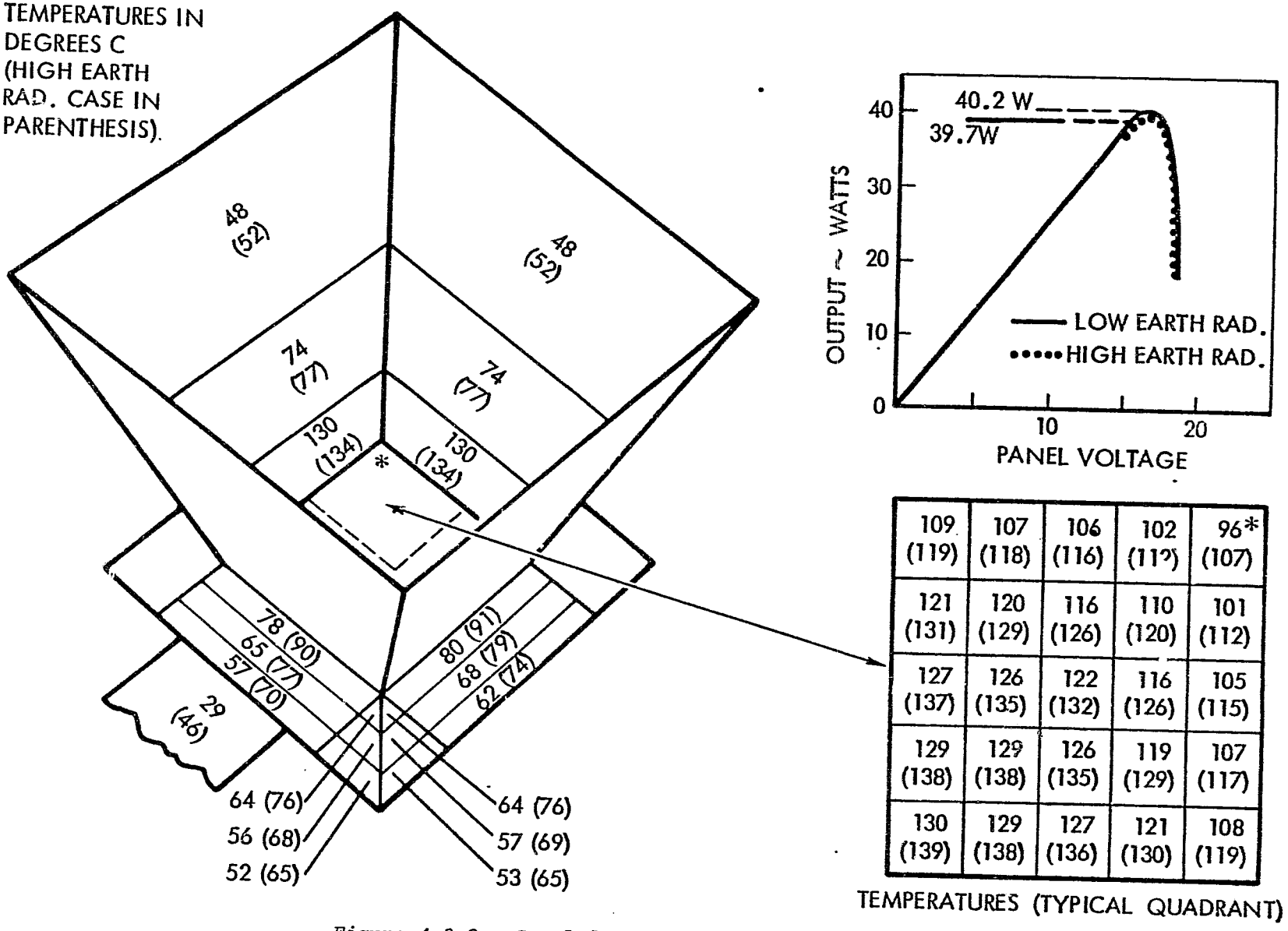

Figure 4.3-2. Coupled Thermal-Electrical Model Results (GaAs Baseline)

ORIGINAL PAGE IS OF POOR QUALITY

ORIGINAL PAGE IS
OF POOR QUALITY

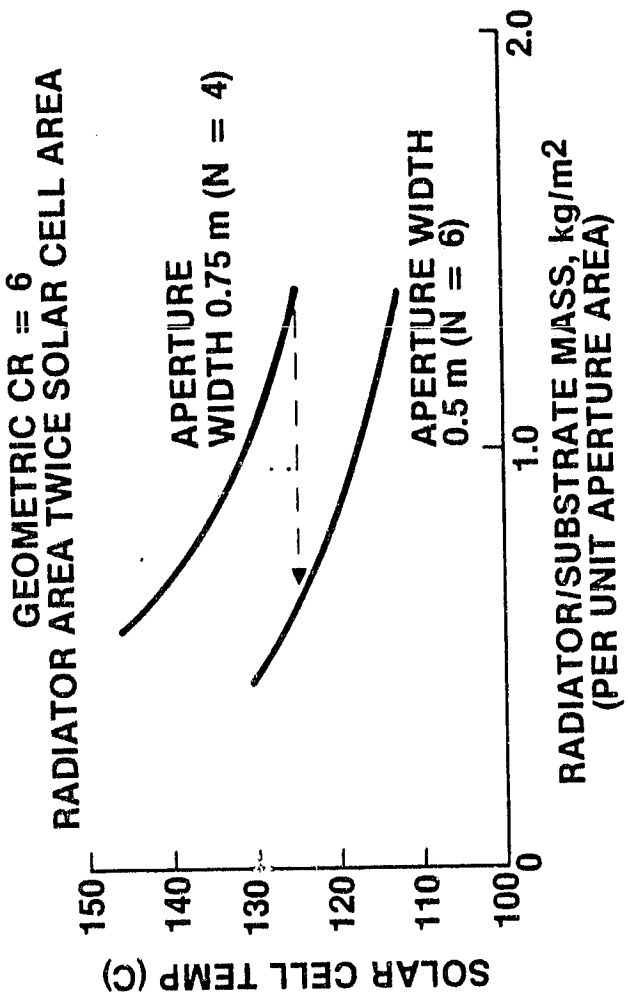

Figure 4.3-3. Scale Effect on Radiator/Substrate

reflector film must be under moderate tension in order to maintain a flat, wrinkle-free mirror surface.

During the orbital cycle, the reflector panels will alternately heat up and cool down. However, due to the substantial differences between the thermal capacities of the two, frame temperature will lag film temperature. This will result in reduced stress at the beginning of the sunlit period and increased stress at the beginning of eclipse. Figure 4.3-4 illustrates this transient behavior. It is clear however that the temperature gradients between film and frame are much less than the steady-state temperature difference assumed in early structural analysis.

4.3.4 MODULE THERMAL DISTORTION

Solar heating of the sun-facing side of caps and containers can result in thermal distortion of the module when concentrators are extended. Absorption of solar energy by the top surfaces and shadowing of the lower ones results in a thermal gradient estimated to be 25°C. The resulting differential expansion produces bending of the structure and a corresponding rotation of the concentractor optical axis (Figure 4.3-5). However, as shown in Table 4.3-1 the pointing errors introduced by this effect are not large and will not result in significant light loss.

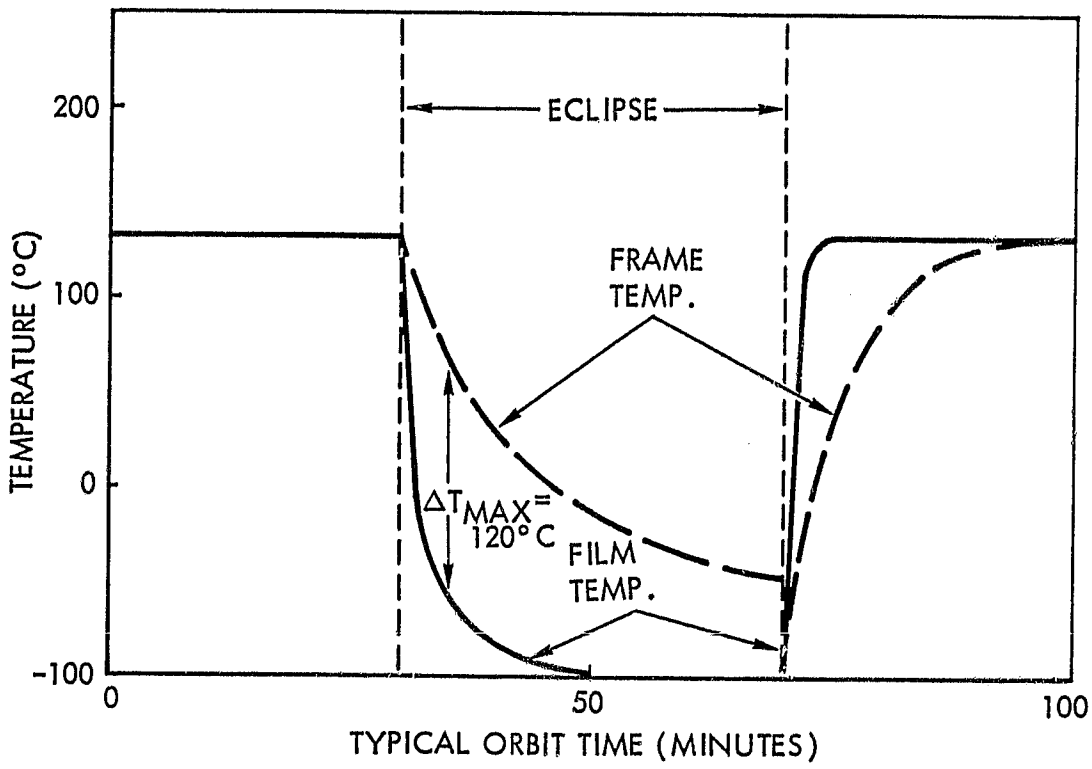

Figure 4.3-4. Transient Temperatures for Frame-Film Reflectors

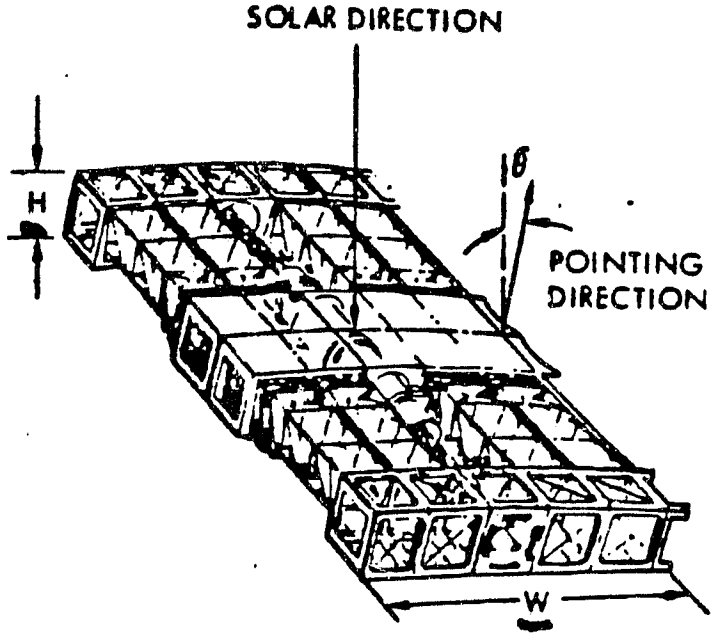

Figure 4.3-5. Differential Expansion Results

ORIGINAL PAGE IS
OF POOR QUALITY

Table 4.3-1. Container Thermal Distortion

Configuration	Container Depth, H (m)	Module Width, W (m)	Pointing Error, (Deg)
N = 4	0.81	13.0	0.25
N = 6	0.54	19.5	0.57

4.4 OPTICAL PERFORMANCE

The distribution of illumination produced by the reflecting panels of the concentrator is important for two reasons: first, differential illumination of the solar cells may have an adverse effect on output; second, the non-uniform illumination can result in large temperature gradients. These effects have been investigated by means of a Rockwell-developed ray-tracing program RAYPYR. Incoming light is represented by a large number of equally spaced, parallel rays emanating from the solar direction. Off-axis pointing is characterized by the direction angles with respect to the coordinate axes. The program follows each ray individually, through multiple reflections if necessary, until it either reaches the truncated bottom (representing the solar panel) or is reflected back out the entrance aperture.

4.4.1 GEOMETRY OF THE OPTICAL SYSTEM

The concentrators treated by RAYPYR have the shape of a right, four-sided pyramid, truncated to form a base which corresponds to the solar cell panel (see Figure 4.4-1). The larger, upper square is the aperture, the smaller, bottom square is the base and the trapezoidal sides are the reflectors.

The coordinate system is a right-hand cartesian one, with the Z-axis parallel to the optical axis and the X- and Y-axes aligned with the sides of the base. Ray directions are characterized by direction angles with respect to the three coordinate directions.

The shape of the concentrator is determined by three parameters; base width (W); concentrator height (H) and reflector slant angle (θ). In a conventionally designed concentrator, these parameters are chosen so that an incoming ray parallel to the optical axis, which strikes an edge of the aperture, produces a reflected ray which strikes the opposite edge of the base. This condition is satisfied (See Figure 4.4-2) when

$$\frac{W}{H} = -(\tan 2\theta + \cot\theta) \qquad (1)$$

Each reflector is divided into sections and the amount of energy absorbed in each is calculated. The truncated bottom surface is divided into a square grid representing the cells making up the solar panel. The energy reaching each cell is calculated by summing the contribution of all rays which reach

ORIGINAL PAGE IS
OF POOR QUALITY

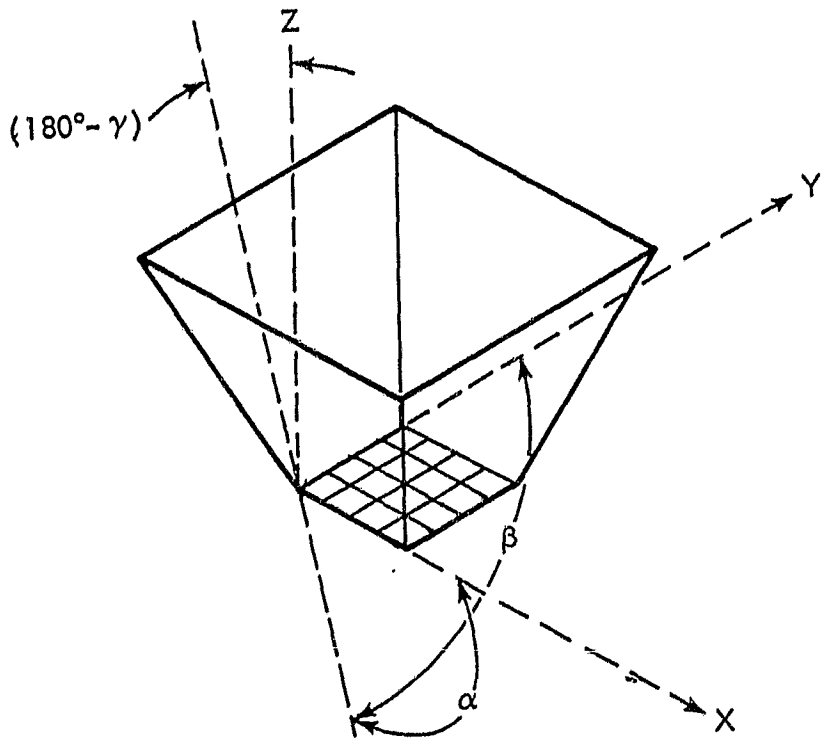

Figure 4.4-1 Coordinate System for Pyramidal Concentrators

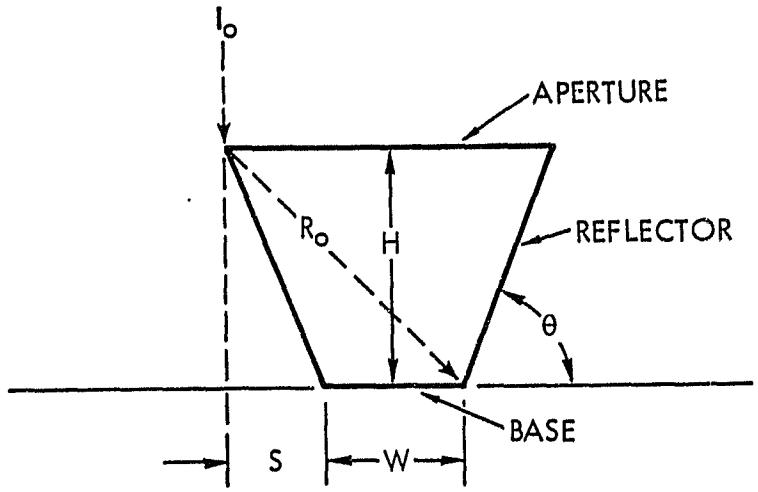

Figure 4.4-2. Geometry of Limiting Ray (Conventional Design)

it. Even though a large number of incoming rays are used (typically 90,000), uneven distributions can result due to the fortuitous pileup of equally spaced incident rays in certain grid squares. This problem is alleviated by introducing random spacing for the incident rays.

4.4.2 RAY REFLECTION

The basic relationship governing specular reflection is Snell's law: The angle of incidence equals the angle of reflection. In vector form (Reference 6).

$$\overline{R} = \overline{I} - 2(N \cdot I)\ \overline{N} \tag{2}$$

The incident ray is expressed in terms of its direction cosines.

$$\overline{I} = \cos\alpha_1 \overline{X} + \cos\beta_1 \overline{Y} + \cos\gamma_1 \overline{Z} \tag{3}$$

The normal to the reflector is given in general terms as

$$\overline{N} = -\sin\theta\,(P_{k_1} \overline{X} + P_{k_2} \overline{Y}) + \overline{Z}\cos\theta \tag{4}$$

The coefficients P_{kj} take on the values -1, 0, +1 depending on which of the four reflectors is involved.

The dot product in Equation becomes

$$N \cdot I = -\sin\theta\,(P_{k_1} \cos\alpha_1 + P_{k_2} \cos\beta_1) + \cos\theta\,\cos\gamma_1 \tag{5}$$

The components of the reflected ray (the direction cosines) are obtained by substituting Equations (3), (4) and (5) into Equation (2):

$$\cos\alpha_2 = \cos\alpha_1 + 2\,(N \cdot I)\,P_{k_1}\,\sin\theta$$

$$\cos\beta_2 = \cos\beta_1 + 2\,(N \cdot I)\,P_{k_2}\,\sin\theta$$

$$\cos\gamma_2 = \cos\gamma_1 - 2\,(N \cdot I)\,\cos\theta$$

The ray tracing process follows individual rays from their initial positions in the aperture plane through one or more intersections with reflector, base or aperture planes. In general, a given ray may intersect more than one reflector plane. The intersection of interest is the one having the smallest Z change, after eliminating backward intersections and the trivial case of intersection with the plane containing the initial point. If there are no reflector intersections between the aperture and the base, the ray is terminated and its contribution is added to the base (if downward directed) or considered lost through the aperture.

Figure 4.4-3 illustrates typical ray trace histories. Shown in projection are the paths of rays which strike different regions of the concentrator. Those striking the base (region I) directly undergo no reflections. Those striking the sides (region II) have only one reflection, provided Equation 1 applies, as it does in the baseline concentrator design. Rays striking region III in the corner experience two reflections before reaching the base and rays striking region IV undergo several reflections before being reflected out the aperture without illuminating the base.

4.4.3 RAY TRACE RESULTS FOR THE PYRAMIDAL CONCENTRATOR

Ray trace analyses of the GCR = 6 pyramidal concentrator gave optical efficiencies and detailed distributions of illumination for three reflector configurations for moderate pointing errors (0 to 5 degrees). The configurations include reflector designs with fully reflecting, non-reflecting and partially reflecting corners. Table 4.4-1 summarizes the results. They show that:

1. Penalties for off-axis pointing are rather small (3-4%) for angles up to 3 degrees.
2. Tilt orientation has only a slight effect on optical efficiency (see Figure 4.4-4).
3. Making the corner "gaps" transparent (that is, non-reflecting) reduces heat load on the reflector panels by a factor of three and makes panel illumination uniform (Figure 4.4-5), but at the cost of over 20% loss in optical efficiency.
4. Making the tips of the corners non-reflecting (Figure 4.4-6) substantially decreases reflector heat loads and increases the uniformity of illumination at only a modest cost (4%) in optical efficiency.

It is interesting to note that optical performance of pyramidal concentrators falls slowly with pointing error, even up to 15 degrees (see Figure 4.4-7). Thus there is no catastrophic loss of power, even for large concentrator rotations.

ORIGINAL PAGE IS
OF POOR QUALITY

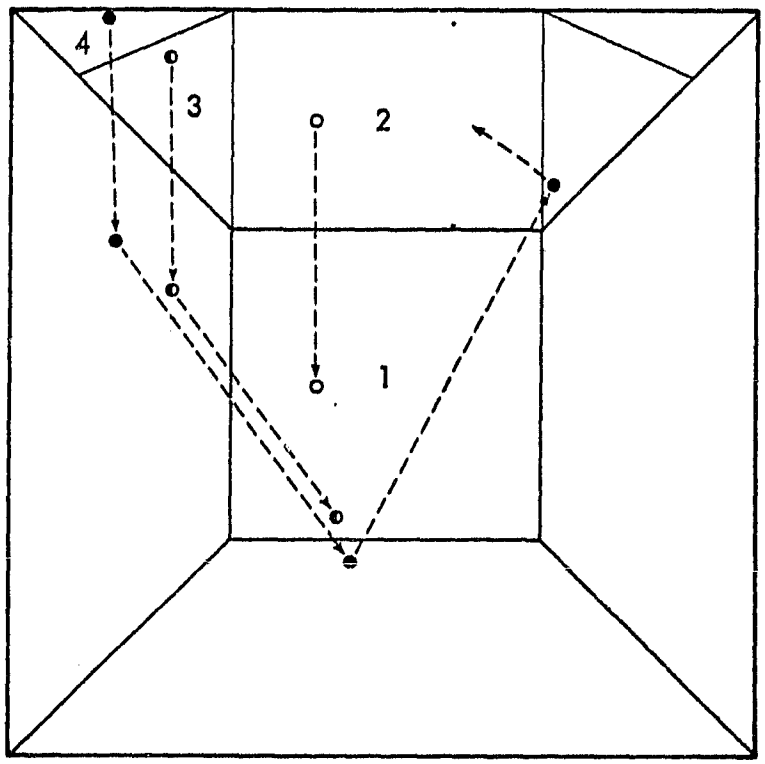

Figure 4.4-3. Typical Ray Trace Histories

ORIGINAL PAGE IS
OF POOR QUALITY

Table 4.4-1. Optical Performance of CR = 6 Concentrators

Configuration	Delta (δ) Pointing Error (°)	Effective CR	Energy Distribution (percent)			
			Base	Reflectors	Gaps	Reflected out
Fully reflective corners	0	4.64	77.3	14.5	0.0	8.2
	1	4.62 4.63*	77.0 77.2	14.6 14.6	0.0 0.0	8.3 8.2
	3	4.49 4.47*	75.0 74.6	15.1 15.3	0.0 0.0	9.9 10.2
	5	4.37 4.29*	73.1 71.8	15.2 15.7	0.0 0.0	11.7 12.6
Nonreflective corners	0 1 3 5	3.61 3.59 3.47 3.36	60.2 59.9 57.9 56.2	4.8 5.0 5.5 5.8	35.0 35.0 35.0 35.0	0.0 0.1 1.6 2.9
Corner tips nonreflective	0 1 3 5	4.46 4.44 4.28 4.11	74.3 74.0 71.4 68.8	9.0 9.1 9.7 12.1	16.7 16.7 16.8 14.8	0.0 0.2 2.1 4.4

Note: * Values with asterisk represent tilt along diagonal. Others are for tilt parallel to sides.

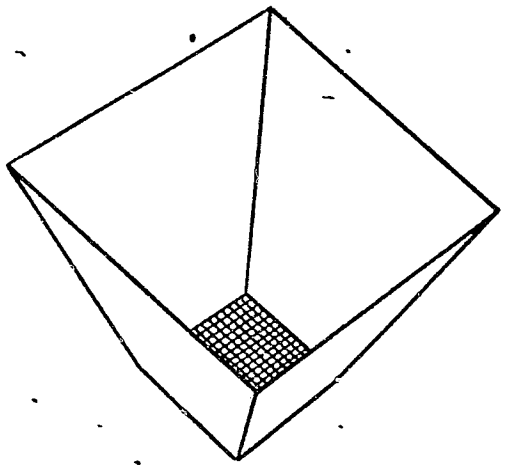

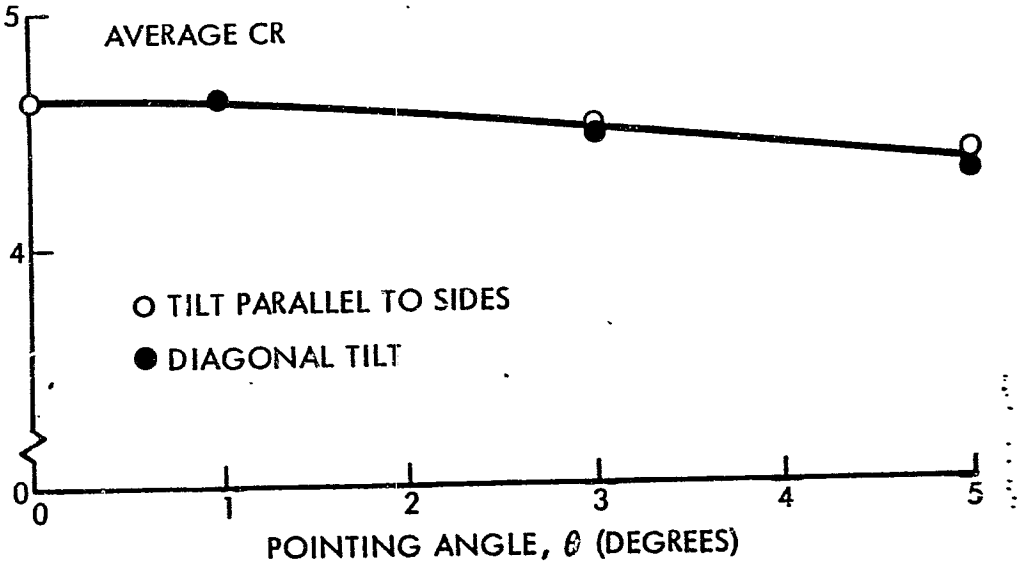

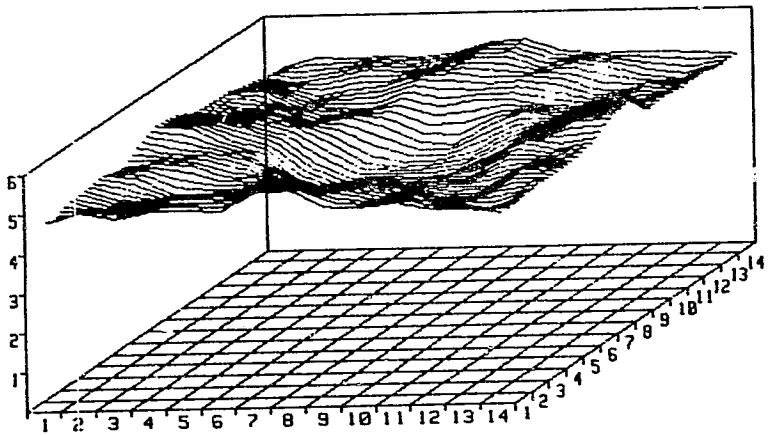

CASE 1
0. DEG. INCIDENCE, FULL CORNERS.

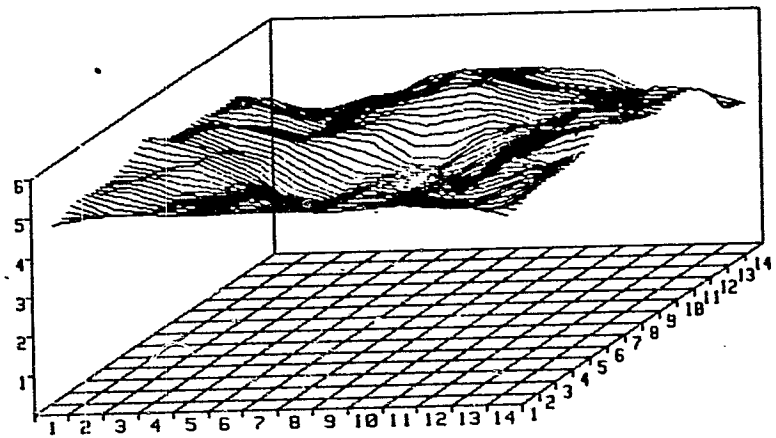

CASE 3
3. DEG. INCIDENCE, FULL CORNERS.

Figure 4.4-4. Optical Performance—Fully Reflecting Corners (Geometric CR = 6.0; Reflectivity 90%)

ORIGINAL PAGE IS
OF POOR QUALITY

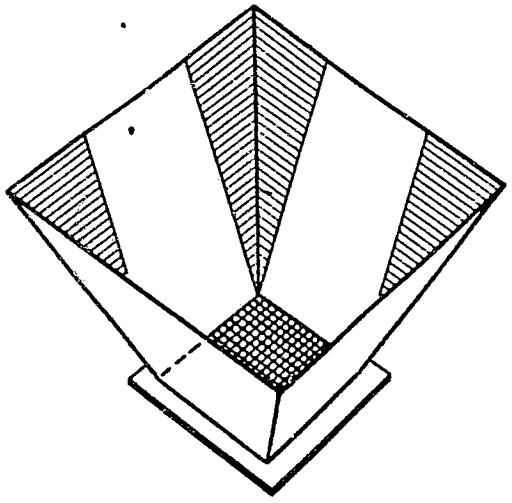

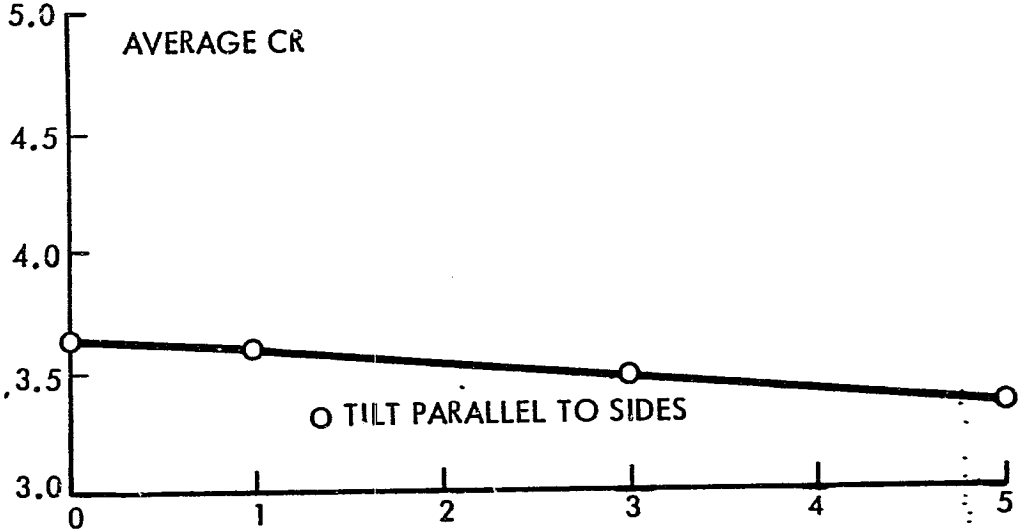

- REDUCES REFLECTOR HEAT LOADS
- ILLUMINATES SOLAR CELLS MORE UNIFORMLY
- BUT REDUCES OPTICAL EFFICIENCY ~ 20%

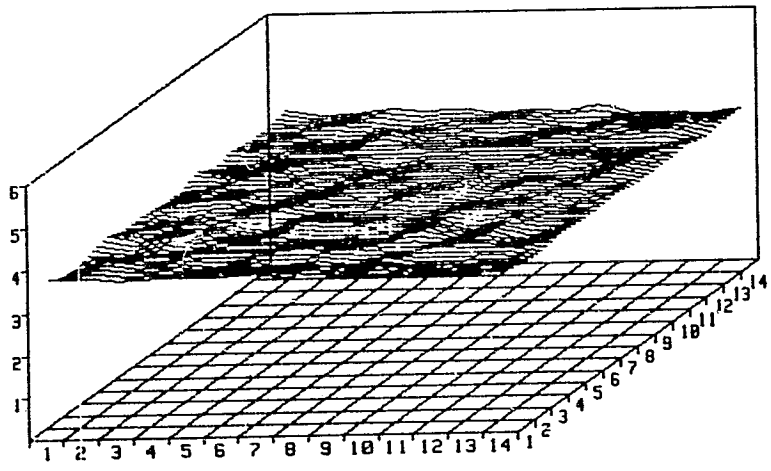

CASE 5
0. DEG. INCIDENCE, NO CORNERS.

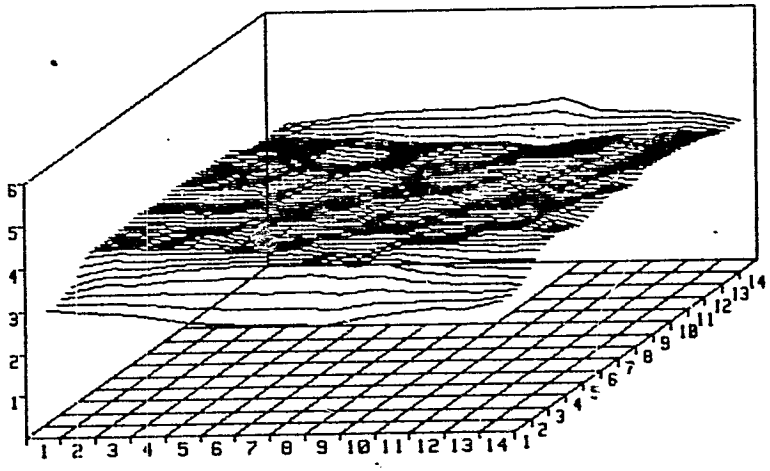

CASE 7
3. DEG. INCIDENCE, NO CORNERS.

Figure 4.4-5. Optical Performance—Nonreflecting Corners (Geometric CR = 6.0; Reflectivity 90%)

ORIGINAL PAGE IS
OF POOR QUALITY

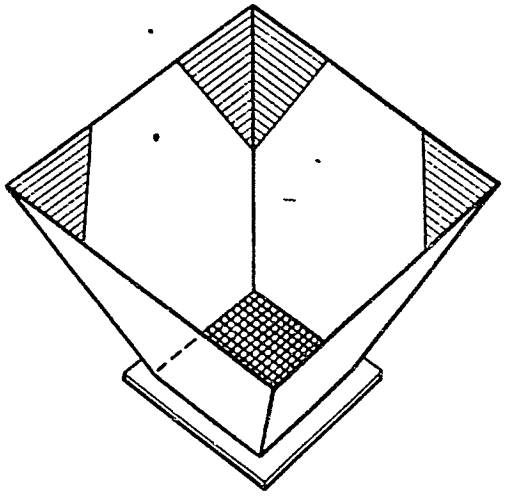

- REJECTS MAINLY RAYS WHICH HEAT REFLECTORS WITHOUT REACHING SOLAR CELLS
- LOSES ONLY ~ 5%

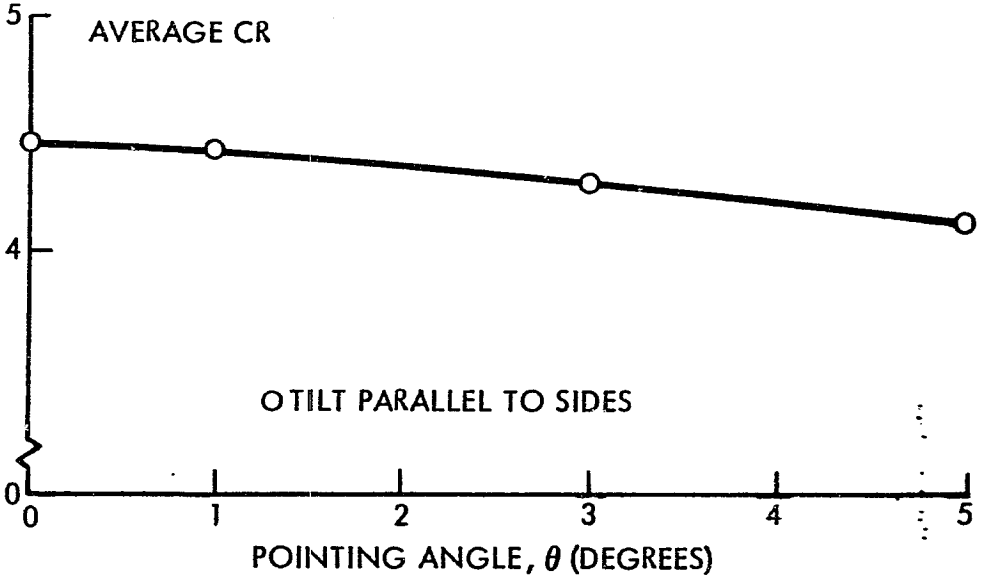

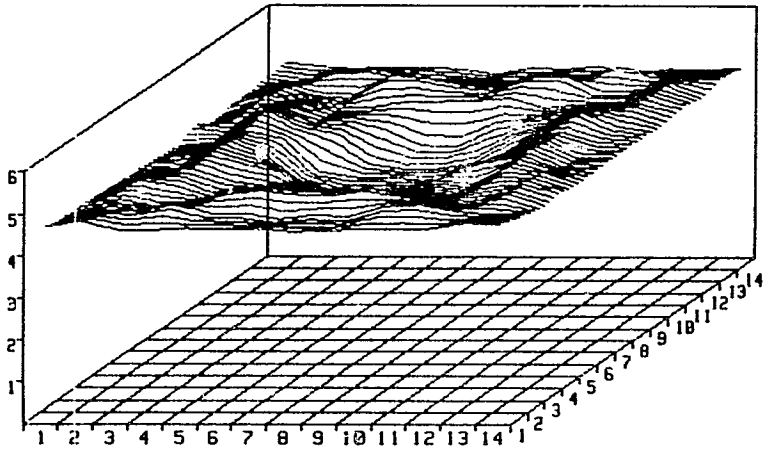

CASE 9
0. DEG. INCIDENCE, CORNER TIPS.

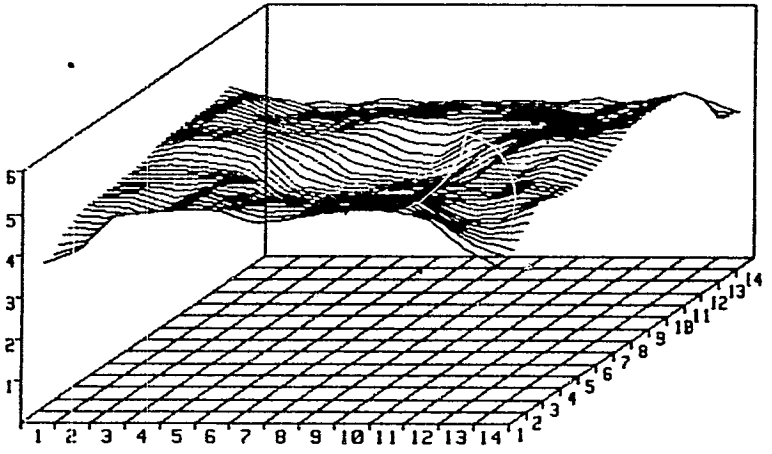

CASE 11
3. DEG. INCIDENCE, CORNER TIPS.

Figure 4.4-6. Optical Performance—Nonreflecting Corner Tips (Geometric CR = 6.0; Reflectivity 90%)

ORIGINAL PAGE IS OF POOR QUALITY

ORIGINAL PAGE IS
OF POOR QUALITY

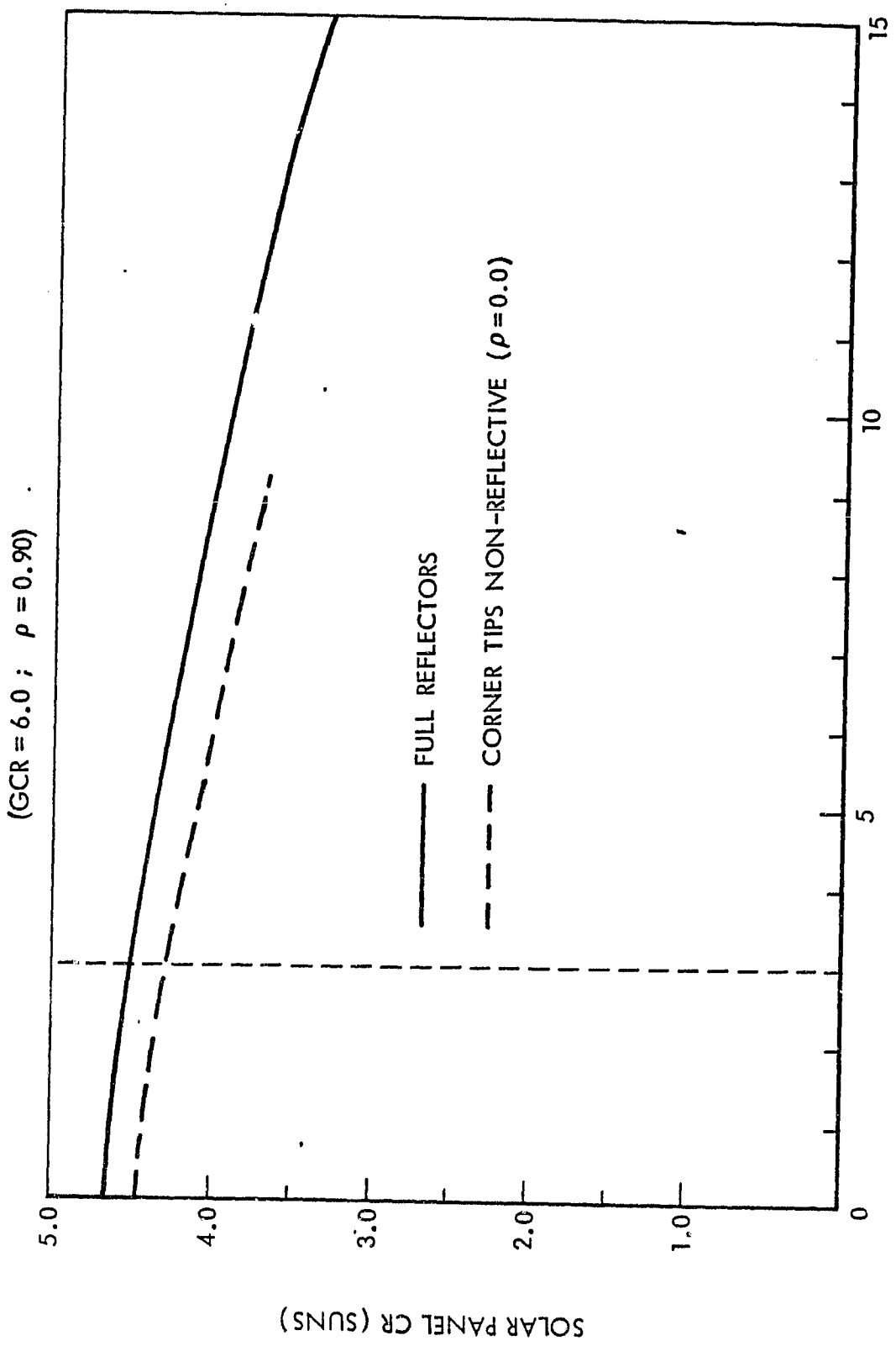

Figure 4.4-7. Ray-Tracing Results—Average Flux Incident on Solar Panel

4.5 ELECTRICAL ANALYSIS

The electrical design of the array requires consideration of the output characteristics of individual solar cells, their behavior in groups when interconnected into panels and electrical strings of panels, and the large-scale collection and distribution of power at the module and array level. Since compatibility with both silicon and gallium arsenide is a requirement, the final design will embody compromises brought about by the differing cell sizes and output characteristics of the two types.

4.5.1 SOLAR CELL MODELS

A detailed mathematical model of silicon cell performance has been projected from experimental current and voltage (I-V) data obtained from the subcontractor (ASEC) for 20 mm x 20 mm low CR optimized cells identical to those which will be supplied for the demonstrator panels. This size is of course, smaller than the 50 mm x 50 mm cells chosen for the baseline silicon design. The smaller cells have been chosen for use in the demonstrator because space qualified cells are immediately available. Their characteristics are well-known and have been used here to forecast performance of the larger cells.

Figure 4.5-1 shows typical AMO spectrum, 28°C performance at one, six and ten Suns. Short circuit current was found to be accurately proportional to the illumination intensity. Open circuit voltage shift was small and logarithmically proportional to the incident flux. The normalized current-voltage curves are almost independent of illumination level. The values at six Suns are used in constructing the silicon model described in Figure 4.5-2.

The above relationships have been supplemented with temperature coefficients obtained from the extensive JPL data on silicon cells given in Reference 7.

4.5.2 COUPLED ELECTRICAL-THERMAL PERFORMANCE ANALYSIS

An accurate evaluation of concentrator performance must take into account the coupled thermal and electrical behavior of the solar cell panel. This includes the (non-uniform) absorption of solar energy, heat loss by radiation and conduction and the conversion of light to electrical power. The problem involves the simultaneous solution of the thermal and electrical networks (see Figure 4.5-3). This was accomplished by means of a Rockwell-developed

ORIGINAL PAGE IS
OF POOR QUALITY

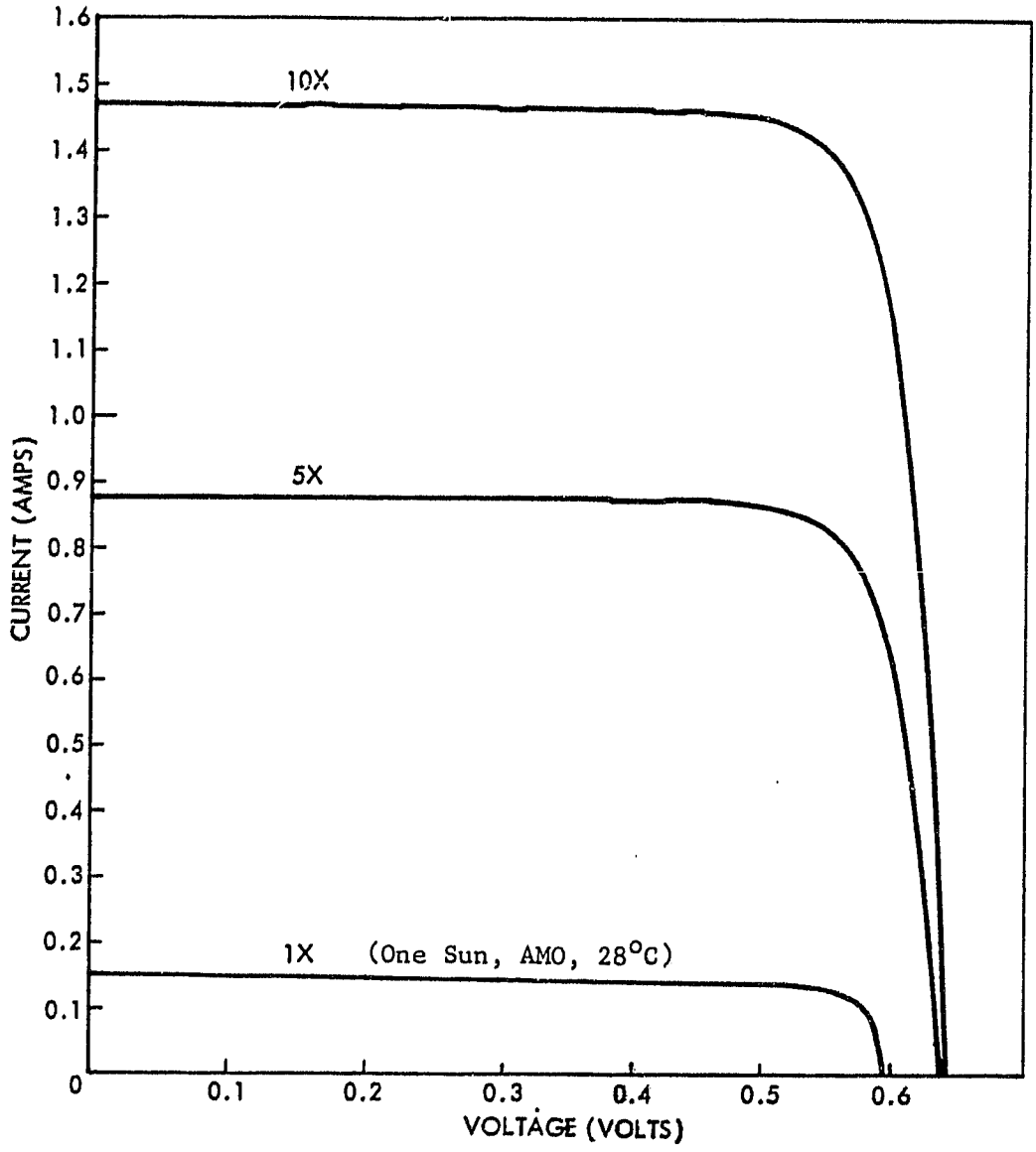

Figure 4.5-1. Measured Low CR Optimized Solar Cell Output Characteristics

ORIGINAL PAGE IS
OF POOR QUALITY

	SILICON	GALLIUM ARSENIDE
CELL SIZE (NOM.)	50mm X 50mm X 0.25mm	20mm X 20mm X 0.3mm
SURFACE PROPERTIES SOLAR α THERMAL ϵ	0.70 0.85	0.75 0.85
CURRENT-VOLTAGE CHARACTERISTICS (T = 100°C CR= 4.0 SUNS)	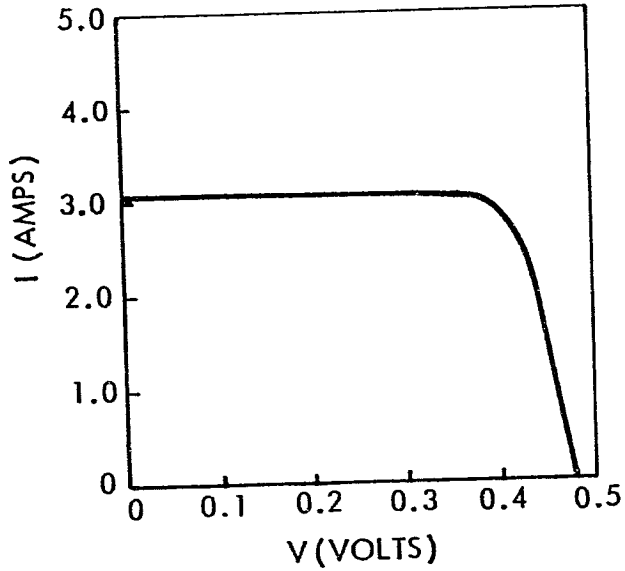	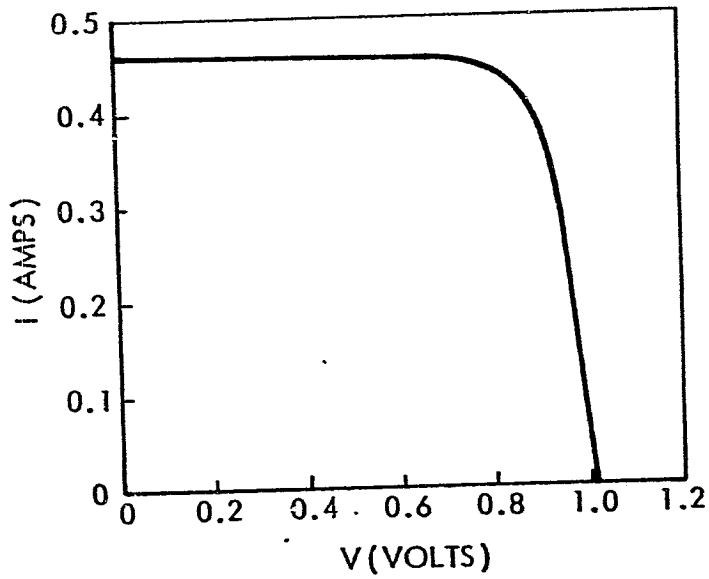
I_{SC} (AMPS)	[3.100 + .000504 (T-100)] • [CR/4.0]	[0.458 + .000040 (T-100)] • [CR/4.0]
V_{OC} (VOLTS)	0.477 - .0021 (T-100) + .0215 Ln (CR/4.0)	1.003 - .0014 (T-100) + .028 Ln (CR/4.0)

Figure 4.5-2. Solar Cell Characteristics and Performance Models (BOL)

Space Operations/Integration & Satellite Systems Division
Rockwell International

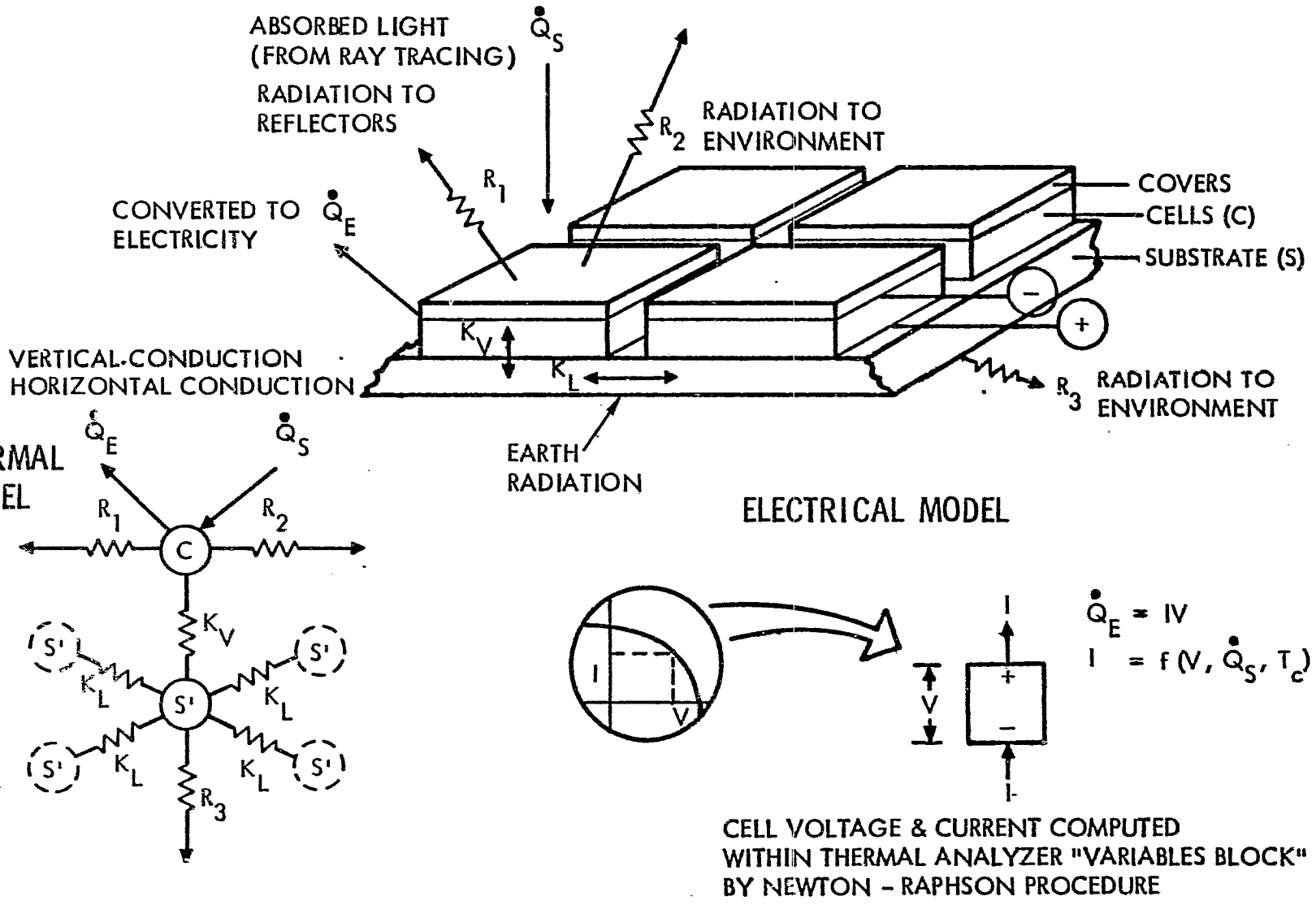

Figure 4.5-3. Coupled Thermal-Electrical Math Model

ORIGINAL PAGE IS
OF POOR QUALITY

thermal analyzer code which has the capability of adding Fortran-like statements in a "variables block" to manipulate program variables as required by a specific problem. In the present case, the thermal behavior or the concentrator was solved by the built-in logic of the analyzer code while the electrical behavior of the solar cell network was solved in the "variable blocks". Thermal-electrical coupling occurs because of the temperature dependence of solar cell characteristics and because of variations in the amount of solar energy converted into electrical power as the electrical load is varied.

Electrical performance curves for both GaAs and Si concentrators, along with temperature distributions, are shown in Figures 4.3-1 and 4.3-2. Individual solar cell characteristics are given in Figure 4.5-2. The current-voltage output curves were obtained from a series of steady-state solutions for different assigned panel currents. (The temperature distributions apply only to the peak power conditions.) The higher efficiency and lower temperature coefficients of the GaAs cells result in a peak power output over twice that for silicon for the same illumination conditions.

4.5.3 HARNESS OPTIMIZATION

A flat flexible cable was selected to interconnect individual concentrator elements within an electrical string. This type of cable also collects electrical power from all the strings and distributes it to the user attach fitting. The selection was based upon the need for flexibility and high packing density as well as the usual space design requirements such as low outgassing and environmental resistance. The variables which are important to the design of the cables are: physical configuration of the solar array, solar array system electrical characteristics, physical properties of the cable materials, and the cost estimating relationships (unit costs) of both the solar array and the harness. The contractual requirement which governs the design is to minimize the system recurring cost of power.

An optimum current density (J_H) in the electrical distribution system can be determined as a tradeoff of harness cost (C_H) and the cost of added concentrator capability (C_C) to compensate for harness losses while delivering constant power to a load. This statement embodies the cost optimization concept expressed below, where C_T is total system cost, and A_H is the harness cross-sectional area:

$$\frac{dC_T}{dA_H} = \frac{dC_H}{dA_H} + \frac{dC_c}{dA_H} = 0 \qquad (1)$$

The assumptions made in deriving the expression below are two. The first is that the harness material is available on a cost per square meter of surface area basis (not cross-sectional area) when purchased in the large quantities which would be needed to support this program. Not independent of this is the assumption that the thickness of the metal laminate layer does not significantly affect the cost per square meter of the harness. This cost is assumed to be driven by the number of parts to be processed and the number of process steps per part and not the variation in time it takes to complete one of several steps involved (i.e., the etching of the metal circuitry). Hence, the cost optimized current density is given by:

$$J_H = \sqrt{\frac{1}{\rho t}\,\frac{C_H'}{C_c'}} \qquad (2)$$

where ρ is the bulk resistivity of the conductor, t is the selected thickness of the metal laminate layer, C_H' is cost per square meter of harness surface area and C_c' is the cost per watt of electrical power.

Once a conductor current density is determined all other relevant harness characteristics are fixed. The previously mentioned variables such as configuration and electrical properties, of course, must be known. The parametric cost optimized characteristics are given below in Table 4.5-1.

I_T is the total current to the load. V_c is the source output voltage before harness losses are incurred and m is the mass density of the conductors. The cost estimating relationships are discussed in Section 4.6 and the electrical characteristics of the strings are covered in Sections 3.4.2.1 and 3.4.2.2 for the silicon and GaAs designs respectively.

TABLE 4.5-1 HARNESS DESIGN CHARACTERISTICS

CHARACTERISTIC	PARAMETRIC EXPRESSION	SI DESIGN	UNITS
RESISTANCE	$R_H = \rho \frac{\bar{\ell}}{A_H} = \frac{\rho \bar{\ell} J_H}{I_T}$	0.012	ohm
VOLTAGE DROP	$V_H = I_T R_H = \rho \bar{\ell} J_H$	2.5	volt
POWER LOSS	$P_H = I_T V_H = \rho \bar{\ell} J_H I_T$	1057	Watt
EFFICIENCY	$E_H = \frac{V_C - V_H}{V_C} = 1 - \frac{\rho \bar{\ell} J_H}{V_C}$	0.99	--
MASS PER MODULE	$M_H = (\text{volume})m = \bar{\ell} \frac{I_T}{J_H} m$	375	kilogram
MATERIAL COST PER MODULE	$C_H = (\text{surface})C_H' = \frac{\bar{\ell}}{t} \frac{I_T C_H'}{J_H}$	55,000	dollar
EFFECTIVE LENGTH	$\bar{\ell}$ = (see text)	119	meter

The preceding optimization would differ if the system were to be optimized for minimum mass. The current density would then be given by:

$$J_H = \sqrt{\frac{m}{\rho} P_c'} \quad , \tag{3}$$

where P_c' is the specific power (Watts/kg) of the array. All the other harness characteristics would follow.

The term $\bar{\ell}$ in the preceding expressions refers to the average length of harness over which power must be transmitted to reach the user attach fitting. For the Si design configuration shown in Figure 4.5-4, this is given by:

$$\bar{\ell} = \sqrt{\frac{A_d}{R_a}} + \frac{2(n-1)}{p} \sqrt{\frac{A_d}{R_a GCR}} + \sqrt{R_a A_d} \left(2 - \frac{1}{n}\right) \tag{4}$$

where R_a is the electrical aspect ratio, A_d is the array deployed area, n is the number of concentrators per string and p is the number of strings per array.

For the harness layout chosen, ℓ tends toward a value of approximately 1.5 times the minimum distance between the user attach fitting and the tip of the median concentrator element assembly. The GaAs harness is slightly different due to the four electrical strings per row of deployed concentrator elements.

ORIGINAL PAGE IS
OF POOR QUALITY

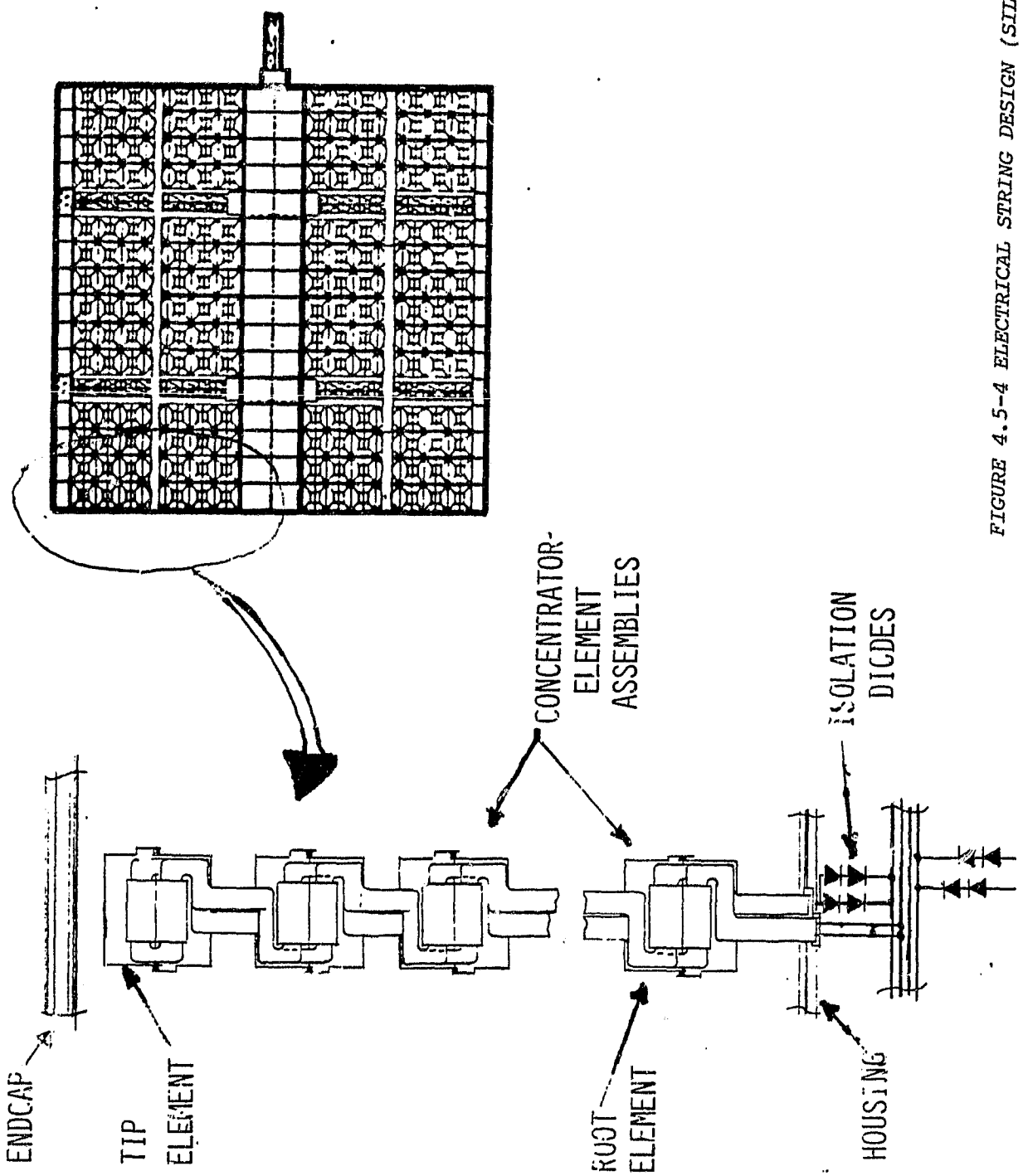

FIGURE 4.5-4 ELECTRICAL STRING DESIGN (SILICON)

4.6 ARRAY MODULE PERFORMANCE

4.6.1 COMPONENT WEIGHTS AND COSTS

The existence of a baseline design provides the basis for better prediction of array weight and cost than have been possible based on design concepts alone. Weight in particular can be established fairly accurately once part dimensions and materials have been defined. Costs are more uncertain, since they depend on projections of fabrication costs extrapolated ahead in time and from a few units to thousands. Several different approaches have been used to arrive at component costs.

The canister-mast units are developed components for which reliable costs can be determined by the subcontractor. Weights for baseline design are also readily estimated. This weight is a significant item, and the possibility of reducing it significantly will be studied later in the program. If feasible, such a design refinement would have its own cost impact.

The mass-based cost algorithm developed in Reference (1) has been used to derive the cost of the main structural components from their weights. Reflector panel costs are based on large-volume production of the rigid panel option, considering the unit costs of material, molding process, and aluminization. Solar cell cost projections for both silicon and gallium arsenide are NASA PEP (Power Extension Package) solar array and Air Force GaAs development program cost goals, respectively. Table 4.6-1 summarizes the cost and weight breakdown for a module. Separate totals have been included for silicon and GaAs cell types.

4.6.2 CONCENTRATOR PERFORMANCE

Performance equations, such as those employed in References (1) and (5) make use of estimated optical, radiator and solar cell efficiencies in order to arrive at concentrator electrical power output. This approach is useful as a method of investigating parametric variations in concentrator design and as a preliminary estimate of array performance. The accuracy of the projection is improved when calculated values of optical efficiency, solar cell temperature distribution and panel electrical output can be introduced. Such improved estimates have now been obtained for the GaAs and Si baseline configurations as described in Section 4.5. This output calculation, together with cost, weight and area values for the modules as a whole result in the module performance values shown in Table 4.6-2.

Table 4.6-1. Weight and Cost Estimates for Baseline Modules

COMPONENT OR SUBSYSTEM	MASS (kg)	COST (1982 $M)		
		GaAs	EITHER	Si
CABLE EXTENSION MECHANISMS	156		.62 (a)	
CANISTERS & MASTS	600		1.15 (b)	
CONTAINER END CAP	72		.18 (a)	
CONTAINER HOUSING & LATCHES	227		.95 (a)	
CONCENTRATOR TENSIONERS	117		.47 (a)	
DEPLOYMENT ACTUATORS	5		.09 (a)	
ELECTRICAL HARNESS & INSULATION	500		1.99 (a)	
REFLECTOR PANELS	1250		0.31 (c)	
REFLECTOR HARDWARE	122		0.49 (a)	
SOLAR PANELS & RADIATORS	1328	12.89 (d)		3.75 (e)
TOTALS	4377	19.14		10.00

NOTES: (a) BASED ON MASS ALGORITHM; COSTS APPORTIONED BY MASS
(b) SUBCONTRACTOR ESTIMATE
(c) MATERIALS & SEMI-AUTOMATED PROCESSING
(d) MANTEC GOAL
(e) PEP GOAL

ORIGINAL PAGE IS
OF POOR QUALITY

Table 4.6-2. Performance Estimates for Baseline Modules

SOLAR CELL TYPE	MASS (kg)	COST ($M)	POWER (kW BOL)	WATTS / m^2	WATTS/ kg	$/ WATT
GALLIUM ARSENIDE	4377	19.1	172	130	39	116
			(169)	(128)	(39)	(117)
SILICON	4377	10.0	80	61	18	134
			(76)	(58)	(17)	(141)

NOTES:
1. AREA 1320 m^2; 4356 CONCENTRATOR ELEMENTS
2. POWER UNDER HIGH EARTH RADIATION IN PARENTHESIS

ORIGINAL PAGE IS
OF POOR QUALITY

It is interesting to compare the above specific power and cost projections with those of a state-of-the-art lightweight planar silicon arrays which delivers about 100 W/m^2, 60 W/kg and 300-400 $/W recurring cost. The silicon concentrator is bigger and heavier for the same output but has a factor of three or more advantages in cost.

The concentrator design allows the substitution of the higher performance but more expensive GaAs cells without incurring an overall cost disadvantage. The GaAs concentrator specific power (W/kg) is improved, matching the SEP on an area basis and coming closer on a mass basis. When end-of-life performance is considered, the added mass and the enclosure provided by the concentrator design confers a definite advantage over a planar one. This is also reflected in a life cycle cost (LCC) of energy comparison between the low CR concentrator array and lightweight planar array designs (see Figure 4.6-1). This energy gain is especially important when considering long duration missions and/or high radiation flux orbital profiles.

ORIGINAL PAGE IS
OF POOR QUALITY

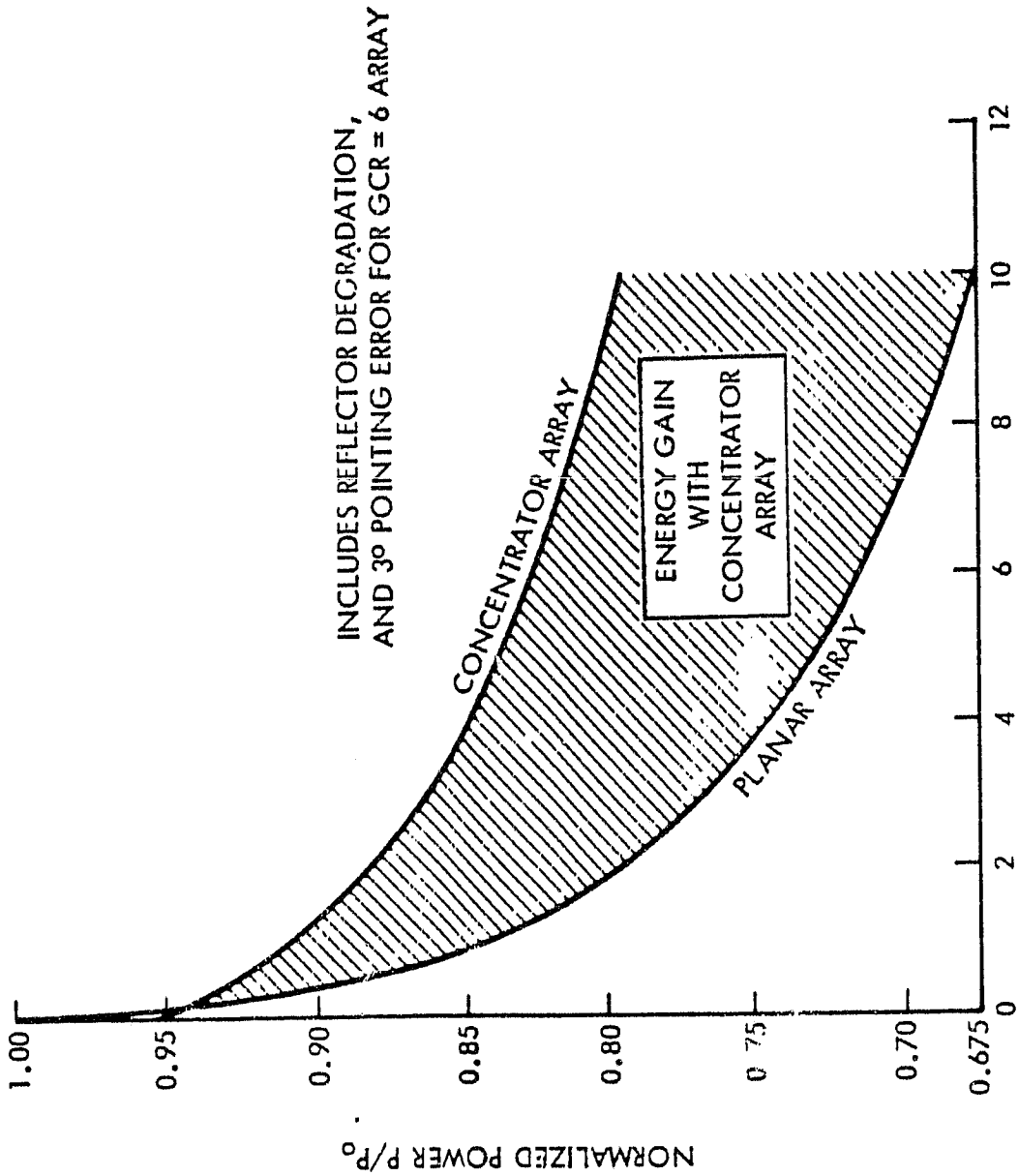

Figure 4.6-1. Life Cycle Energy Comparisons

5.0 COMPONENT DEMONSTRATION TESTS (TASK II)

The prediction methods described in Section 4.0 provide considerable insight into the adequacy of a design but analytical models do not necessarily account for all factors which might affect array performance. In particular, reflector optical quality, concentrator dimensional accuracy, and solar cell variations are all difficult to characterize and incorporate into performance prediction methods. Similarly, kinematic behavior and fabrication feasibility are difficult to assess from a drawing alone. Therefore, in a later phase of the design effort, planned testing will demonstrate the optical, thermal and electrical performance of a full-scale concentrator under terrestrial conditions and provide more insight into the mechanical behavior of the design. Terrestrial performance will be compared to an analytical model of the terrestrial behavior.

5.1 STRUCTURAL AND DYNAMIC MODELS

Two mock-ups of the array have been constructed by a subcontractor (Penwal Industries) according to drawings and instructions prepared by Rockwell. These models are intended as aids to the visualization of the kinematics of the array module during deployment and extension.

5.1.1 ONE-FIFTEENTH SCALE DEPLOYMENT SIMULATOR

Figure 5.1-1 shows the deployment simulator mock-up photographed in conjunction with a scale model of the Shuttle orbiter. The mock-up consists of six sections and provides a means of visualizing the relative positions of module components such as canisters, attachments and hinge lines during various stages of deployment. It will also be useful in the design of integration hardware components for attaching the module to the Shuttle payload bay or a user spacecraft.

5.1.2 TWO-BY-TWO DYNAMIC SIMULATOR

Figure 5.1-2 shows an intermediate stage in the dynamic simulator, which represents a two-element by two-element segment of the full scale array. Only the cable support system end cap attachment and folding concentrator reflector

ORIGINAL PAGE IS
OF POOR QUALITY

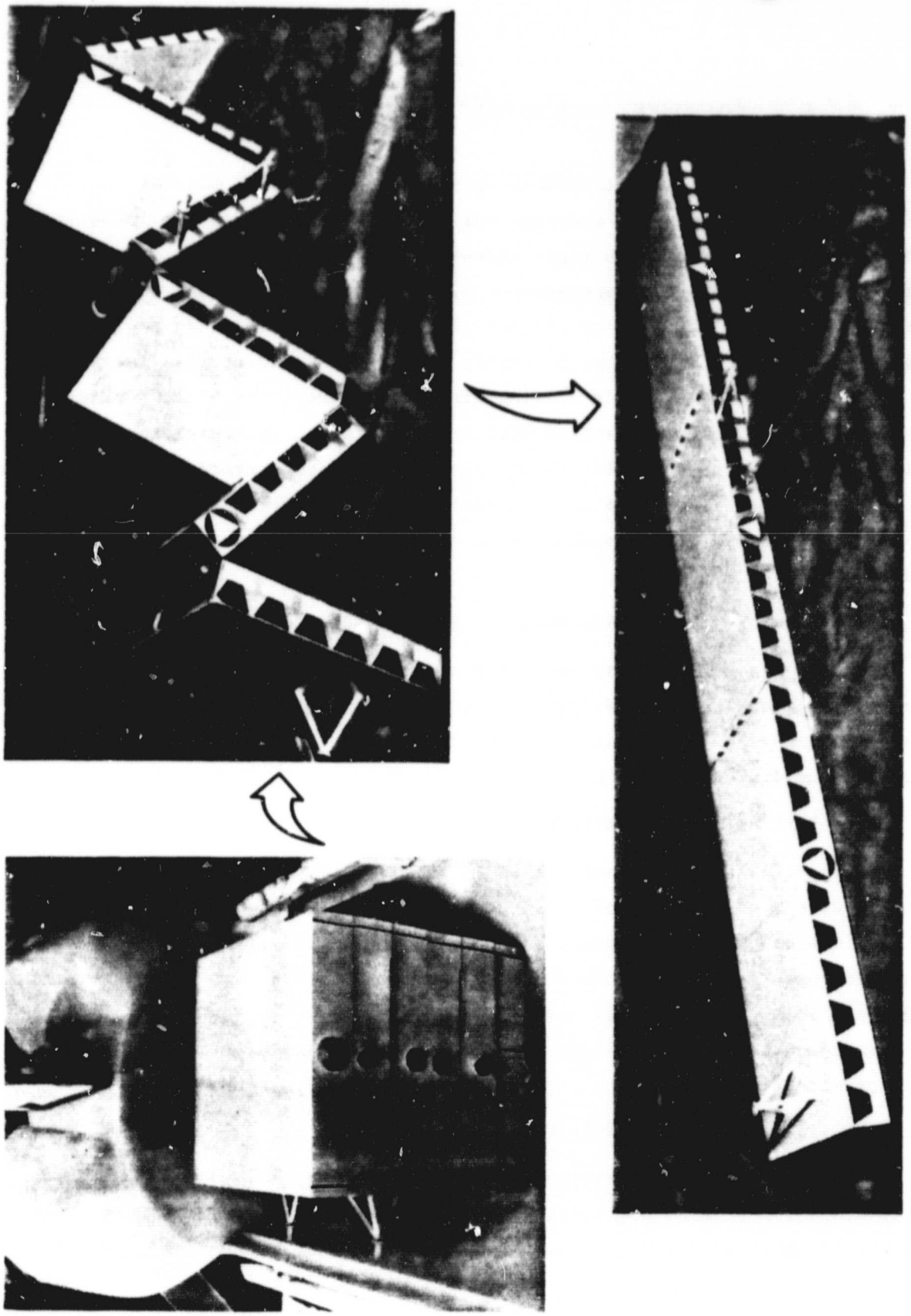

Figure 5.1-1. Articulated Model Deploying from Stowed Position

ORIGINAL PAGE IS
OF POOR QUALITY

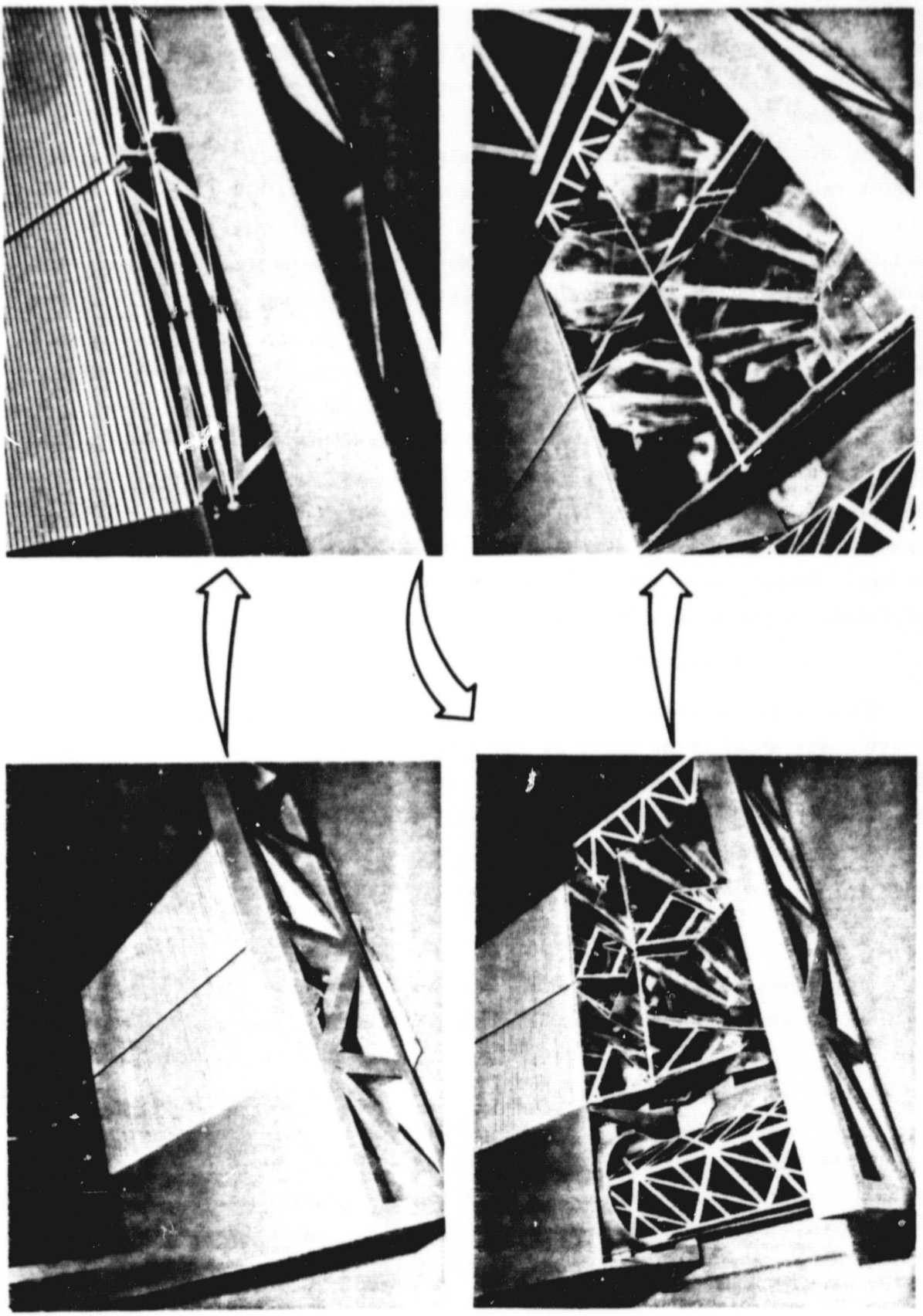

Figure 5.1-2. Four Element Model Undergoing Extension

panels are simulated in this model. The surface representing solar panels are non-functional and end cap extension is activated by means of a hand-driven screw instead of an astromast.

The simulator is designed to demonstrate the kinematics of extension and retraction for side-by-side concentrator elements under the action of end cap motion. The end caps and masts are made from expanded polyvinyl chloride (PVC) sheets 3.2 mm (1/8 inch) thick. Reflector frames are also 3.2 mm PVC covered with aluminized mylar to make reflector surfaces. The substrate/radiators are made from 0.63 mm (25 mil) aluminum sheet on which are bonded 0.76 mm (30-mil) aluminum panels to simulate the thickness of the solar cell stack. The model housing is made from 9.5 mm (3/8 inch) plywood with PVC sheets representing stacked concentrator elements. There are three support cables made of (3.2 mm) plastic-coated stainless steel attached to negators within the housing. Mast extension is simulted by means of a 25.4 mm (one-inch) diameter screw jack (8 threads to the inch) which extends and retracts the end cap. Monofiliment trip lines actuated by dead weights are used to retract individual concentrator elements.

5.2 REFLECTOR MATERIAL AND FABRICATION TESTS

These tests are informal shop and laboratory investigations of materials or processes about which there is insufficient design information to insure trouble-free fabrication or operation. Not all technology questions can be answered within the scope of the present program. Some issues require separate technology development programs prior to application in a full-scale array. These issues are identified and discussed in Section 4.0.

5.2.1 KAPTON FILM CREEP TEST

A preliminary creep test has been carried out. Specimens were uncoated Kapton film strips, one inch wide and 0.013 mm thick, clamped top and bottom with a ten-inch free length. They were loaded from 0.1 to 0.5 pounds, giving a stress of 0.34 to 6.9 N/mm^2 (50 to 1000 psi). Extension ($\Delta L/L_o$) was measure by cathetometer telescope (least count equivalent to ± 0.0004 units extension) using observations between scribe marks on the sample support rack and the applied weights. All measurements were made at room temperature after movement of the specimen rack to the telescope. For heated samples (heating accelerates the creep rate), a cool-down period of about two hours was introduced before measurement.

The results were inconclusive. Some (not all) samples failed after very small percent extensions and at stress levels far below published ultimate strength values. Test procedures and sample preparations are being reviewed and evaluated.

5.2.2 REFLECTOR FABRICATION SAMPLES

5.2.2.1 Film Reflector

A demonstration panel of the stretched film rigid frame type has been fabricated by adhesive bonding of a 0.05 mm Kapton sheet to a 3.3 mm thick epoxy impregnated graphite frame. The film has retained a drum tight condition over a period of 6 months. However, the film thickness is greater than the baseline design and no systematic temperature cycling has been performed. Further fabrication experiments are planned with more realistic panel samples.

5.2.2.2 Rigid Panel

A full-sized rigid panel with integral stiffening ribs has been molded from chopped graphite fiber filled polysulfone stock at Rockwell's Downey facility. Some curvature remains after removal from the mold and further work is planned on a thermal treatment to flatten the pannel. A surface treatment is required prior to aluminization to meet the specular reflectance requirements.

5.2.2.3 Concentrator Element

A full-size concentrator element designed for visual demonstration has been constructed using 3.2 mm thick aluminum sheet to simulate polysulfone graphite reflector frames. The reflectors were made of 0.051 mm (2 mil) aluminized Kapton bonded to the frames with room-temperature-cured epoxy. The substrate/radiator is made from 0.81 mm (32-mil) aluminum (compared to 0.63 mm planned for the flight version) and the solar cell stack is simulated with a sheet of 0.63 mm aluminum. Functional folding of reflector panels and substrate/radiator is accomplished using simple tape hinges made of 0.025 mm (one-mil) Kapton.

5.2.3 REFLECTOR SPECULAR QUALITY TESTS

The objectives of these tests is to screen candidate materials and process considered for fabrication of reflector panels and to provide a comparative evaluation of the specular reflectance.

5.3 SOLAR PANEL FABRICATION AND TESTING

5.3.1 PANEL PROCUREMENT STATUS

5.3.1.1 Silicon Solar Panel

A subcontract agreement was executed with Applied Solar Energy Corporation (ASEC) on April 29, 1982. Hardware items to be delivered are to supply two half panels and ten individual cells. Each panel consists of fifty 20 mm x 20 mm silicon cells laid down on Rockwell-supplied substrate/radiators. Each half-panel will consist of two electrical strings of configurations 2Px10S and 3Px10S. The string layout was selected to allow experimental data to be collected on power losses due to series interconnection of identical strings under non-uniform illumination. Each string is protected by a by-pass diode and parallel redundant isolation diodes. The cell size (20 mm x 20 mm) was selected to minimize the development requirements on the subcontractor. Large area, low CR optimized devices do not exist in either silicon or GaAs types. Also a one to one performance comparison with the GaAs cells will be facilitated. The GaAs are only available in approximately 20 mm x 20 mm size.

The Rockwell-fabricated radiator/substrate panels have been cut and formed. They will require additional surface processing before being shipped to the subcontractor. The subcontractor has fabricated all cells covered them, and has interconnected them into the requires strings. The ten individual cells have interconnects installed. The latest available test data, prior to string assembly, demonstrated the average conversion efficiency to be 14% at AMO, 28°C, CR = 6. The panel wiring diagram has been completed.

ASEC will also provide engineering data and a technology readiness review on a low CR optimized solar cells and panels.

5.3.1.2 GaAs Solar Panel

A subcontract agreement was executed with Spectrolab on June 1, 1982. Hardware items to be delivered are one half-panel and fifteen individual cells. The electrical and mechanical configuration of the GaAs half-panel will be almost identical to one of the silicon half-panels although the current-voltage characteristics (and the resultant conversion efficiency) will be markedly different. The commonality of cell layout will remove any configuration related factors in determining panel performance relative to the silicon panel.

Spectrolab will also be providing a technology readiness review on low CR optimized GaAs solar cells and panels. Spectrolab will be supported by Hughes Research Lab (HRL) as a second tier subcontractor. HRL is currently preparing mechanical samples of the GaAs cells for use in preliminary assessments on solderability and previously developed assembly techniques for the new low CR optimized devices and their plated (not evaporated) ohmic contacts.

5.3.2 PANEL ELECTRICAL TESTS

The subcontracts for both silicon and GaAs panels require the subcontractors to prepare a test plan and to carry out acceptance tests on the components to be delivered. Table 5.3-1 summarizes the performance requirements.

In addition to the measurements described in Table 5.3-1 a conductor isolation will be tested by imposing a minimum of 1000 V for 120 seconds. Leakage current should be less than 10^{-6} amps. Also a short-term thermal cycling test for the purpose of workmanship verification will be performed. Panels will be exposed to ten temperature cycles from 100°C to -100°C.

Table 5.3-1. Test Requirements for Solar Panels

Panel Performance (One Sun, AMO spectrum, 28°C)	Silicon	GaAs
Voltage at maximum power, volts/cell	0.454	0.830
Current at maximum power, amps/cell	0.135	0.98
Conversion Efficiency, percent	11.3	15.0
Diode Performance (100°C)		
Minimum forward current, amps	0.5	0.5
Maximum forward voltage, volts	1.0	1.0
Maximum reverse current, mA	0.5	0.5
Minimum reverse voltage, volts	150.	150.
Thermo-Optical Properties		
Normal emittance, minimum	0.81	0.81
Solar absorptance minimum	0.73	0.75

Rockwell will perform the tests described below prior to full scale concentrator testing. These tests are intended to fulfill two basic functions. These tests will verify the acceptability of the hardware as received from the

subcontractors ("buy-off") and will establish the photovoltaic characteristics of the hardware under known and controlled conditions (calibration and benchmarking).

The buy-off procedures are rudimentary checks of the current-voltage characteristics at standard test conditions (AMO, CR=1, 28°C). If the Rockwell measured values are in reasonable agreement with the subcontractors, the hardware will be found to be acceptable and the purchase order will be closed-out. This check will be performed on all hardware (cells and panels) received from the subcontractors.

Next, the hardware will be subjected to a more rigorous series of tests designed to accurately establish its photovoltaic characteristics. These tests will provide data which will be used to uncouple, as much as possible, the inherent device characteristics from the response of the devices to the extremely complex thermal-electrical-optical environment of the full scale concentrator testing. These calibration procedures consist basically of:

- Illuminated current voltage characteristics in reverse bias as well as normal power generating conditions
- Current-voltage characteristics versus illumination intensity
- Temperature coefficients on both current and voltage

These procedures will be performed in a manner such that they are not destructive to the devices under test. To this end, the individual cells will be characterized before testing the half-panels. This is of importance to the GaAs panel as not much data is available on low CR optimized GaAs devices and protecting the GaAs half-panel is of primary importance. In addition to providing a performance benchmark the reverse bias characteristics will be used to determine the requirements for the current bypass protection diodes in the array module design.

Based upon the available data two Si cells and two GaAs cells will be selected for further calibration testing. These cells will be established as viable intensity and spectrum correction standards. They will be segregated from the balance of the hardware and protected from handling damage by a water cooled mounting fixture. These devices will be calibrated against the best

available primary or secondary reference standard. These standards will be of paramount importance to the full scale concentrator element testing in natural sunlight as they will contribute to the corrections in panel performance due to terrestrial operation.

If, due to schedule considerations, any significant time elapses and/or handling of the solar panels occurs between the benchmark testing and the natural sunlight testing a pretest checkout of the panels will be performed. This checkout would identify any possible damage which had occurred to the panel in the interim. A similar test and comparison to benchmark results would be performed after completion of the natural sunlight testing for similar purposes. In this way, any change in device characteristics can be isolated from concentrator element system effects; the least it will allow is identification of a change in device characteristics which may affect interpretation of the test data.

5.4 FULL SCALE CONCENTRATOR TESTS

These tests are designed to demonstrate the combined optical, thermal and electrical performance of a full-scale concentrator element under terrestrial conditions. A further objective is to compare experimental performance with analytical predictions of terrestrial performance made by the same methodology and software used for design analysis of the on-orbit concentrator performance, thus validating the methodology.

5.4.1 TEST EQUIPMENT DESIGN

The minor differences between the baseline design and test hardware, documented in Table 5.4-1, require separate drawings for the two designs. An important additional item is the equatorial mount and support frame (fixture) on which the concentrator is mounted for testing. This equipment will be used in both the illumination tests and the electrical tests. It consists of a clock-driven equatorial mount, supporting a rigid frame (see Figure 5.4-1). The rigid frame is provided with adjustments of up to five degrees with respect to the tracker optical axis. The concentrator element will be attached to the support frame by steel pins which match, as closely as possible, the supports and attachments to be used in the preliminary design. The attachment system will be provided with means of making controlled distortions in reflector

Table 5.4-1. Differences between the Baseline Design and Test Hardware

ITEM	PRELIMINARY DESIGN	TEST HARDWARE
	MECHANICAL DESIGN COMPARISON	
Rigid Reflector	0.25 mm pocket 3.25 mm rib 500 Å VDA	0.38 mm pocket 3.25 mm rib VDA/Kapton laminate
Film Reflector	3.25 mm frame	3.25 mm frame (Polysulfone) 1.52 mm frame (AL)
Substrate/ Radiator	Stamped AL White silicone paint Bonded hinge No connector	Brake formed AL White epoxy paint Screwed hinge Connector bracket
Radiator to Reflector Hinge	Molded plastic pins cottered to fixed radiator hinge	Bonded steel pins thru removable hinge
Concentrator Suspension	Molded plastic lugs	Bonded steel pins
	ELECTRICAL DESIGN DIFFERENCES	
Wire Harness	Flat cable Welded assembly Hard wired	Round wires Soldered assembly Connector output
Silicon Half-Panel Array	50 mm x 50 mm cell $N_s \times N_p$ = 4x2 FEP cover adhesive Frosted cover 14% efficiency (panel)	20 mm x 20 mm cell $N_s \times N_p$ = 10x3, 10x2 DC93-500 cover adhesive MGF AR coat 18% efficiency (cell)
GaAs Half-Panel Array	20 mm x 20 mm cell $N_s \times N_p$ = 10x5 18% efficiency	22 mm x 20 mm cell $N_s \times N_p$ = 9x3, 9x2 15% efficiency
Interconnect	Welded Silver mesh	Soldered Kovar "Solaflex" (GaAs only)
Bypass Diodes	One per half-panel (Si)	One per electrical string
Isolation Diodes	Series/parallel redundant	Parallel redundant

ORIGINAL PAGE IS
OF POOR QUALITY

DETERMINE TERRESTRIAL OPERATING TEMPERATURES

- COMPARISON TO ANALYTICAL MODEL
- ESTABLISH M&P CRITERIA

Figure 5.4-1. Full Scale Concentrator Tests

geometry and also to allow controlled deployment and storage of the concentrator element.

For the illuminations tests the solar cell panel is replaced by a light receiver, a diffuse translucent sheet of material (e.g., ground glass) located in the plane which would be occupied by the solar cells in a complete concentrator assembly. The lower surface of the receiver is ruled in a rectangular grid. A camera provided with a flat-field, close-focus lens is mounted below the light receiver. The region between receiver and camera is maintained light-tight by means of a housing.

For the verification tests electrical and thermal instrumentation will be added as shown in Figure 5.4-1. The solar panel output will be assessed through a connector which is attached to the radiator. A wire harness will be mated to this connector and will be terminated in a breakout box (patch panel). This box will serve as the interface between the data acquisition system and the panel under test. It is at this box that the electrical strings will be configured (series or parallel) for a specific test. Type T thermocouples (5 minimum) will be used to monitor operating temperatures during the test. Junctions will be temperature compensated. Solar cell surface temperatures will be measured before and after test by means of a hand-held infrared radiometer capable of resolving an individual 20 mm x 20 mm solar cell. These measurements will be correlated with the thermocouple measurements.

Local meteorology measurement equipment (weather instrumentation) is required to measure air temperature, wind velocity, relative humidity and diffuse solar radiation content. A reference standard solar cell, for intensity and spectrum corrections, is located on the support frame so as to be oriented normal to the sun. In order that conditions most closely approach those expected in space, tests will be carried out at high altitude in clear air under minimum wind conditions.

Jet Propulsion Lab's Table Mountain Observatory, Wrightwood, California is recognized by the industry as an acceptable natural sunlight test facility. Preliminary tests of all equipment will be carried out at Rockwell's Seal Beach facility.

5.4.2 CONCENTRATOR ILLUMINATION TESTS

This test is designed to measure the distribution of illumination over the plane of the solar cell panel produced by full scale reflector panels assembled in a realistic concentrator configuration.

5.4.2.1 Photometric Calibration

Reflector panels are replaced by black, non-reflecting surfaces and the lower surface of the light receiver is covered by a black sheet fitted with a slide which can be withdrawn to expose progressively more of the receiver. With the receiver exposed to one sun (no significant reflection from black panels) a multiple exposure is made (at identical shutter speeds) as the slide is withdrawn one position at a time. The resulting developed film provides a calibration curve relating optical density to relative exposure in suns.

5.4.2.2 Illumination Tests

The calibration described above should be performed prior to installation of a set of reflector panels. A set of panels are then installed and illumination patterns on the receiver plate are photographed for a series of pointing angles and for conditions of controlled distortion of the panel holders if desired. A photographic series should end with a calibration frame.

Film from the illumination tests should be developed in a reproducible manner. The negatives should be analyzed by densitometer using multiple scans across the image of the light receiver. The calibration curve(s) from the same film are used to convert optical density to illumination level in suns.

The experimental illumination patterns obtained from this test will be compared with analytical predictions obtained from the ray-tracing program RAYPYR. The multiple source capability of RAYPYR will be used to approximate the strong diffuse component of sunlight coming from angles near the solar direction.

5.4.3 CONCENTRATOR VERIFICATION TESTS

This test is designed to obtain experimental performance on a full-scale concentrator element under conditions simulating as closely as possible to the flight conditions for which it has been designed. This experimental performance will be compared with analytical predictions using the comprehensive

thermal-electrical math model.

5.4.3.1 Calibration and Pre-Test Operations

A series of electrical tests will be performed on the solar cell half-panels prior to their assembly into a concentrator element. These tests, which are described in Section 3.4.2, include conductor isolation checks and I-V determinations for each electrical string under AMO simulation. Panel thermocouples will be calibrated against a suitable secondary standard over the range 25 to 150°C. The concentrator will be aligned with the support frame by means of adjustable attachments. Attachment settings after alignment will serve as a zero reference, from which controlled distortions of reflector geometry can be accomplished.

5.4.3.2 Environmental Measurements

Tests will be conducted in clear weather during the mid-day hours (10:00 to 14:00 solar time) with wind less than 3 meters per second. Wind velocity, air temperature, relative humidity and reference solar cell output should be measured prior to the initiation of testing and periodically during the test period. If wind velocity exceeds 3 mps, air temperature varies by more than 5°C or reference solar cell output varies by more than 5% testing should be discontinued until all parameters are again within range.

5.4.3.3 Verification Tests

Performance tests of complete concentrator assemblies will be performed in natural sunlight. Two identical series will be carried out, one for a panel consisting of two silicon cell half-panels and the other for a mixed panel made up of a silicon cell and a GaAs cell half panel. For each series, the concentrator will be aligned with zero pointing angle and no distortion and allowed to come to thermal equilibrium while tracking the sun. When equilibrium is reached, the I-V characteristics of each electrical string will be recorded by sweeping the applied voltage. I-V characteristics will then be obtained for the desired pointing angles and concentrator distortions, one after the other. No special thermal equilibration time is required between I-V recording. When a new panel is installed, prior to starting a new series, a warm up is required.

5.4.3.4 Post-Test Operations

Following the verification tests, concentrator alignment is checked and panel electrical characteristics are determined as described under "pre-test" operations". Analytical predictions will be made of individual electrical string outputs using the coupled thermal-electrical math model written for the Rockwell XF25. The model will be similar to that used for space performance predictions. Detailed differences between the demonstration unit and the baseline concentrator will be taken into account in the math model. These include: difference in the electrical network; difference in solar cell characteristics and spectral quality of the light; the presence of diffuse sky radiation; atmospheric attenuation; absence of adjacent concentrators and finally the existence of convective cooling.

These tests will provide an assessment of the performance of a full-scale concentrator prototype and a comparison between analytical predictions and experimental results.

6.0 DEVELOPMENT PLANNING AND FUTURE EFFORT

The development planning objectives are: to identify the technology deficiencies which must be overcome in order to achieve the desired performance and cost goals; to develop a supporting research and technology plan, including funding and schedule information, by which the technology deficiencies may be removed; to develop a plan to fabricate a ground test model.

6.1 TECHNOLOGY ASSESSMENT

The design studies carried out in the process of defining the baseline solar array configuration have led to the identification of several technology areas in which more effort will be required than can be applied under the demonstration phase of the present program. They are summarized in Table 6.1-1. These areas are those in which knowledge is deficient either as to the performance of a component or as to methods of achieving needed cost or weight improvement. The four areas are briefly discussed below.

Table 6.1-1. Technology Assessment— Identification of Technology Definciencies

Technology Deficiency	Remarks
Module weight	Candidates for weight reduction: • Canister/mast assembly • Substrate radiator • Concentrator reflector panels
Stability (lifetime) of surface optical properties	Surfaces critical for array performance • Reflectors • Radiator selective coating
Silicon solar cell fabrication	Characteristics/capabilities • Interconnect welding • Thinner, higher efficiency cells • Low-cost covers/bonding
GaAs solar cell fabrication	Characteristics/capabilities • Interconnect welding • Low-cost covers/bonding • Cell producibility • Lower cost, higher efficiency cells

The solar array is not weight-critical for low-earth, moderate-inclination orbits. However, weight would become a problem for possible future extended orbit applications. Moreover, weight reduction is often (though not always) associated with cost reduction. The three heaviest components are identified as candidates for technology programs aimed at weight reduction.

Because of the difficulties of simulating the particulate and radiation environment of space there is presently no useful data with which to predict the long-term (10 year) stability of thermo-optical surface coatings with any certainty. The advent of operational Shuttle flights makes possible the controlled exposure and recovery of representative surfaces after long flights in low earth orbit as piggy-back experiments on a Shuttle-launched satellite. Functional tests and microscopic examination of the recovered samples will provide a sound basis for degradation projections out to a 10-year lifetime or more.

Both gallium arsenide and silicon solar cells fall short of their ultimate projected efficiencies and are therefore candidates for further performance improvement. The severe thermal cycling environment associated with concentrating arrays makes welded interconnects desirable. Again, both cell types show deficiencies as far as high-yield production welding is concerned.

Gallium arsenide solar cells have entered the development and production cycle later than silicon cells. Therefore, the volume production of low-cost, high-performance GaAs cells suitable for low CR application remains to be demonstrated. The low cost bonding of fused silica covers to GaAs cells has not yet been developed. The GaAs solar cells are quite brittle and do not conform readily to the curved platen technique used for bonding silicon cells.

6.2 SUPPORTING RESEARCH TECHNOLOGY (SRT) PLAN

For each item identified under the technology assessment (Table 6.1-1) procedure, a concise statement of the problem will be generated and a summary of the individual tasks required to resolve it will be prepared. The corresponding funding by individual task will be estimated by government fiscal year. For each item, a justification of need to resolve the technology deficiency will be prepared. This justification will relate the tasks identified with this program to other applicable efforts within NASA and the

other government agencies. For each task a schedule will be prepared containing realistic milestones, the dates of availability of supporting technology and a final due date for resolution of the technology deficiency. A time-phased cost estimate will be accumulated for the SRT plan as a whole.

6.3 GROUND TEST MODEL FABRICATION PLAN

The purpose of this subtask is to develop a comprehensive plan for the fabrication of the ground test demonstration model and its associated special test equipment and required tooling. The plan will address requirements for model design, supporting design analysis, material selection, tooling, fabrication, final assembly and test. Schedule and cost estimates will be provided in the plan.

Pursuant to discussions held during the first quarterly briefing in February, consideration has been given to the fabrication of a combined ground and prototype flight test article. Table 6.3-1 summarizes the pros and cons of this approach. Such an approach would yield design and operational information more rapidly than separate ground and flight test phases. The cost impact of introducing flight capability could be minimized by designing a fractional-power model consisting of full-scale concentrators and other components reduced in number from those making up a full-size module. For example, the model could consist of a single mast/canister assembly, extending concentrator elements from a housing in one direction only.

The incorporation of flight test capability to the model would provide significantly greater realism in the areas of: thermal performance in a vacuum environment; kinematic behavior under zero g and the behavior of sliding contacts under vacuum. An earlier ground test phase on the same hardware could be used to "wring out" problems of assembly, optical alignment and functioning of mechanisms.

6.4 DESIGN UPDATE

6.4.1 ISSUES TO BE RESOLVED

In order to complete the baseline design, certain decisions have been made in advance of demonstration tests and design studies scheduled later in the program. Such decisions are tentative and may be changed to produce a refined array design of later test results warrant. In fact all design details remain

Table 6.3-1. Model Fabrication Plan

Objectives: Comprehensive fabrication plan for demonstration model and associated test equipment.		
Options	Advantages	Disadvantages
Ground Test Model	Accessibility of test item for observation, measurement and modification or repair	Effects of zero-g, vacuum and space radiation very difficult to simulate accurately
	Size restrictions are minimal	
Shuttle-Launched Space Model (first opportunity STS-26, 4/12/85)	Technical realism	Substantial integration and launch costs
	Recoverable test item	Volume, weight and schedule constraints

subject to refinement if new information indicates a significant improvement in array weight, cost or performance can be achieved. Certain design issues have been deliberately left for later decision.

6.4.1.1 Reflector Panels

Two options are being carried along in parallel for the fabrication of the reflector panels, the stretched film and the aluminized rigid panel. One of these will be selected for the final design upon completion of fabrication and optical tests.

6.4.1.2 Solar Cell Size

For reasons of cost and performance large-area cells may be preferred. In particular, if GaAs cells are larger than the 20 mm x 20 mm baseline size can be used, array costs can be reduced. This issue will be explored in conjunction with the subcontractor later in the program.

6.4.1.3 Payload Bay Support for Stowed Modules

A strong structural support is required to carry the launch loads on the stowed modules out to attach points in the Shuttle payload bay. Several approaches have been considered including the use of cradles or bridge fittings and shear panels.

6.4.2 CONTINUING STUDIES

Major emphasis during the second half of the program will be placed on design and demonstration testing. However, some analytical studies will be carried out in support of these activities.

6.4.2.1 Structures

Working with the subcontractor effort will be made to reduce the weight of the canister/mast subsystem. Detailed design of suitable deployment latches for container housing and end cap segments will be carried out. Design of internal support structures for stowed modules will also be accomplished during the second half of the program. The baseline cable extension mechanism configuration will be reviewed in order to achieve weight reduction if possible. The acoustic response of the stowed concentrator elements (particularly the solar panel) to Shuttle launch environment will also be determined. Generic designs will be developed for the hardware components needed to interface with a typical user spacecraft.

6.4.2.2 Reflector Panels

A continued effort will be made to reduce reflector panel weight. Literature study and analysis will be used to project estimates of long-term degradation of surface reflectivity.

6.4.2.3 Electrical Performance

A combined thermal-electrical math model will be developed, which considers air-mass-one effects on the incident light and convective cooling of the solar panel, will be developed for use in evaluating the ground demonstration tests.

7.0 REFERENCES

1. *Study of Multi-kW Solar Arrays for Earth Orbit Applications, Final Report*, (NASA-MSFC NAS8-32988) Rockwell International Corporation, SSD 80-0064; May 15, 1980.

2. *NASA-MSFC Study of Multi-kW Solar Arrays for Earth Orbit Application, Final Report*, Lockheed Missiles and Space Company, LMSC-D715841; April 1980.

3. *Study of Multikilowatt Solar Arrays for Earth Orbit Applications, Final Report*, TRW, 33295-6001-UT-00; September 19, 1980.

4. *Space Shuttle Program, Level II Program Definition and Requirements, Space Shuttle System Payload Accommodations*, NASA, JSC 07700, Volume XIV, Revision G; September 26, 1980.

5. French, Edward P., *Heat-Rejection Design for Large Concentrating Solar Arrays*, Prepared for and contained in the Proceedings of the 15th IECEC, Seattle, Washington; August 18-22, 1980, pp. 394-399.

6. Burkhard, Donald S., et. al., *Solar Concentrating Properties of Truncated Hexagonal, Pyramidal and Circular Cones,* Applied Optics, Volume 17, No. 15, pp 2431; August 1, 1978.

7. Patterson, R. E. and Yesui, R. K., *Parametric Performance Characteristics and Treatment of Temperature Coefficients of Silicon Solar Cells for Space Application,* JPL Technical Report 32-1582, May 15, 1973.

APPENDIX A.

DRAWINGS

This appendix provides three drawings that describe the general array module preliminary design and the concentrator element test configuration. A complete list of drawings planned for this contract contract effort is shown in Figures 3.0-1 and 3.0-2 in Section 3.0.

Drawing V416-935002 - The assembly of the six container assemblies comprising the array module is shown. All of the interfaces from container to container including latches, hinges and motors are detailed as well as the overall assembly envelope are defined.

Drawing V416-935100 - The housing assembly with all of the subassemblies and components installed is shown. The housing dimensional envelope is provided and a typical housing structure is depicted. The concentrator element stacks are shown in the stowed as well as extended condition.

Drawing D416-450000 - The test hardware concentrator element is shown including the test fixture. The fixture is designed to allow for racking and misalignment of the concentrator element for obtaining performance characteristics for both aligned and misaligned conditions. The concentrator element shown is for a combination solar panel consisting of one silicon cell half panel and one gallium arsenide half panel. The test configuration will also include a solar panel consisting of two silicon cell half panels.

ORIGINAL PAGE IS
OF POOR QUALITY

3.2
127.6

FOLDOUT FRAME

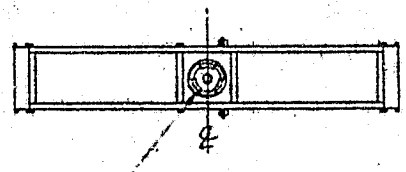

℄

℄ USER SPACECRAFT ATTACH POINT

ORIGINAL PAGE IS
OF POOR QUALITY

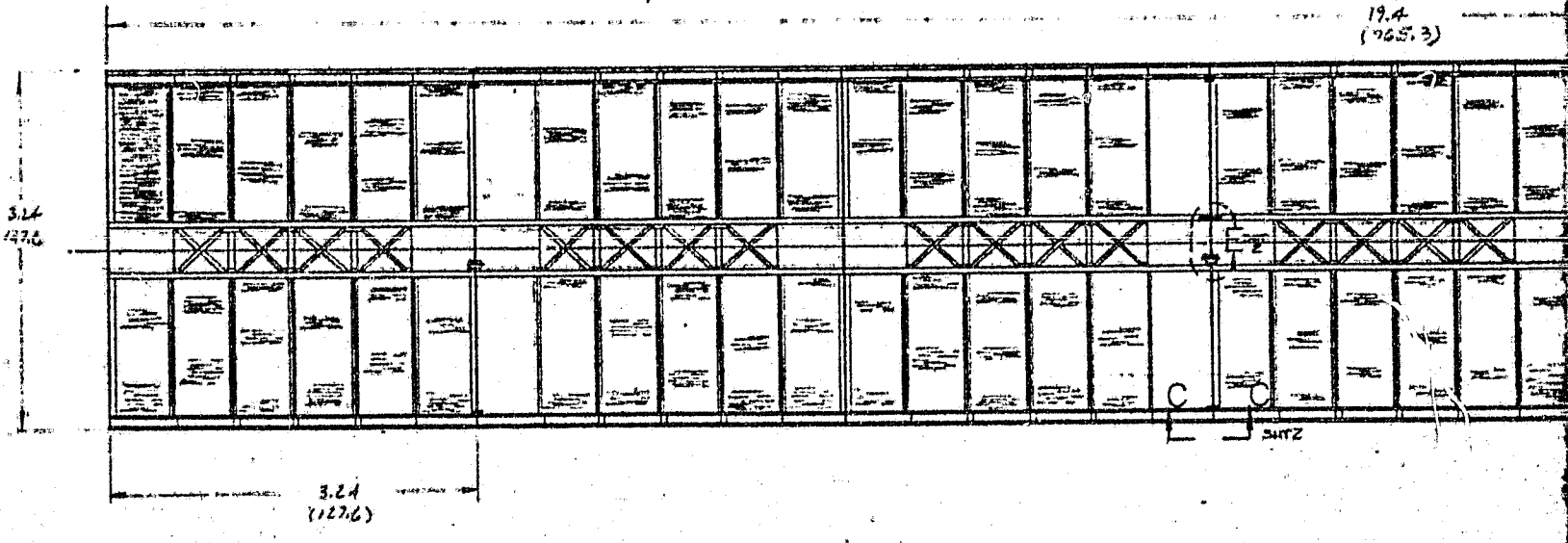

2 FOLDOUT FRAME

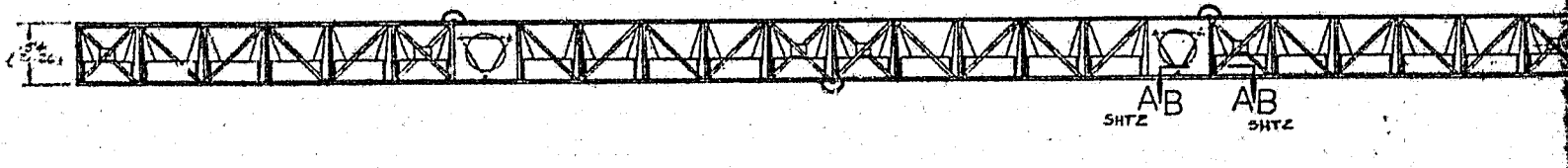

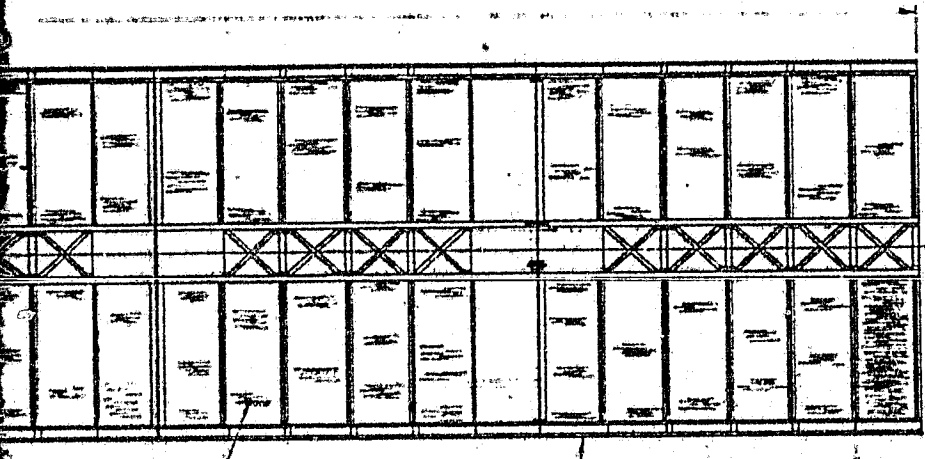

3 FOLDOUT FRAME

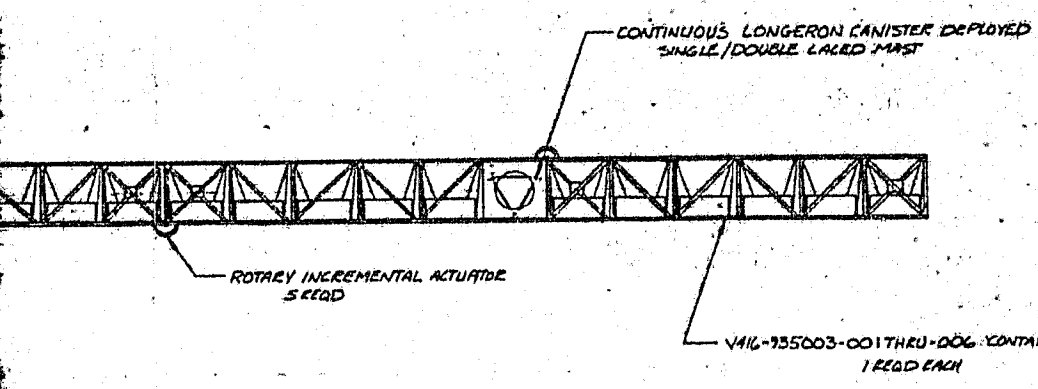

ORIGINAL PAGE IS
OF POOR QUALITY

NOTES: UNLESS OTHERWISE SPECIFIED
1. ALL DIMS ARE IN M, INCHES IN ( )

4 FOLDOUT FRAME

ORIGINAL PAGE IS
OF POOR QUALITY

QTY REQD	QTY REQD	QTY REQD	QTY REQD	QTY REQD	QTY REQD	DASH ENDIT	PART OR IDENTIFYING NUMBER	NOMENCLATURE OR DESCRIPTION	MATERIAL	DATA SPECIFICATIONS SIZES, NOTES, SUPPLIERS	ZONE
						5		DEPLOYMENT MOTOR			
						16	V416-935305	WIRE HARNESS ASSY			
						1	-006	V416-935002	CANNISTER ASSY		
						1	-005				
						1	-004				
						1	-003				
						1	-002				
						1	-001	V416-935003	CANNISTER ASSY		
						-001		V416-935002			

PARTS LIST

FROM	QTY	NEXT ASSY	USED ON	END ITEM NO.	THRU
-001	1	V416-935001	LCRSA		

NEED FOR DASH ITEM | APPLICATION | EFFECTIVITY

UNLESS OTHERWISE SPECIFIED: DIMENSIONS ARE IN INCHES. TOLERANCES ON: DECIMALS .XX ±0.01, .XXX ±0.005, FRACTIONS ±1/64, ANGLES ±0° 30'. FINISH NOTED "SMALL". .001 THRU .063 +.005 −.001, .064 THRU .124 +.006 −.001, .125 THRU .249 +.007 −.002, .250 THRU .499 +.010 −.002, .500 THRU .749 +.012 −.003, .750 THRU 1.000 +.015 −.003, 1.001 THRU 2.000 +.020 −.003

DR BY MBAS 7/30/86
CHK BY
APPROVED BY

Rockwell International Corporation
Rocket Division
12214 Lakewood Boulevard • Downey, California

SOLAR ARRAY MODULE
LCRSA

SIZE J | CAGE/DRAWING NO. 03953 | DRAWING NO. V416-935002
SCALE 1/4=1 | SHEET 1/1

V416-935002

4 3 2 1

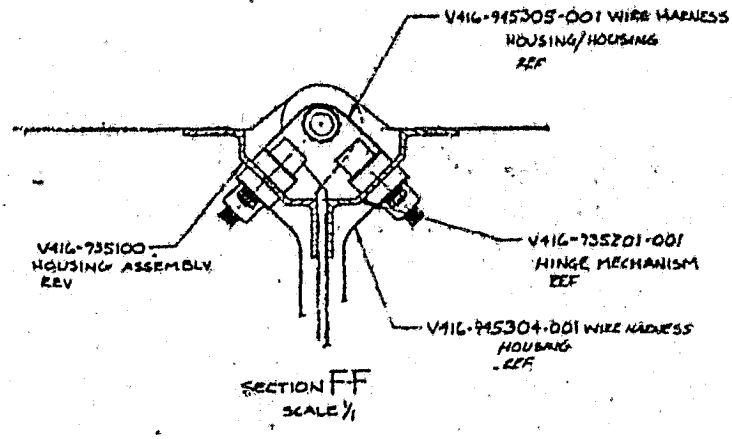

SECTION FF
SCALE 1/1

ORIGINAL PAGE IS
OF POOR QUALITY

FOLDOUT FRAME

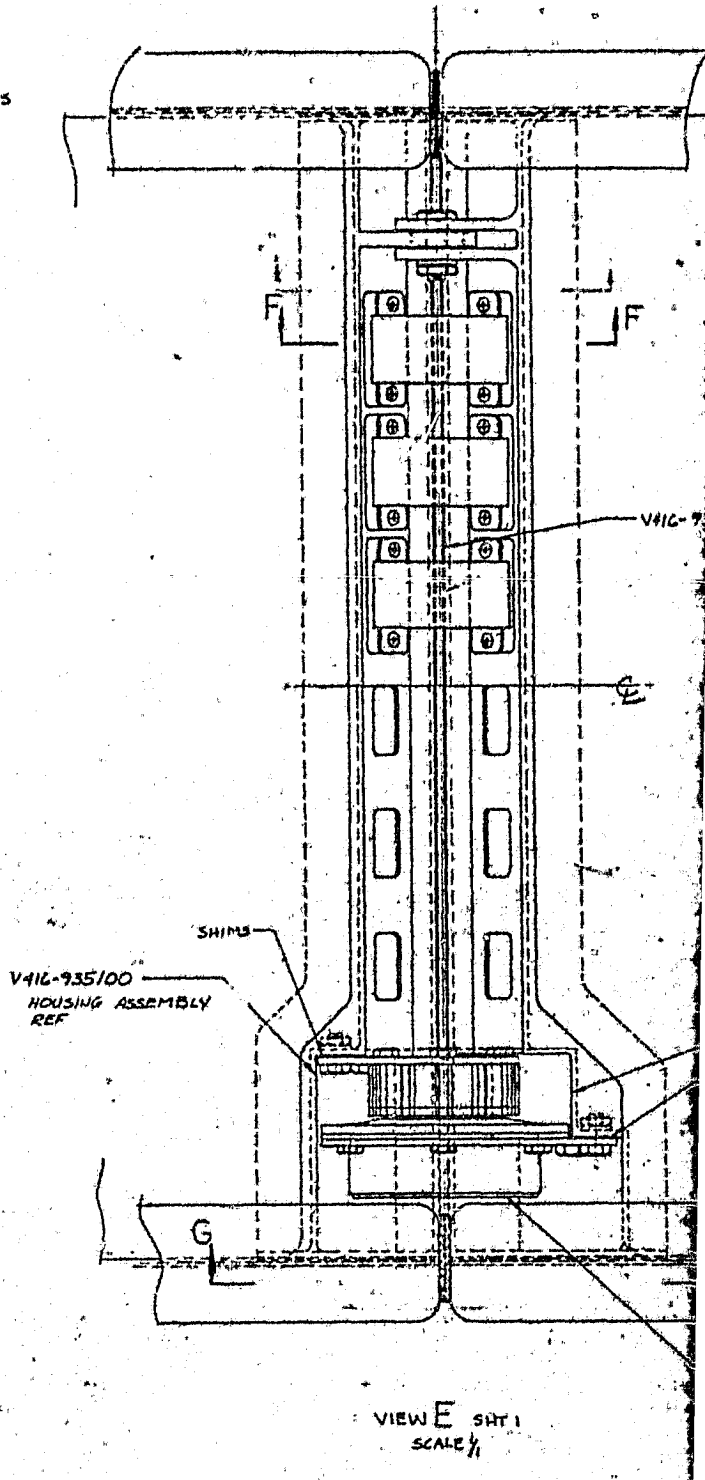

VIEW E SHT 1
SCALE 1/1

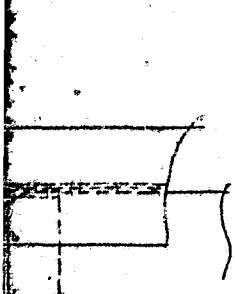

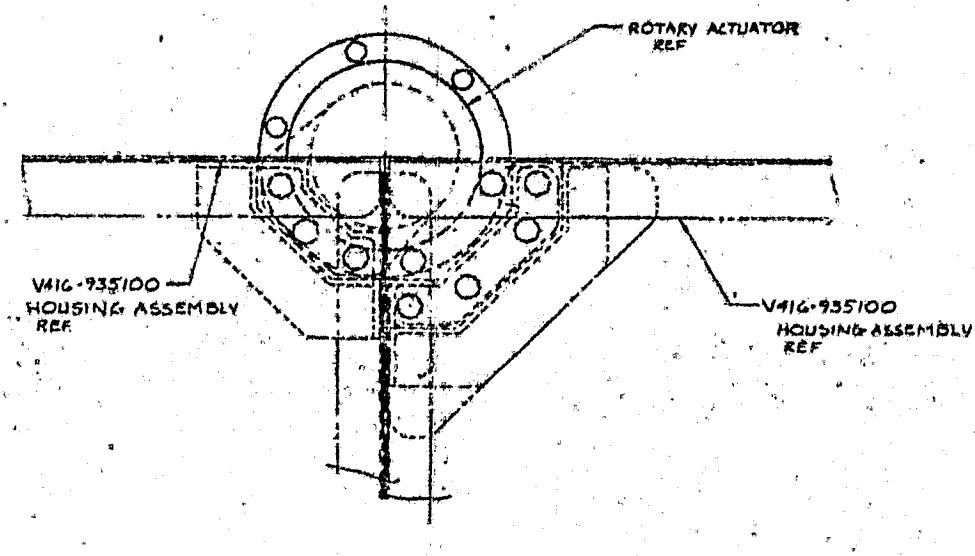

F

V416-935201-001 HINGE MECHANISM
REF

VIEW GG
SCALE 1/1

ORIGINAL PAGE IS
OF POOR QUALITY

℄

2

FOLDOUT FRAME

V416-935100
HOUSING ASSEMBLY
REF

SHIMS

G

ROTARY INCREMENTAL ACTUATOR
OUTPUT STEP ANGLE; .0200 DEGREES
HARMONIC DRIVE RATIO; 100
OUTPUT STEP RATE; 450 STEPS/SEC, 9.0 DEG/SEC
OUTPUT CAPABILITY; 6.8 N-m (100 in-lbs) FRICTIONAL
HOLDING TORQUE; 17.0 N-m (150 in-lbs) POWERED
WEIGHT; .91 Kg (2.0 LBS)

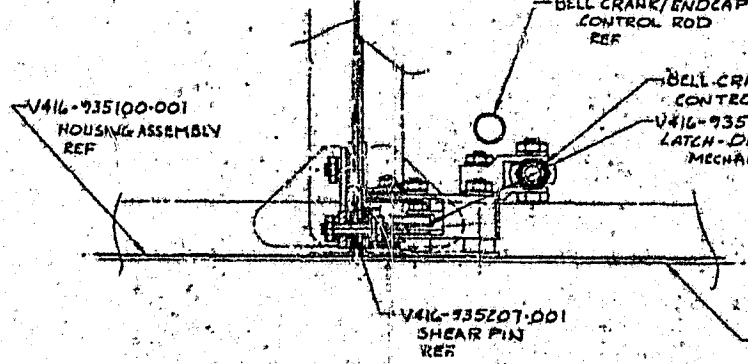

SECTION D-D
SCALE 1/1

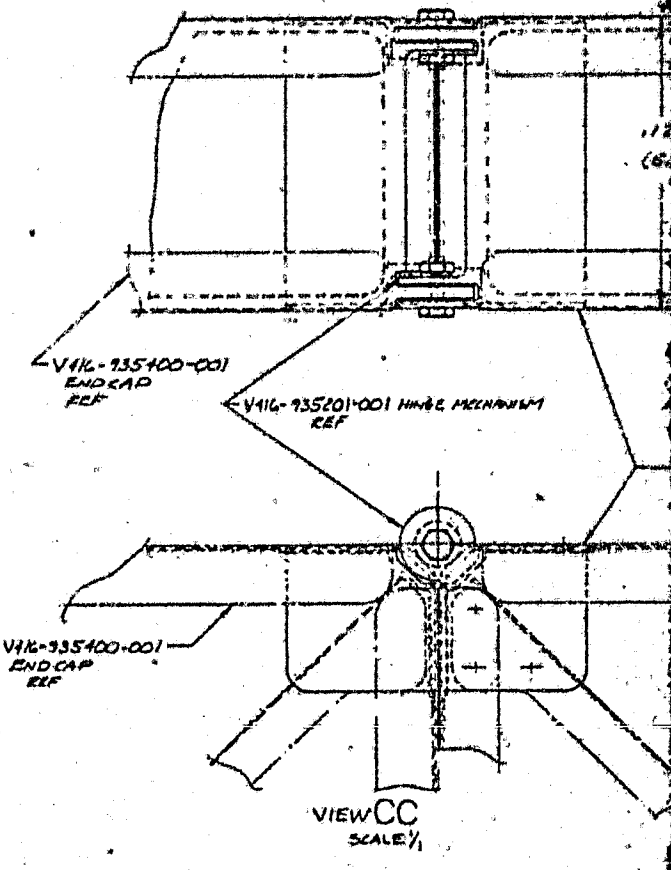

VIEW CC
SCALE 1/1

ORIGINAL PAGE IS
OF POOR QUALITY

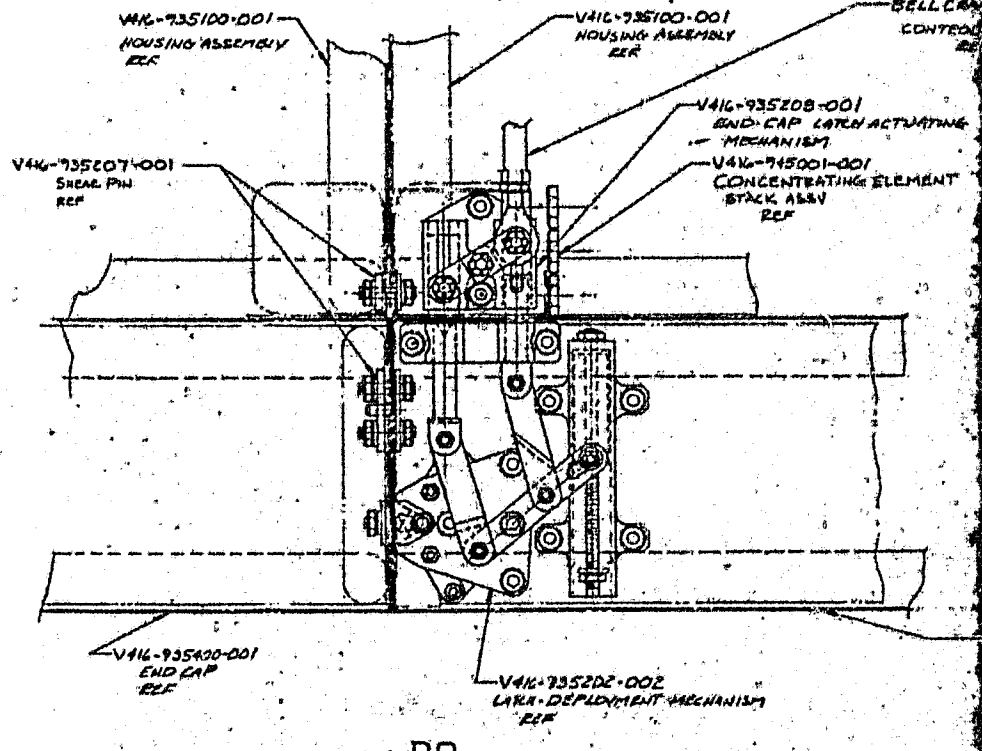

VIEW BB
SCALE 1/1
(VIEW TYPICAL OF END CAP BASE/BASE LATCH MECHANISM)

3

FOLDOUT FRAME

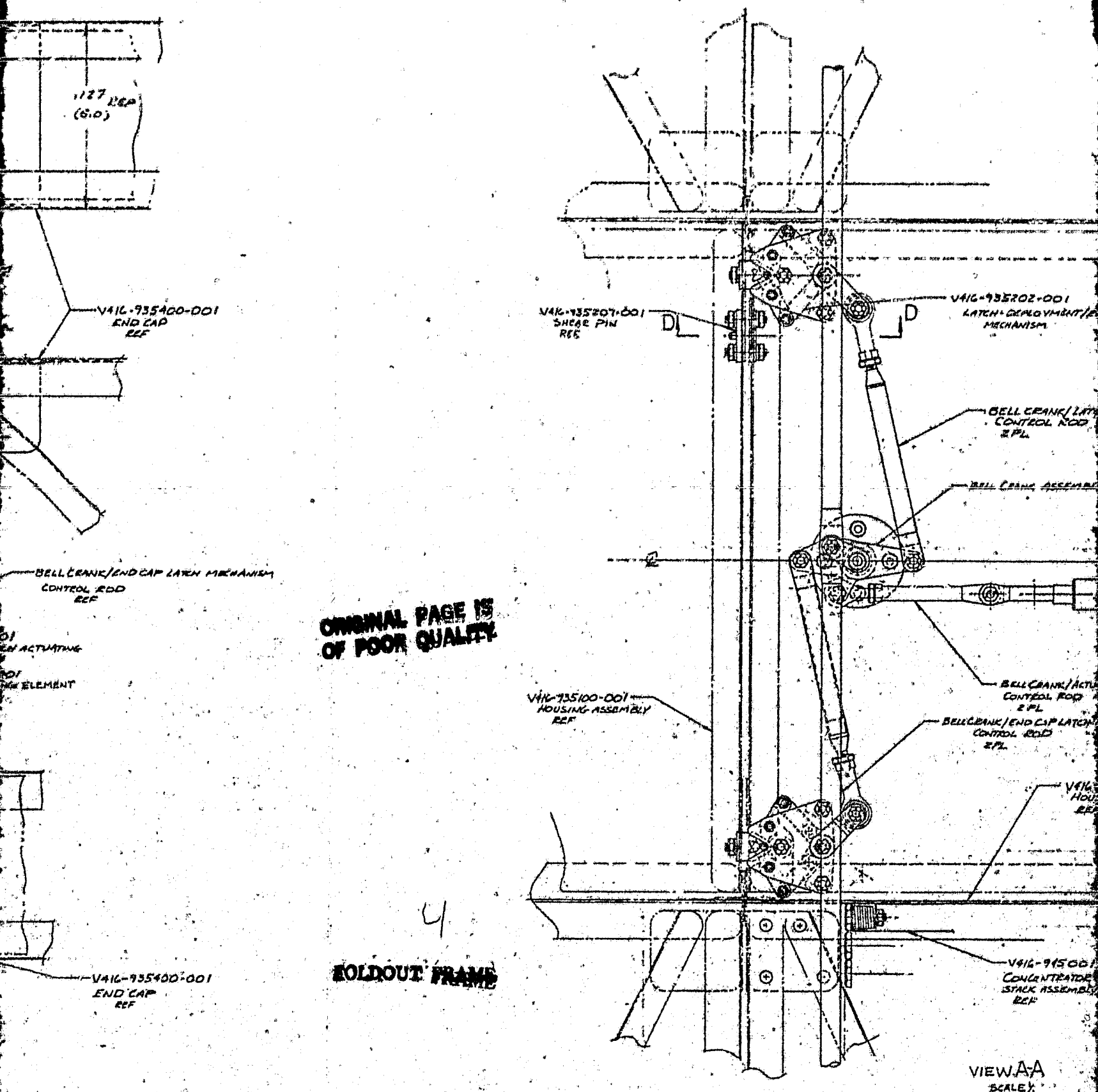

ORIGINAL PAGE IS OF POOR QUALITY

4

FOLDOUT FRAME

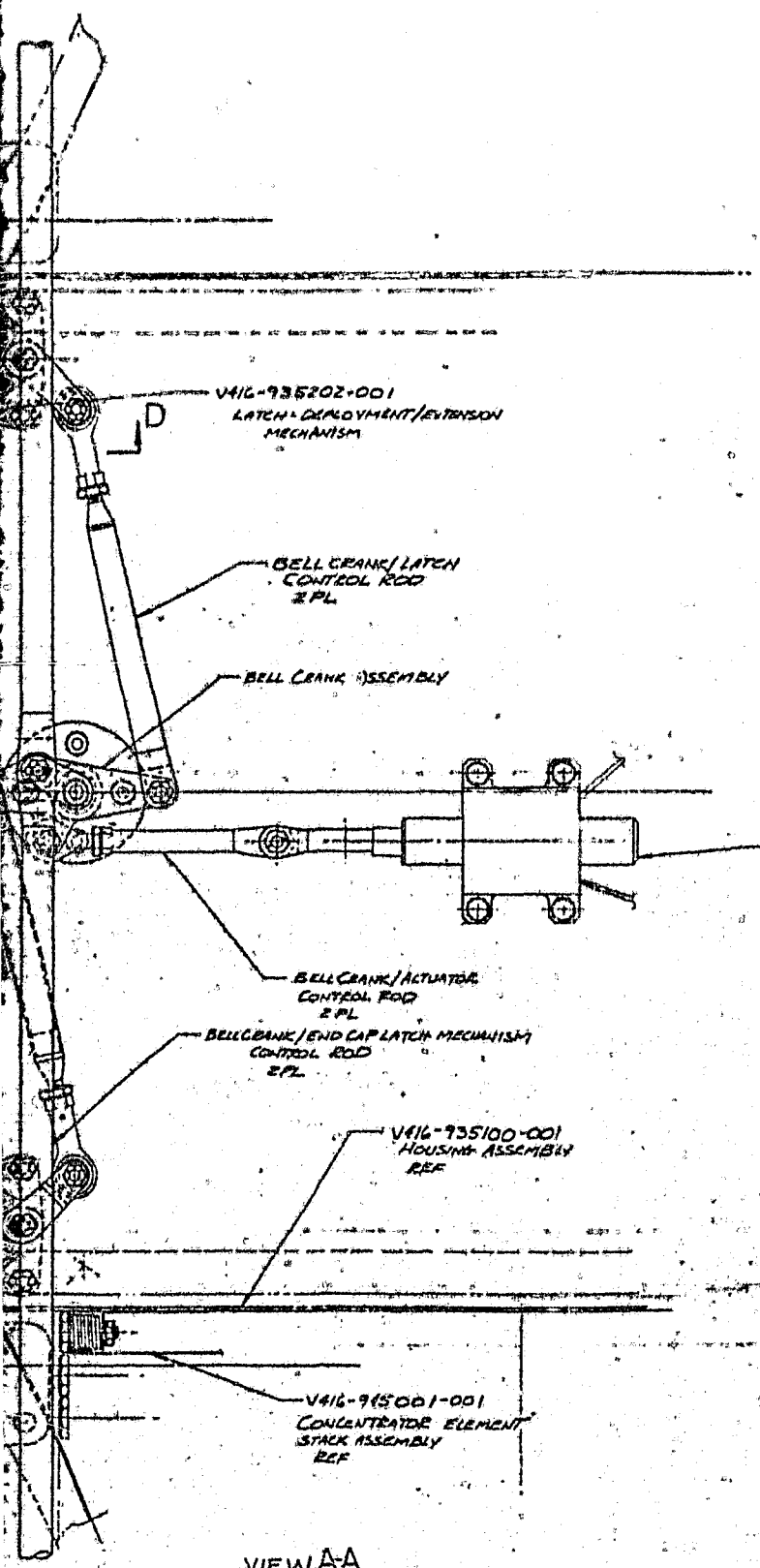

VIEW A-A
SCALE 1/1
(VIEW TYPICAL LATCHING MECHANISM)

LINEAR INCREMENTAL ACTUATOR

GENERAL SPECIFICATIONS
OUTPUT STEP INCREMENT .0141 mm (.000536 in)
STEPS PER mm) 70.9 (1 INCH) 1800)
DRIVE MOTOR; 4.0 DEGREE PERMANENT MAGNET STEPPER
STEP RATE; 0-600 STEPS/SECOND (11 8.48 mm, .333 in PER SEC)
OUTPUT FORCE; 44.5 N (10.0 LBS) MIN.
HOLDING FORCE 13.3 N (3.0 LBS) MIN.
TOTAL ASSEMBLY WEIGHT 2.1 Kg (4.7 LBS)

ORIGINAL PAGE IS
OF POOR QUALITY

FOLDOUT FRAME

A-5, A-6

DR BY	M. BIES	9/23/82
CHK'D		
APPROVED BY		

SOLAR ARRAY MODULE

SIZE	CAGE CODE NO.	DRAWING NO.
J	03953	V416-935002

SCALE 1/8 SHEET 3 OF 8

ORIGINAL PAGE IS
OF POOR QUALITY

QTY REQD	QTY REQD	QTY REQD	QTY REQD	QTY REQD	QTY REQD	CHG NO.	PART OR IDENTIFYING NUMBER	NOMENCLATURE OR DESCRIPTION	MATERIAL	BASIC SPECIFICATIONS SPEC, NOTES, SUPPLIERS	ZONE
10	10	10	8	8	8	-003	V416-935202	SLIDE ASSEMBLY			
132	132	132	132	132	132	-002	1	1			
650	650	650	520	520	520	-001	V416-935202	SLIDE ASSEMBLY			
2	2	2				-002	1	1			
			2	2	2	-001	V416-935206	EJECTOR TRAP ASSY			
2	2	2	1			-002	1	1			
			2	2	2	-001	V416-935205	EJECTOR TRAP ASSY			
5	2		4	3	1	-003	V416-935304	WIRE HARNESS HOUSING			
1	1	1	"			-002					
			1	1	1	-001	V416-935304	WIRE HARNESS HOUSING			
12	12	12	10	10	10	-001	V416-935302	WIRE HARNESS ELEMENT/SLIP			
14	14	14	12	12	12	-001	V416-935204	CONT. STR. TRAP ASSY			
14	14	14	12	12	12	-001	V416-935203	CONT. CAL PROBE			
12	12	12	10	10	10	-001	V416-935001	CONCENTRATING STRUC. ASSY			
"			2	2	2	-001	V416-935103	MAST / CANISTER ASSY			
1						-005	V416-935101	HOUSING			
"	1					-004					
		1				-003					
			1			-002					
				1	1	-001	V416-935101	HOUSING			
-006	-005	-004	-003	-002	-001		V416-935100				

-002 THRU -006 = SAME (EXCEPT AS NOTED)
-001 SHOWN

PARTS LIST

-006	1	V416-935003	LCESA		
-005	1				
-004	1				
-003	1				
-002	1				
-001	1	V416-935003	LCESA		
FIND NO.	QTY	NEXT ASSY	USED ON	END ITEM NO.	THRU

UNLESS OTHERWISE SPECIFIED DIMENSIONS ARE IN INCHES
TOLERANCES ON: DECIMALS ANGLES
.XX in ± .03 ± 0° 30'
.XXX in ± .010
UNLESS NOTED "SHALL"
.06 THRU .250 = ± .005 — .010
.251 THRU .500 = ± .005 — .015
.501 THRU .750 = ± .005 — .020
.751 THRU 1.000 = ± .005 — .025
1.001 THRU 2.000 = ± .010 — .030

DR BY M BISS 9/25/84
CHK BY
APPROVED BY

Rockwell International Corporation
Rocketdyne Division
Canoga Laboratories Rocketdyne • Downey, California 90241

HOUSING ASSEMBLY
LCESA

SIZE	CODE IDENT NO.	DRAWING NO.
J	03953	V416-935100

SCALE FULL | SHEET 1/2

ORIGINAL PAGE IS
OF POOR QUALITY

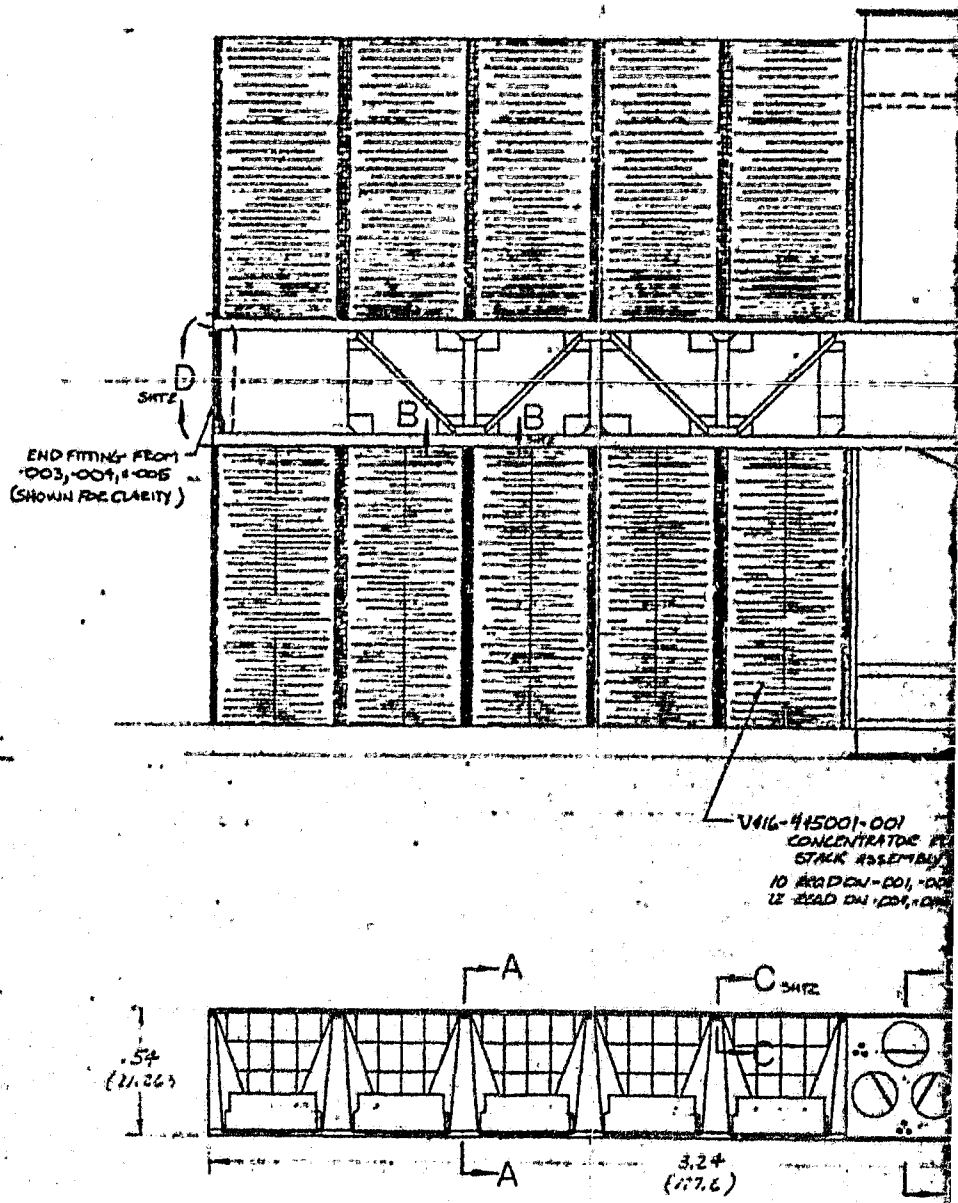

FOLDOUT FRAME

V416-935100

ORIGINAL PAGE IS
OF POOR QUALITY

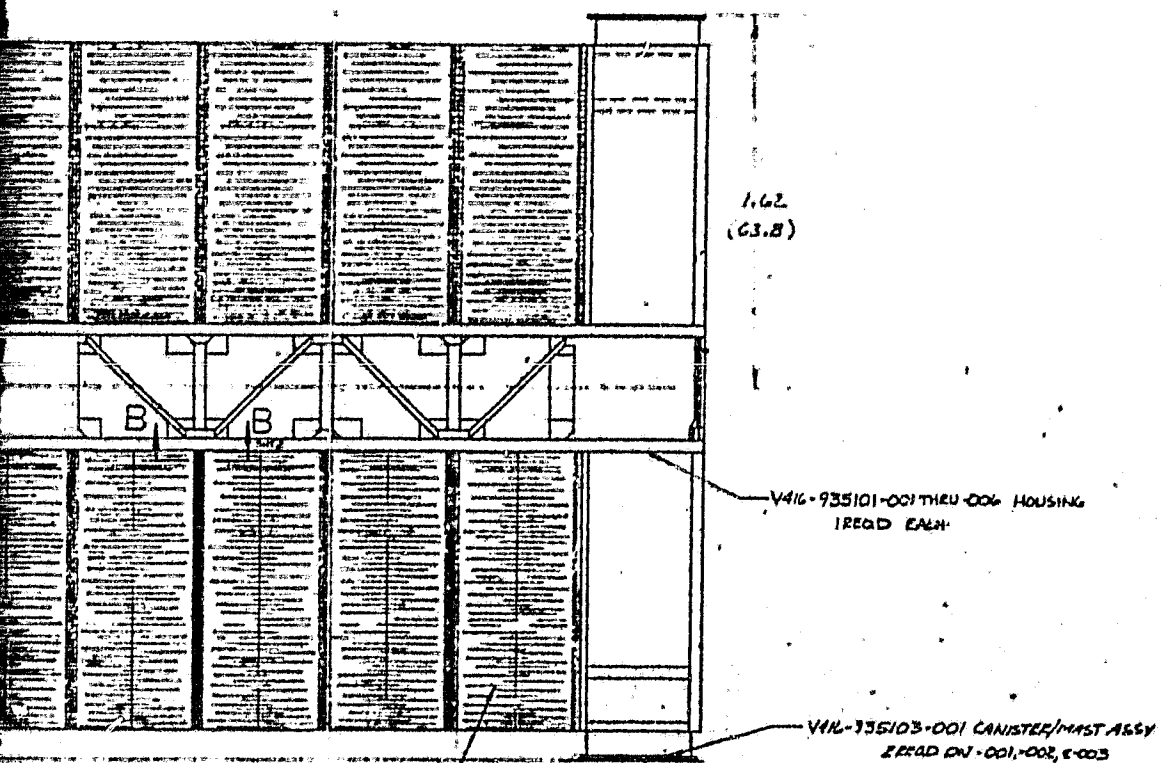

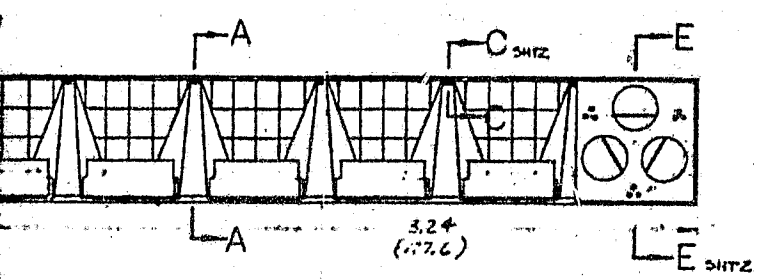

2 FOLDOUT FRAMES

NOTES: UNLESS OTHERWISE SPECIFIED
1. ALL DIMENSIONS ARE IN MM (INCHES)

ORIGINAL PAGE IS
OF POOR QUALITY

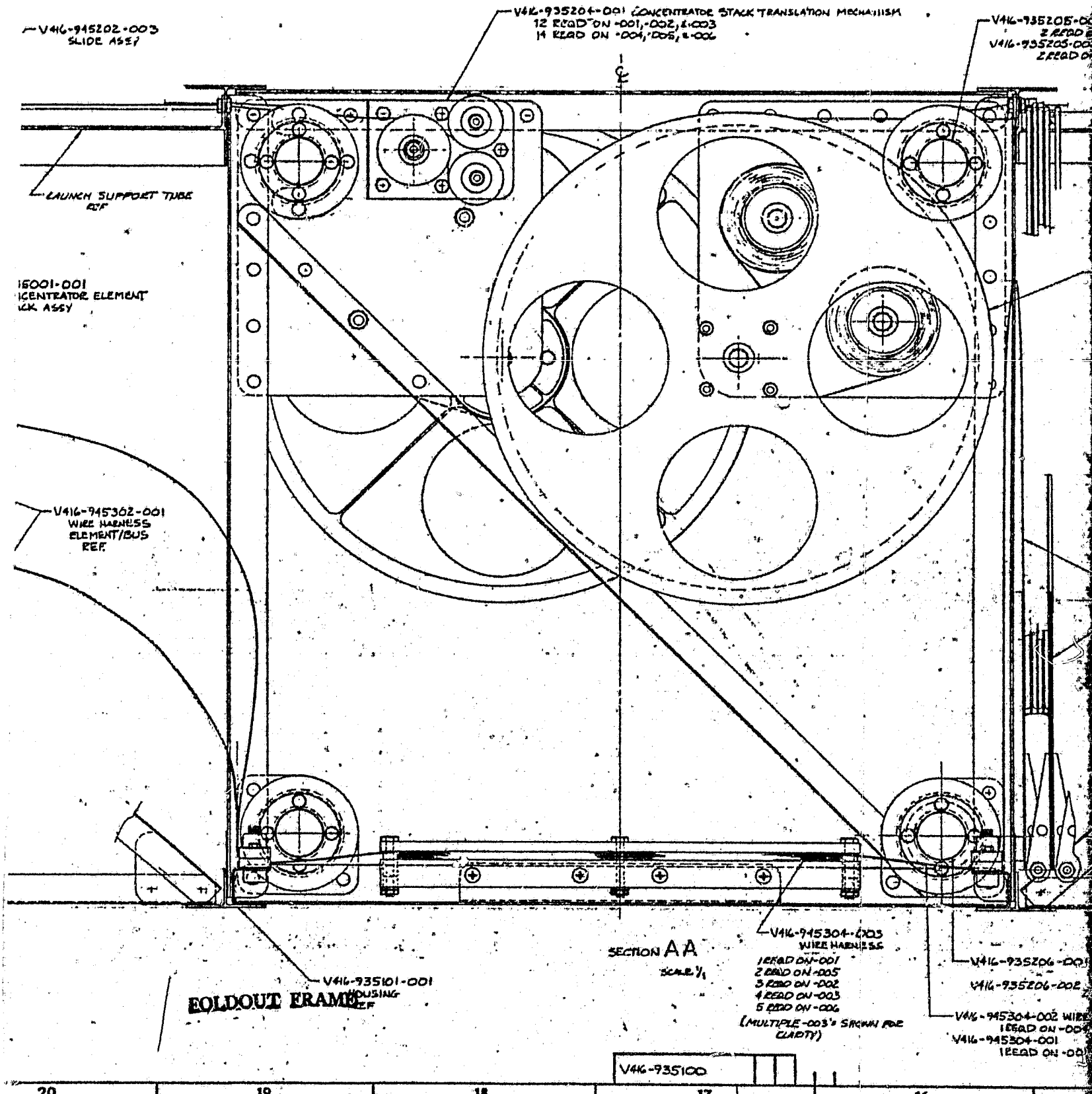

ORIGINAL PAGE IS
OF POOR QUALITY

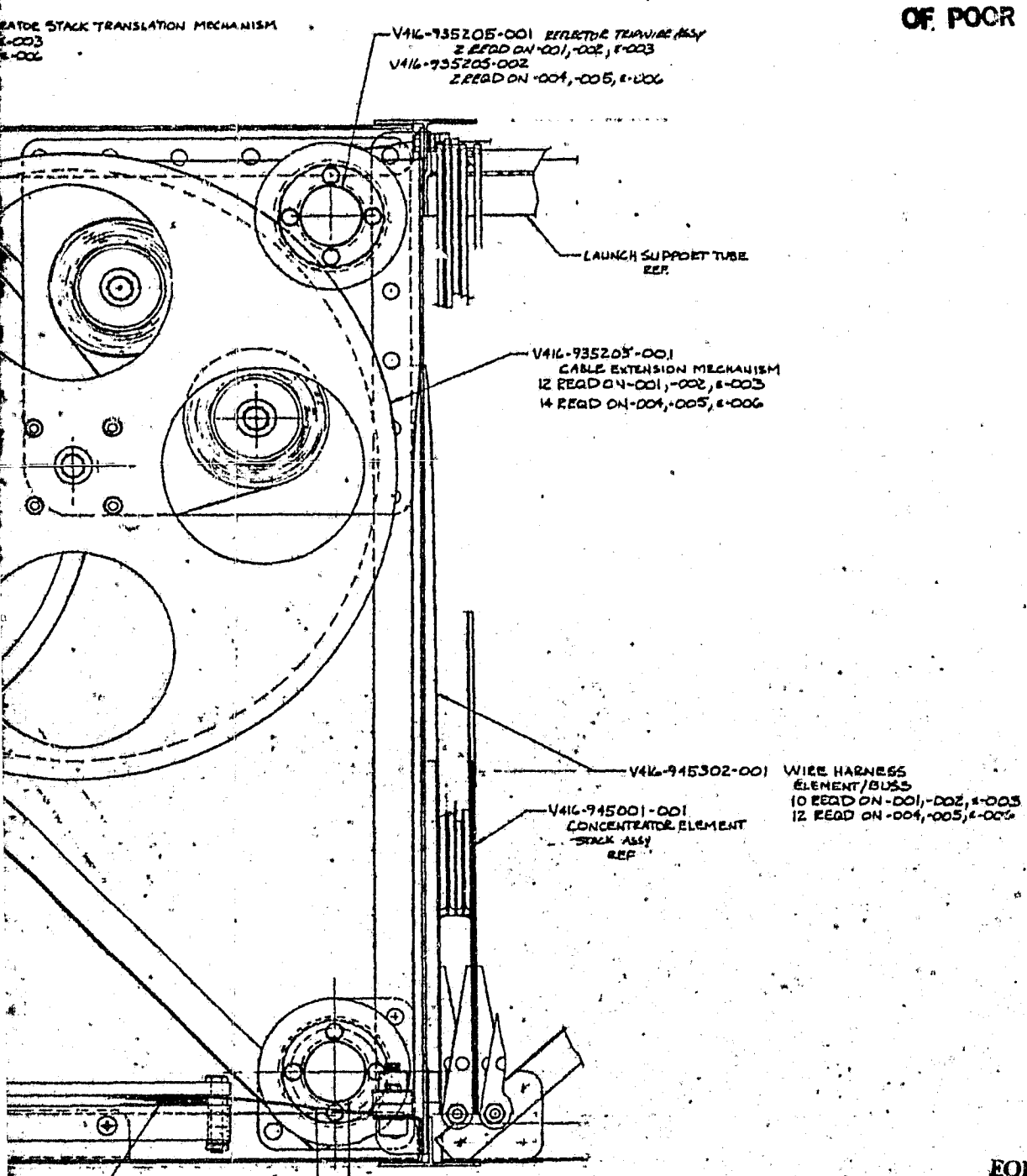

2

FOLDOUT FRAME

ORIGINAL PAGE IS
OF POOR QUALITY

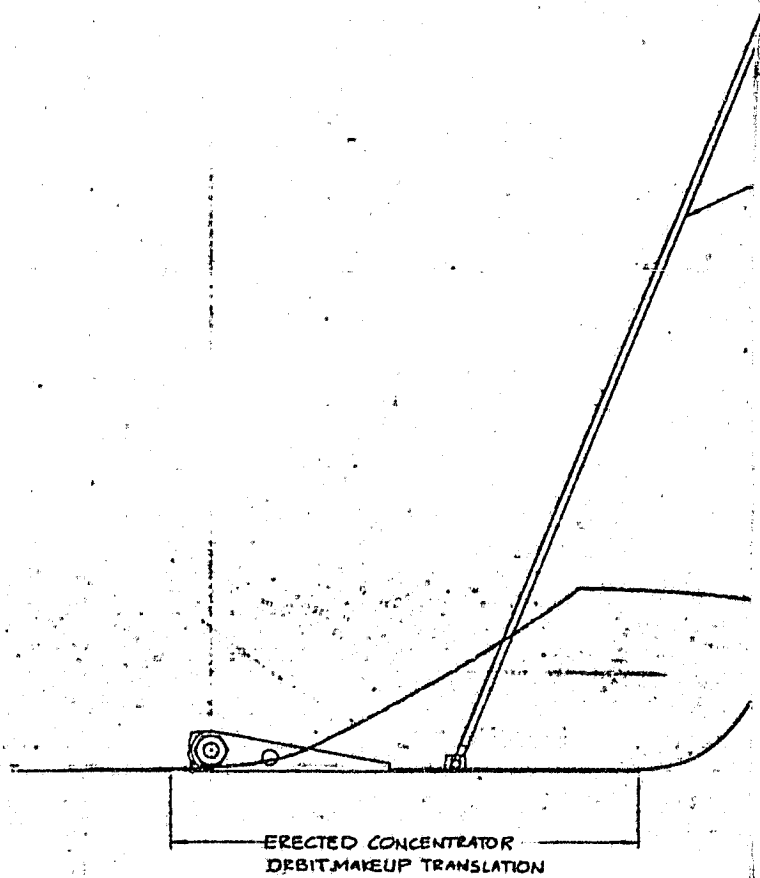

ORIGINAL PAGE IS
OF POOR QUALITY

FOLDOUT FRAME

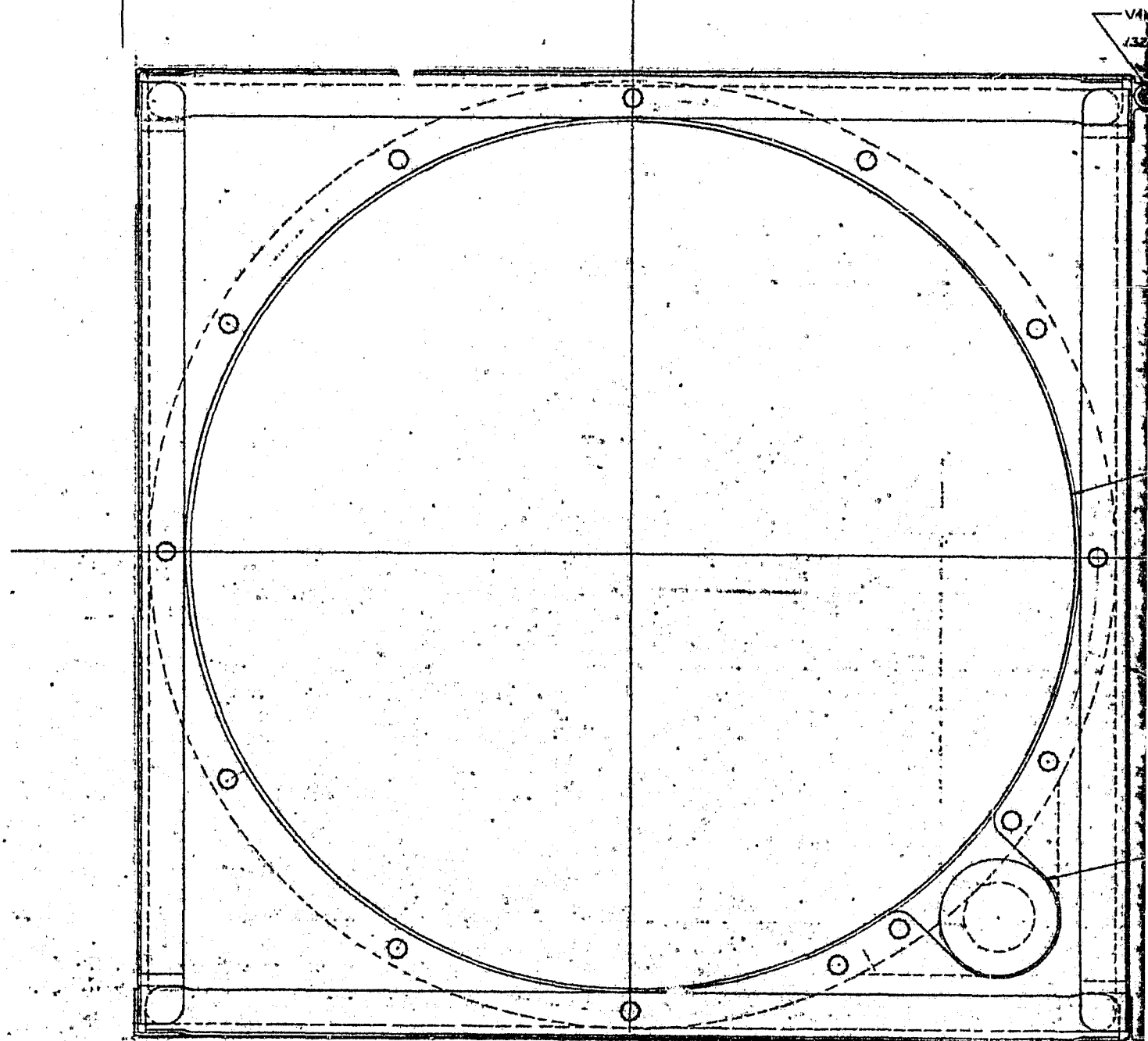

SECTION G G
SCALE 1/1

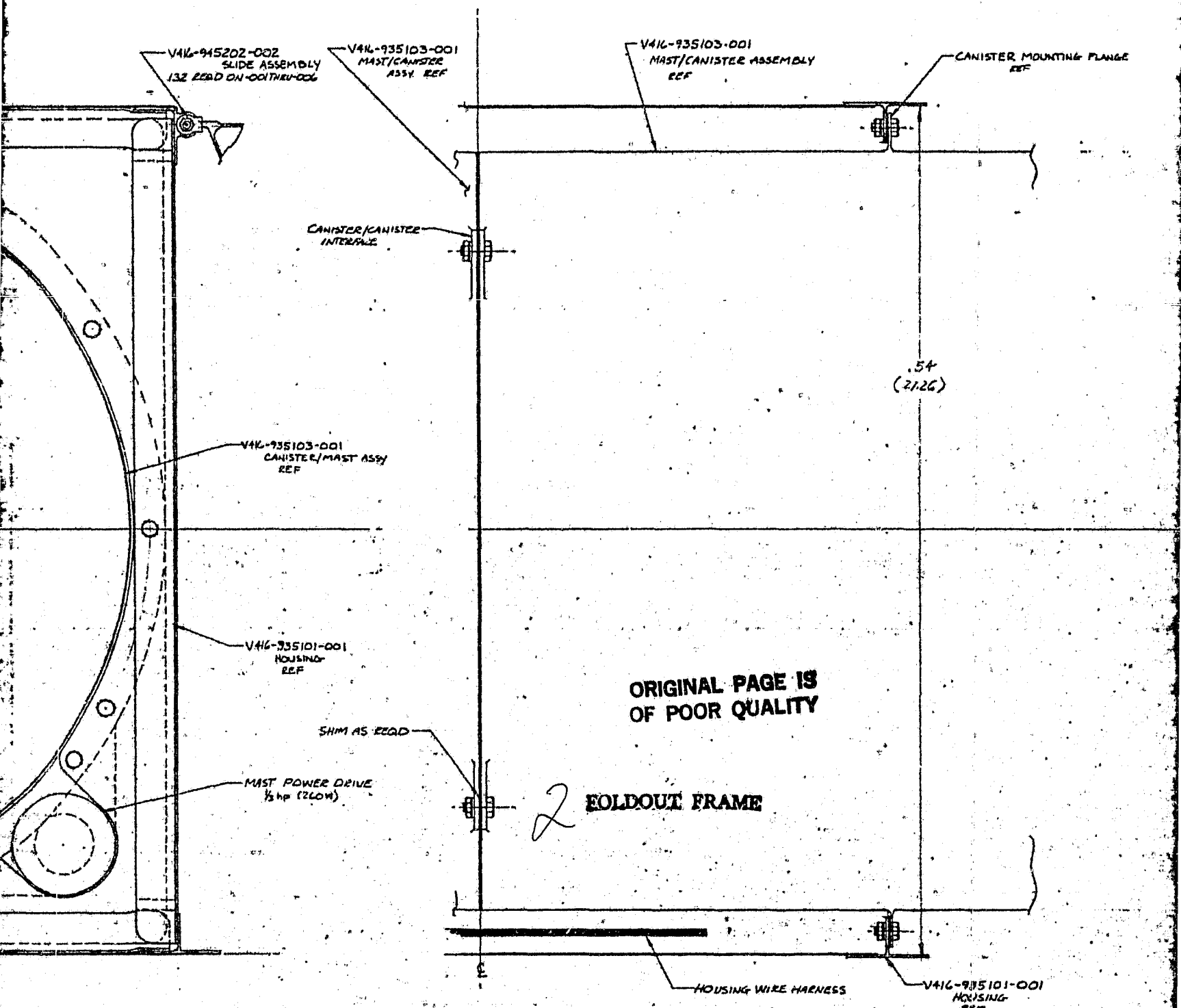

ORIGINAL PAGE IS
OF POOR QUALITY

V416-935100

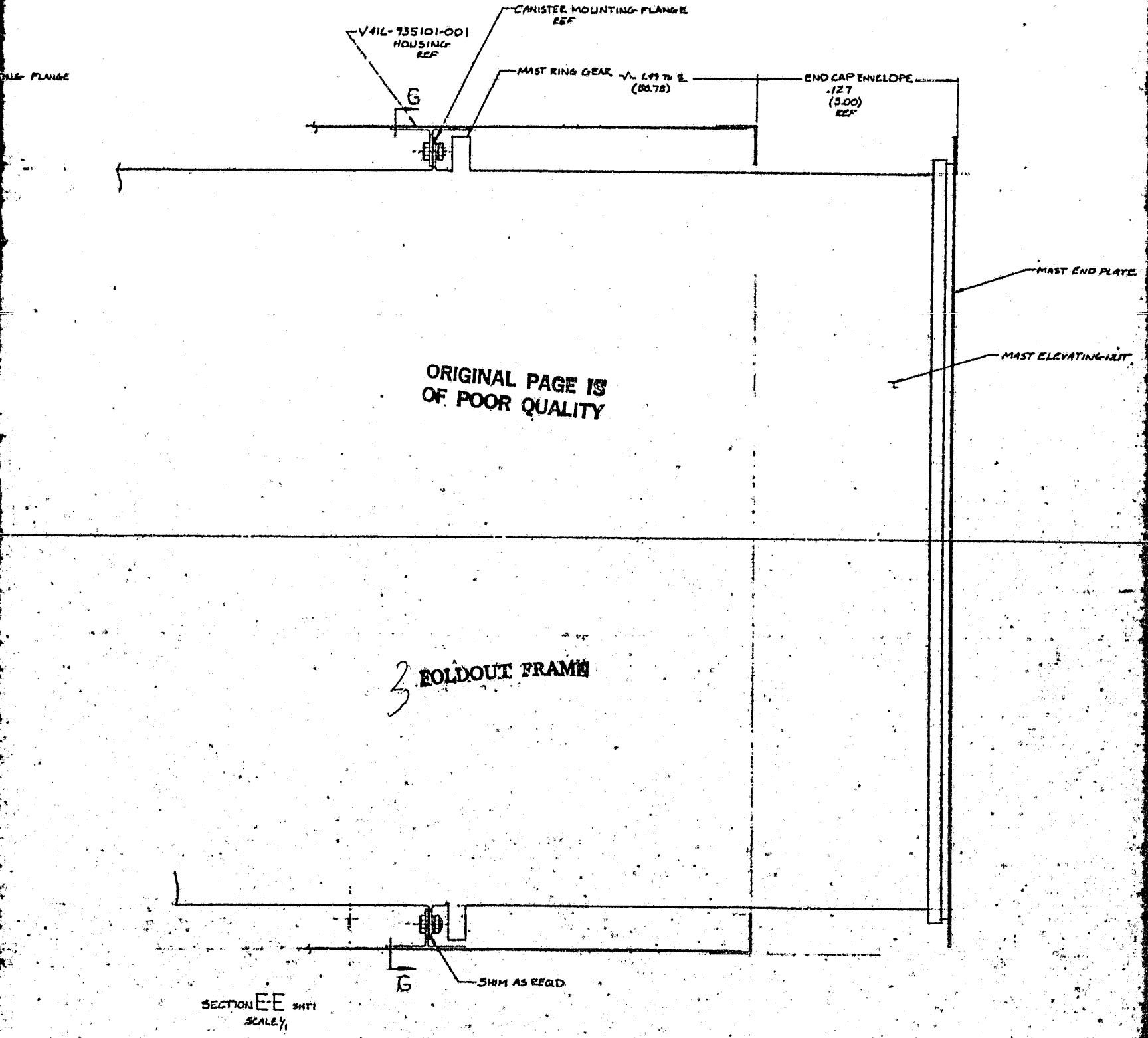

SECTION E-E SHT1
SCALE 1/1

ORIGINAL PAGE IS
OF POOR QUALITY

3 FOLDOUT FRAME

ORIGINAL PAGE IS
OF POOR QUALITY

MAST END PLATE

MAST ELEVATING NUT

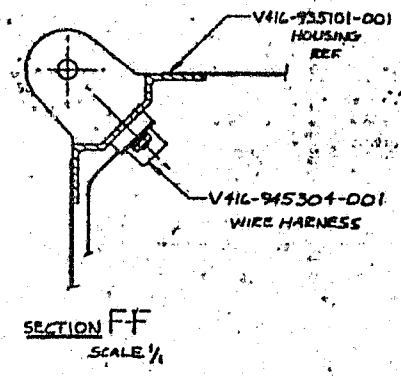

SECTION FF
SCALE 1/1

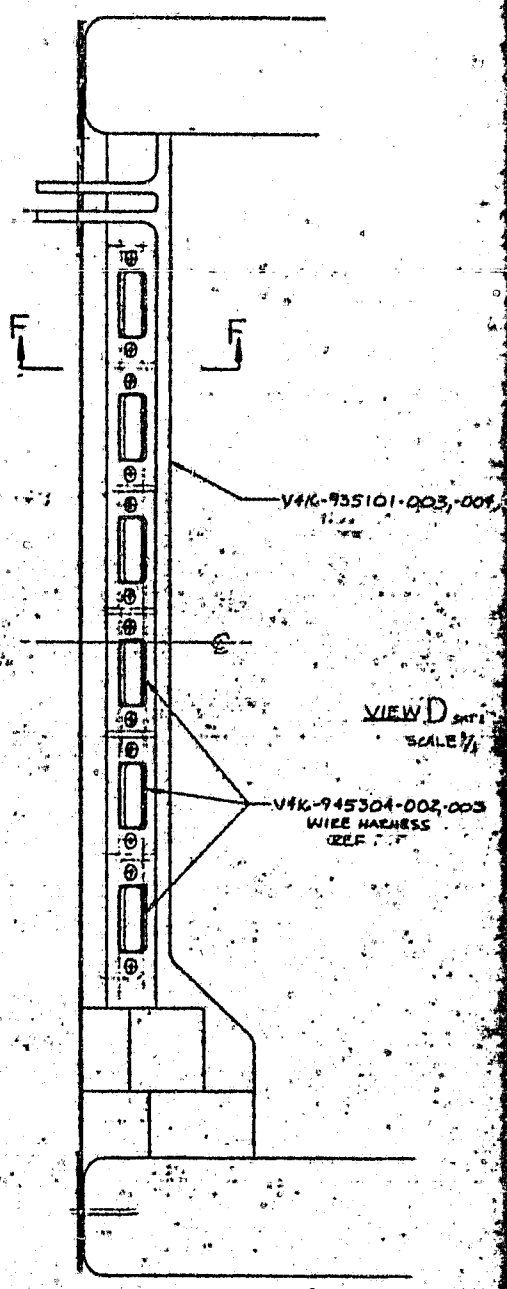

4 FOLDOUT FRAME

V416-935100

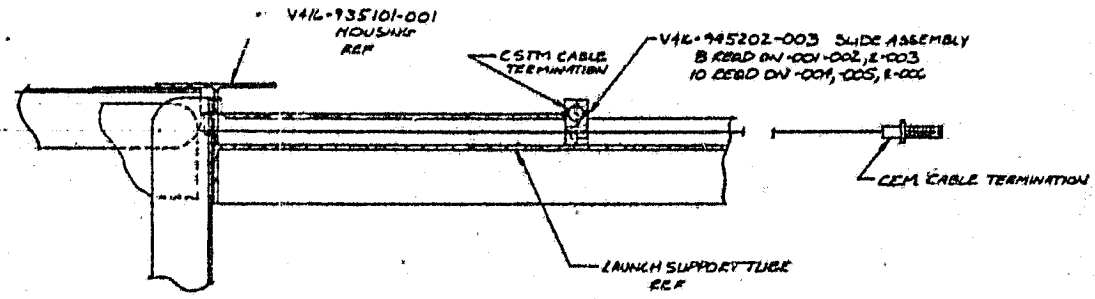

SECTION C-C SHT 1
SCALE 1/1

V416-935101-003, -004, & -005 HOUSING
REF

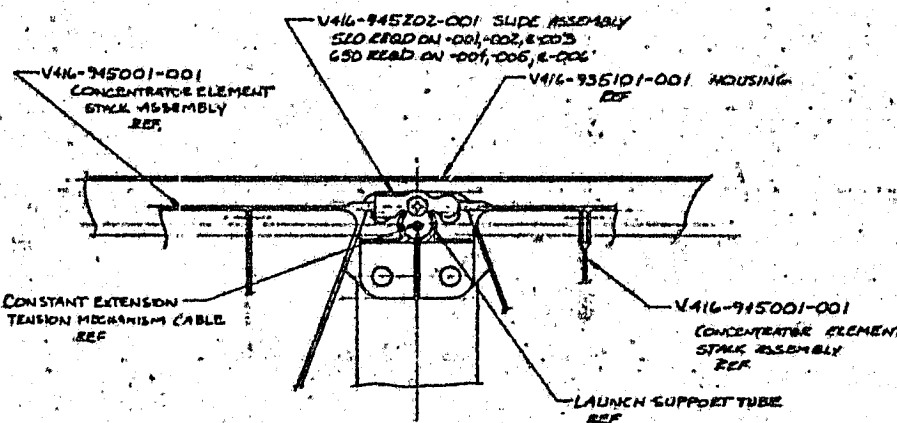

VIEW D SHT 1
SCALE 1/1

V416-945304-002, -003
WIRE HARNESS
REF

SECTION BB SHT 1
SCALE 1/1

FOLDOUT FRAME

ORIGINAL PAGE IS
OF POOR QUALITY

27 | 26 | 25

REVISIONS

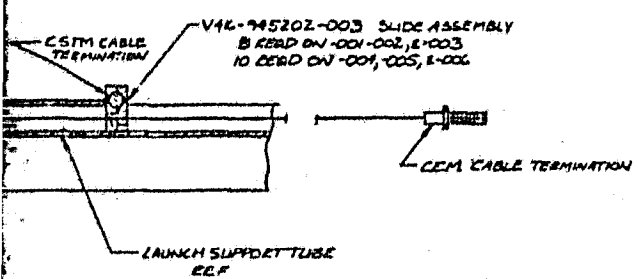

C SHT 1
E 1/1

ORIGINAL PAGE IS
OF POOR QUALITY

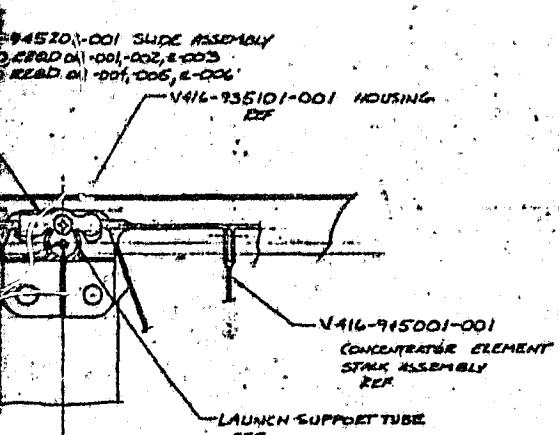

SECTION BB SHT 1
SCALE 1/1

6

FOLDOUT FRAME

A-9, A-10

V416-935100

SIZE	CODE IDENT NO.	DRAWING NO.
J	03953	V416-935100

SCALE FULL | SHEET 1/1

27 | 26 | 25

ORIGINAL PAGE IS
OF POOR QUALITY

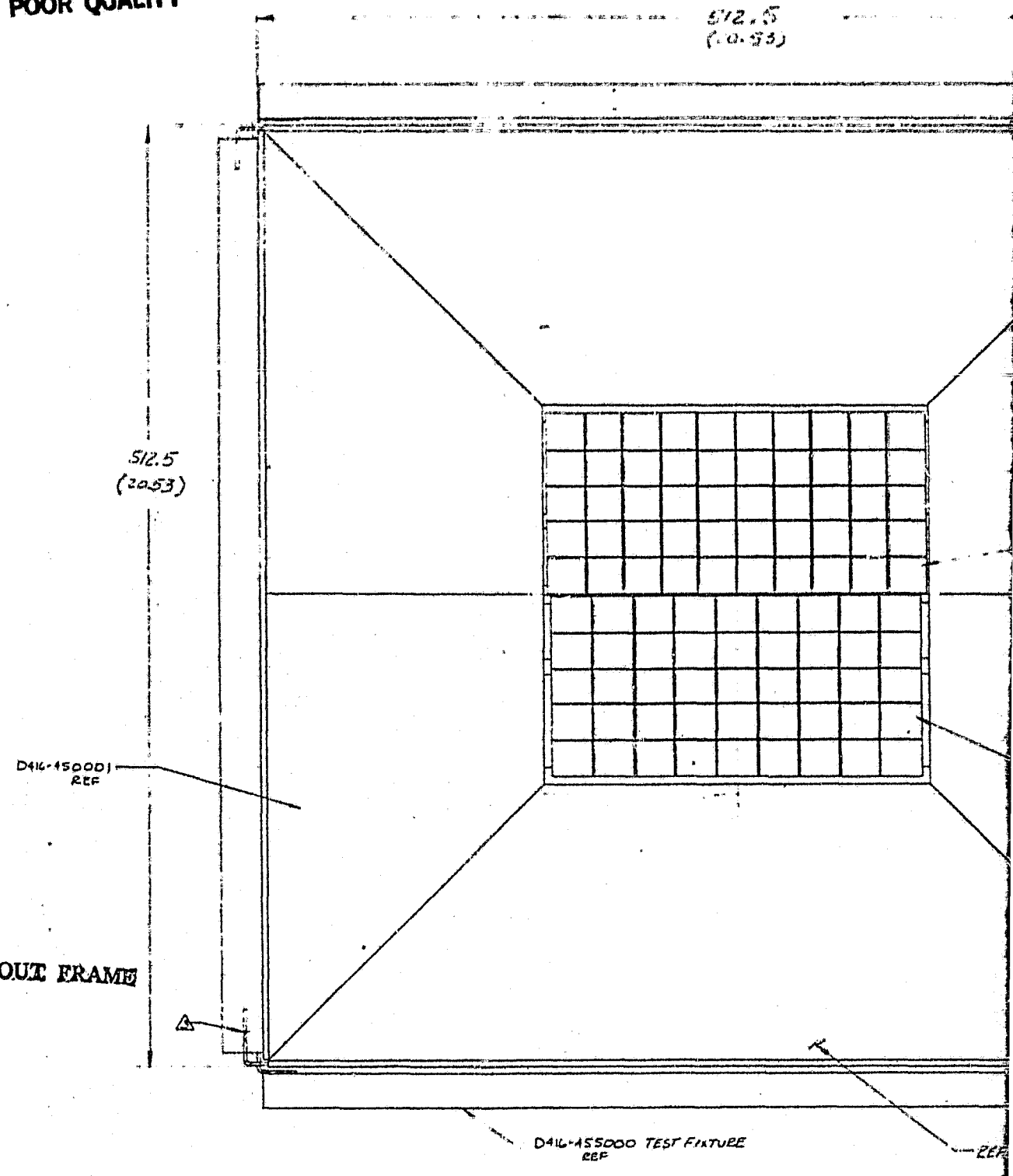

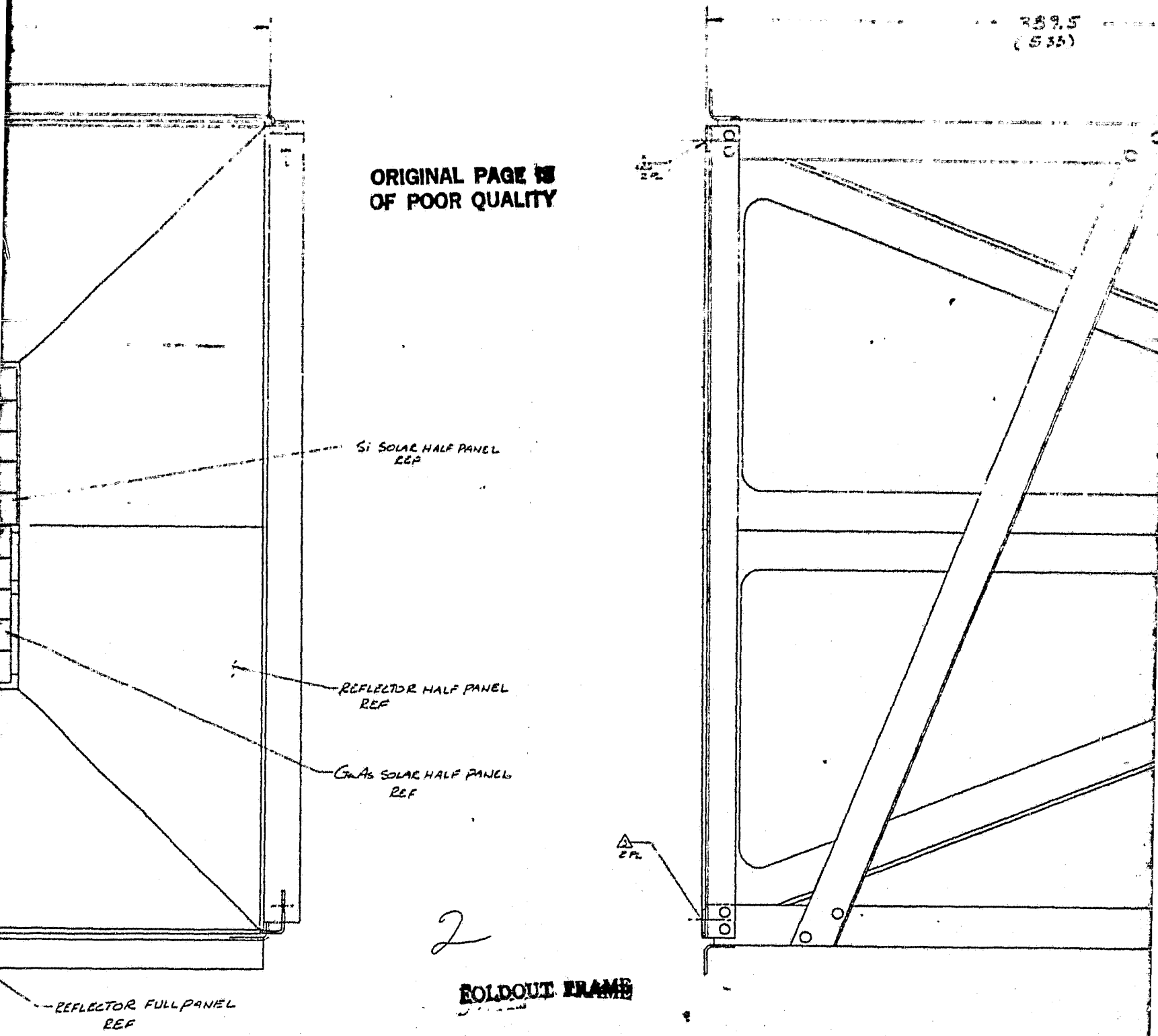

ORIGINAL PAGE IS
OF POOR QUALITY

2

FOLDOUT FRAME

3 FOLDOUT FRAME

ORIGINAL PAGE IS OF POOR QUALITY

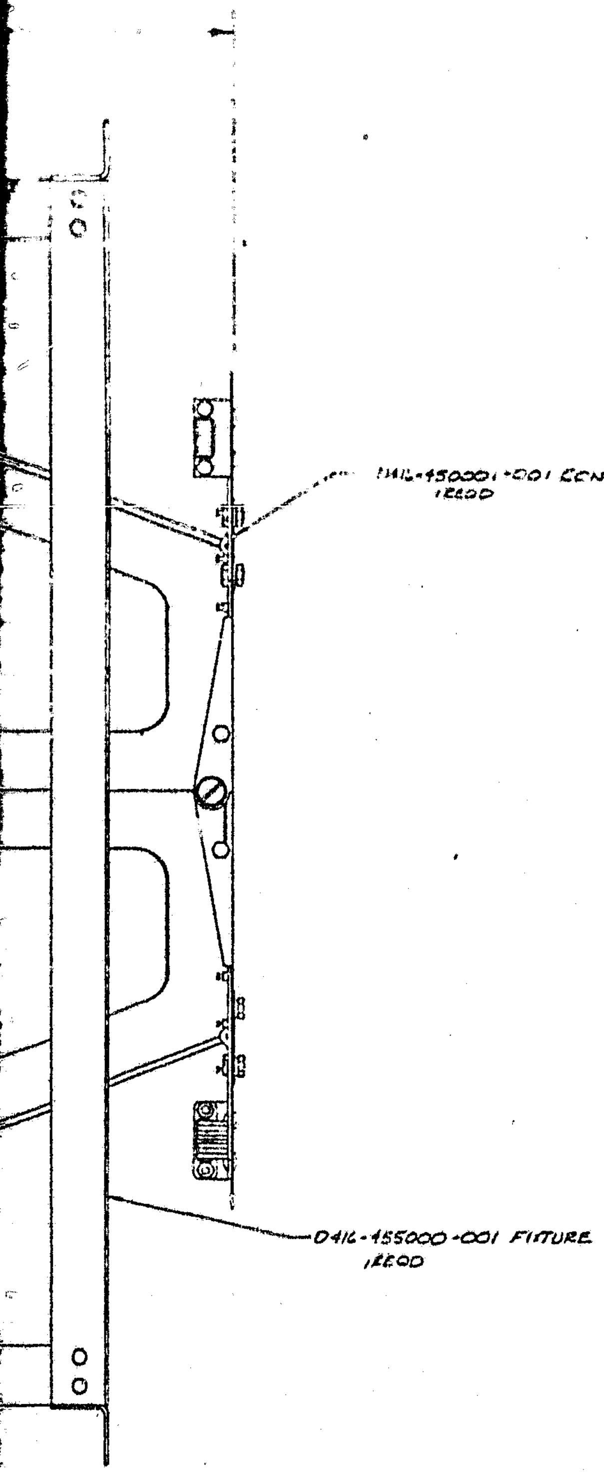

QTY REQD	QTY REQD	QTY REQD	QTY REQD	QTY REQD	QTY REQD	CODE IDENT	PART OR IDENTIFYING NUMBER	NOMENCLATURE OR DESCRIPTION	MATERIAL	DATA SPECIFICATIONS SIZES, NOTES, SUPPLIERS	ZONE
					4			C'CLAMP		0-3" COMMERCIAL GRADE	
					1	-001	D416-455000	FIXTURE			
					1	-001	D416-450001	CONCENTRATOR ELEMENT			
					-001		D416-450000	ASSY			

PARTS LIST

-001 SHOWN

4 [illegible] MM, INCHES IN ( )
3 (triangle) CLAMP AT LOCATION SHOWN
2 SAFTY-WIRE C CLAMPS TO FIXTURE (SHORT LEAD)
1. CONTAMINATION CONTROL PER MF0001-001
NOTES UNLESS OTHERWISE SPECIFIED

ITEM	QTY	NEXT ASSY	USED ON	END ITEM NO.	THRU
-001	1	—	[illegible]		

REQD PER END ITEM | APPLICATION | EFFECTIVITY

UNLESS OTHERWISE SPECIFIED: DIMENSIONS ARE IN INCHES
TOLERANCES ON: DECIMALS, ANGLES

DR BY: M BLISS 5/27/72
CHK BY:
APPROVED BY:

Rockwell International Corporation

CONCENTRATOR ELEMENT TEST ASSEMBLY
LCRSA

SIZE	CODE IDENT NO.	DRAWING NO.
J	03953	D416-450000

SCALE FULL SHEET 1

D416-450000